TECHNISCHE UNIVERSITÄT DRESDEN

Fakultät Maschinenwesen Institut für Festkörpermechanik

Professur für Dynamik und Mechanismentechnik

Diplomarbeit

Zur Erlangung des akademischen Grades Diplomingenieur (Dipl.-Ing.)

Optimale Kombination von strukturmechanischen Modellreduktionsverfahren und Wahl einer geeigneten Zwischendimension

Optimal Combination of Reduction Methods in Structural Mechanics and Selection of a Suitable Intermediate Dimension

Bearbeiter	Jan Paulke
Matrikelnummer	3481040
Studiengang	Maschinenbau
Studienrichtung	Angewandte Mechanik
Betreuer	Dipl.-Ing. Claudius Lein
Betreuender Hochschullehrer	Prof. Dr.-Ing. Michael Beitelschmidt
Tag der Einreichung	1. April 2014

TECHNISCHE UNIVERSITÄT DRESDEN

Fakultät Maschinenwesen Institut für Festkörpermechanik

Professur für Dynamik und Mechanismentechnik

Aufgabenstellung für die Diplomarbeit

im Studiengang	**Maschinenbau (Angewandte Mechanik)**
Name des Diplomanden	**Paulke, Jan**
Matrikelnummer	3481040
Thema:	Optimale Kombination von strukturmechanischen Modellreduktionsverfahren und Wahl einer geeigneten Zwischendimension Optimal Combination of Model Reduction Methods in Structural Mechanics and Selection of a Suitable Intermediate Dimension

Zielsetzung:

Die steigende Komplexität von technischen Baugruppen erfordert vermehrt den Einsatz von elastischen Mehrkörpersystemen (EMKS), mit denen mechanische Systeme modelliert und berechnet werden können. Für die Abbildung des elastischen Körpers werden FE-Modelle eingesetzt und einer Modellordnungsreduktion unterzogen.
In Abhängigkeit der Definition des Raumes, in welchem der reduzierte Verschiebungsvektor definiert ist, können die Reduktionsmethoden in anschauungsraumbezogene Verfahren, Verfahren im modalen Raum, Verfahren im allgemeinen Vektorraum sowie Verfahren im hybriden Raum unterteilt werden.
Die Effektivität der Modellordnungsreduktion wird maßgeblich durch die Rechenzeit und die Modellgüte bestimmt. Einen Zielkonflikt stellen exakte Verfahren dar, die jedoch viel Rechenzeit benötigen. Daher kann es sinnvoll sein, Reduktionsmethoden zu kombinieren, d.h. hintereinander auszuführen, was als Mehrschrittreduktion bezeichnet wird. Hierbei wird zunächst auf eine Zwischendimension reduziert.
Das Ziel der Arbeit besteht darin, eine optimale Kombination von Reduktionsverfahren zu erarbeiten, indem zunächst mögliche Kombinationen zusammengestellt werden. Hierfür steht eine breite Auswahl an bereits implementierten Reduktionsmethoden zur Verfügung. Im Anschluss ist für einige vielversprechende Kombinationen eine ideale Wahl der Zwischendimension zu treffen und entsprechende Bewertungskriterien zu finden. Die Wahl der Zwischendimension hängt von dem Reduktionsverfahren ab, wobei z.B. für anschauungsraumbezogene Verfahren eine optimale Auswahl der Master-Freiheitsgrade getroffen werden kann. Die Methode der Effective Independence (EfI) ist hierfür ein vielversprechender Ansatz.

Für die Reduktion und die Auswertung ist das an der Professur entwickelte Programm MORPACK zu verwenden. Die Kombinationsmöglichkeiten sowie die Bestimmung der Zwischendimension sind in die bestehende Software zu integrieren und entsprechende GUIs zu erstellen.
Anhand von Fallstudien sollen Rechenzeit, Speicherbedarf und Modellgüte in Abhängigkeit von der Zwischendimension für verschiedene Kombinationen von Reduktionsverfahren ermittelt werden. Abschließend ist die Funktionalität anhand realitätsnaher Beispielmodelle zu überprüfen. Am Ende der Arbeit sollten Aussagen zur Anwendbarkeit und der mögliche Vorteil im Vergleich zur Verwendung von Einschrittverfahren bzw. hybriden Verfahren herausgestellt werden.

Arbeitsschritte:

- Literaturstudium zu den Themen Modellordnungsreduktion, Mehrschrittverfahren, optimale Wahl der Master-Freiheitsgrade
- Analyse von bereits in MORPACK implementierten Reduktionsverfahren
- Zusammenstellung von Kombinationsmöglichkeiten bzgl. Sinnhaftigkeit und Anwendbarkeit
- Ausarbeitung von Parametern und Auswahlmöglichkeiten für die Zwischendimension in Abhängigkeit des Reduktionsverfahrens
- Implementierung ausgewählter Kombinationsmöglichkeiten und GUI-Erstellung für die Parametrierung
- Einarbeitung und Implementierung von Verfahren zur optimalen Auswahl von Master-Freiheitsgraden (u.a. EfI)
- Auswahl geeigneter Testmodelle und Festlegung von Fallstudien
- Vergleich und Auswertung hinsichtlich Rechenzeit, Speicherbedarf, Modellgüte
- Gegenüberstellung von Mehrschrittverfahren und Einschrittverfahren / hybriden Verfahren
- Behandlung und Umgang mit numerischen Problemen bezgl. der Zwischendimension (Besetztheit, Rang und Bandbreite der Systemmatrizen)
- Erarbeitung von möglichen Kriterien zur Bewertung der Wahl der Zwischendimension, sofern möglich auch a priori
- Gewährleistung der Funktionalität hinsichtlich des Ablaufs anhand eines realen Bauteils
- Integration der funktionsfähigen Algorithmen in die Software MORPACK
- Dokumentation und abschließende Bewertung

Betreuender Hochschullehrer:	Prof. Dr.-Ing. Michael Beitelschmidt, TU Dresden
Betreuer:	Dipl.-Ing. Claudius Lein, TU Dresden
Ausgehändigt am:	01.12.2013
Einzureichen am:	01.04.2014

Die von der Studienrichtung erlassenen Richtlinien zur Anfertigung der Diplomarbeit sowie die Diplomprüfungsordnung sind zu beachten. Nach zwei Dritteln der Bearbeitungszeit ist eine Zwischenpräsentation der Arbeitsergebnisse für den Lehrstuhl zu halten.
Es ist ein digitaler Anhang zur Arbeit einzureichen (Daten-CD o.ä.). Darin müssen alle in der Arbeit dokumentierten Modelle, Berechnungs- und Simulationsergebnisse mit den nötigen Eingabedaten und Parametern, sowie die zur Modellerstellung genutzten Skripte und Programme nachvollziehbar enthalten sein. Gegebenenfalls ist vor der Diplomverteidigung ein Gespräch mit dem Betreuer zu führen, bei welchem die Daten gesichtet und erläutert werden.

Prof. Dr.-Ing. Michael Beitelschmidt Betreuender Hochschullehrer	Prof. Dr.-Ing. habil. Klaus-Georg Eulitz Studienrichtungsleiter

Selbstständigkeitserklärung

Ich erkläre hiermit, die am heutigen Tag eingereichte Diplomarbeit zum Thema "Optimale Kombination von strukturmechanischen Modellreduktionsverfahren und Wahl einer geeigneten Zwischendimension" selbstständig und ohne unzulässige fremde Hilfe angefertigt zu haben. Die verwendeten Quellen und Hilfsmittel sind im Literaturverzeichnis vollständig aufgeführt. Ich versichere, alles kenntlich gemacht zu haben, was aus Arbeiten Anderer unverändert oder mit Abänderungen übernommen wurde.

Dresden, 1. April 2014

Jan Paulke

Kurzfassung

Mehrschrittverfahren der Modellreduktion werden untersucht, um spezielle Probleme konventioneller Einschrittverfahren zu lösen. Eine optimale Kombination von strukturmechanischen Reduktionsverfahren und die Auswahl einer geeigneten Zwischendimension wird untersucht. Dafür werden automatische Verfahren in Matlab implementiert, in die Software MORPACK integriert und anhand des Finite Elemente Modells eines Getriebegehäuses ausgewertet.
Zur Auswahl der Zwischendimension werden Empfehlungen genannt und auf Probleme bei der Kombinationen bestimmter Reduktionsverfahren hingewiesen. Ein Pseudo-Zweischrittverfahren wird vorgestellt, welches eine Reduktion ohne Kenntnis der modalen Größen bei ähnlicher Genauigkeit im Vergleich zu modalen Unterraumverfahren durchführt. Für kleine Reduktionsdimensionen wird ein Knotenauswahlverfahren vorgeschlagen, um die Approximation des Frequenzganges durch die System Equivalent Reduction Expansion Process (SEREP)-Reduktion zu verbessern.

Abstract

A two-step model order reduction method is investigated in order to overcome problems of certain one-step methods. Not only optimal combinations of one-step reductions are considered but also the selection of a suitable intermediate dimension (ID) is described. Several automated selection methods are presented and their application tested on a gear box model. The implementation is realized using a Matlab-based Software *MORPACK*. Several recommendations are given towards the selection of a suitable ID, and problems in Model Order Reduction (MOR) combinations are pointed out. A pseudo two-step is suggested to reduce the full system without any modal information. A new node selection approach is proposed to enhance the SEREP approximation of the system's response for small reduced representations.

Contents

Kurzfassung iv

Abstract iv

Nomenclature ix

1 Introduction 1
- 1.1 Motivation . . . 1
- 1.2 Objectives . . . 1
- 1.3 Outline of the Thesis . . . 2

2 Theoretical Background 3
- 2.1 Finite Element Method . . . 3
  - 2.1.1 Modal Analysis . . . 4
  - 2.1.2 Frequency Response Function . . . 4
- 2.2 Model Order Reduction . . . 5
- 2.3 Physical Subspace Reduction Methods . . . 7
  - 2.3.1 Guyan Reduction . . . 7
  - 2.3.2 Improved Reduced System Method . . . 8
- 2.4 Modal Subspace Reduction Methods . . . 10
  - 2.4.1 Modal Reduction . . . 11
  - 2.4.2 Exact Modal Reduction . . . 11
  - 2.4.3 System Equivalent Reduction Expansion Process . . . 13
- 2.5 Krylov Subspace Reduction Methods . . . 14
- 2.6 Hybrid Subspace Reduction Methods . . . 15
  - 2.6.1 Component Mode Synthesis . . . 16
  - 2.6.2 Hybrid Exact Modal Reduction . . . 19
- 2.7 Model Correlation Methods . . . 21
  - 2.7.1 Normalized Relative Frequency Difference . . . 21
  - 2.7.2 Modified Modal Assurance Criterion . . . 22
  - 2.7.3 Pseudo-Orthogonality Check . . . 22
  - 2.7.4 Comparison of Frequency Response Function . . . 23

3 Selection of Active Degrees of Freedom 25
3.1 Non-Iterative Methods . . . 26
3.1.1 Modal Kinetic Energy and Variants . . . 26
3.1.2 Driving Point Residue and Variants . . . 27
3.1.3 Eigenvector Component Product . . . 28
3.2 Iterative Reduction Methods . . . 29
3.2.1 Effective Independence Distribution . . . 29
3.2.2 Mass-Weighted Effective Independence . . . 32
3.2.3 Variance Based Selection Method . . . 33
3.2.4 Singular Value Decomposition Based Selection Method . . . 34
3.2.5 Stiffness-to-Mass Ratio Selection Method . . . 34
3.3 Iterative Expansion Methods . . . 35
3.3.1 Modal-Geometrical Selection Criterion . . . 36
3.3.2 Triaxial Effective Independence Expansion . . . 36
3.4 Measure of Goodness for Selected Active Set . . . 39
3.4.1 Determinant and Rank of the Fisher Information Matrix . . . 39
3.4.2 Condition Number of the Partitioned Modal Matrix . . . 40
3.4.3 Measured Energy per Mode . . . 40
3.4.4 Root Mean Square Error of Pseudo-Orthogonality Check . . . 41
3.4.5 Eigenvalue Comparison . . . 41

4 Two-Step Reduction in MORPACK 42
4.1 Structure of MORPACK . . . 42
4.2 Selection of an Intermediate Dimension . . . 43
4.2.1 Intermediate Dimension Requirements . . . 44
4.2.2 Implemented Selection Methods . . . 45
4.2.3 Recommended Selection of an Intermediate Dimension . . . 48
4.3 Combination of Reduction Methods . . . 49
4.3.1 Overview of All Candidates . . . 50
4.3.2 Combinations with Modal Information . . . 54
4.3.3 Combinations without Modal Information . . . 54

5 Applications 57
5.1 Gear Box Model . . . 57
5.2 Selection of Additional Active Nodes . . . 58
5.3 Optimal Intermediate Dimension . . . 64
5.4 Two-Step Model Order Reduction Results . . . 66
5.5 Comparison to One-Step Model Order Reduction Methods . . . 70
5.6 Comparison to One-Step Hybrid Model Order Reduction Methods . . . 72

5.7 Proposal of a New Approach for Additional Node Selection 73

6 Summary and Conclusions **77**

7 Zusammenfassung und Ausblick **79**

Bibliography **81**

List of Tables **86**

List of Figures **88**

A Appendix **89**

A.1 Results of Two-Step Model Order Reduction 89

A.2 Data CD 96

Nomenclature

Any symbols not listed in this section are fully explained within the text.

Scalars

Symbol	Description
$\mathcal{H}_2$	Error if the $\mathcal{H}_2$-norm
N	Number of DoF of the full system
N_n	Number of DoF of the full system
f_{full}	Frequency of the full FEM
f_{NRFD}	Element of the NRFD vector
f_{red}	Frequency of the reduced representation
h_{pq}	Modal-based frequency response
i	Imaginary unit
$k1$	Weighting parameter for geometrical vector in MoGeSeC
$k2$	Weighting parameter for modal vector in MoGeSeC
m	Number of mode shapes of the full system ($N \times N$)
$m_{\mathcal{K}}$	Number of Krylov modes
$\Delta_i\sigma^2$	Increase in variance of the covariance matrix $\boldsymbol{A}^{-1}_{\mathbf{FIM}}$ due to a deletion of the i-th DoF
$\varepsilon^{\text{rel}}_{\mathcal{H}_2}$	Error if the $\mathcal{H}_2$-norm
ζ_f	Modal damping coefficient
ϕ_{ip}	value of the j-th mode at p-th output
ω^2	Eigenvalues of the full FEM
ω_f	forcing frequency

Vectors

Symbol	Description
$\boldsymbol{0}$	Appropriately sized column vector with all elements being 0
$\mathbf{1}$	Appropriately sized column vector with all entries being 1
$\boldsymbol{a}_{\mathbf{DPR}}$	Average driving point residue
$\boldsymbol{a}_{\mathbf{MKE}}$	Average modal kinetic energy
$\boldsymbol{d}_{\mathbf{min}}$	Minimum absolute value across the rows of **DPR**
$\boldsymbol{e}$	Alternative formulation of the EfI
$\boldsymbol{e}_{\mathbf{cemw}}$	Mass-weighted formulation of the EfI with a Cholesky factorization of the EMR-reduced mass matrix $\boldsymbol{M}_{\mathbf{EMR}}$
$\boldsymbol{e}_{\mathbf{cmw}}$	Mass-weighted formulation of the EfI with a Cholesky factorization of the mass matrix $\boldsymbol{M}$
$\boldsymbol{e}_{D}$	Effective Independence Distribution
$\boldsymbol{e}_{D_3}$	Triaxial Effective Independence Distribution
$\boldsymbol{e}_{\mathbf{rmw}}$	Mass-weighted formulation of the EfI with a square root decomposition of the mass matrix $\boldsymbol{M}$
$\boldsymbol{f}$	Applied forces $N \times 1$
$\boldsymbol{m}_{\mathbf{min}}$	Minimum absolute value across the rows of **MKE**
$\boldsymbol{q}$	Displacement vector in the modal coordinate system
$\boldsymbol{r}_{\mathbf{SMR}}$	SMR-based selection criteria
$\boldsymbol{r}_{\mathbf{SVD}}$	SVD-based contribution to the determinant of the FIM
$\boldsymbol{w}$	Weight function vector for MoGeSeC
$\boldsymbol{w}_{\mathbf{ADPR}}$	Weighted average driving point residue
$\boldsymbol{w}_{\mathbf{AMKE}}$	Weighted average modal kinetic energy
$\boldsymbol{z}$	Displacement vector of the full system
$\boldsymbol{z}_{\boldsymbol{a}}$	Active displacement vector
$\boldsymbol{z}_{\boldsymbol{o}}$	Omitted displacement vector
$\dot{\boldsymbol{z}}$	Velocity vector of the full system
$\ddot{\boldsymbol{z}}$	Acceleration vector of the full system
$\boldsymbol{\phi}_{\mathbf{ECP}}$	Eigenvector component product
$\boldsymbol{\psi}_{\mathbf{0}}$	Eigenvectors of the singular FIM corresponding to the zero eigenvalues

Symbol	Description
$\bar{\boldsymbol{\psi}}$	Eigenvectors of the projected FIM corresponding to the non-zero eigenvalues during EfI$_3$+

Matrices

Symbol	Description
$\mathbf{0}$	Appropriately sized matrix with all elements being 0
$\boldsymbol{A}_{\mathbf{FIM}}$	Fisher Information Matrix
$\boldsymbol{A}_{\mathbf{FIM}}^{\mathbf{ini}}$	Initial Fisher Information Matrix for EfI$_3$+
$\boldsymbol{C}$	Damping matrix of the full system
$\mathbf{DPR}$	Driving point residue matrix
$\boldsymbol{G}^{\boldsymbol{\rho}}$	Residual flexibility matrix
$\boldsymbol{H}$	Analytical FRF data matrix
$\boldsymbol{I}$	Appropriately sized identity matrix
$\boldsymbol{K}$	Stiffness matrix of the full system
$\boldsymbol{L}$	Lower triangular matrix of a Cholesky decomposition of the mass matrix
$\boldsymbol{M}$	Mass matrix of the full system
$\mathbf{MKE}$	Modal kinetic energy matrix
$\mathbf{ModMAC}$	ModMAC matrix
$\boldsymbol{P}$	Idempotent matrix used as a projector
$\boldsymbol{P}_{\mathbf{obl}}$	Oblique projector used to create a hybrid TAM
$\boldsymbol{POC}$	POC matrix
$\boldsymbol{P}_{\mathbf{orth}}$	Orthogonal projector used to create a hybrid TAM
$\boldsymbol{S}$	Matrix for the computation of the inertia force adjustment during IRS
$\boldsymbol{T}$	Transformation matrix of MOR
$\boldsymbol{U}$	Left-singular vectors of the SVD
$\boldsymbol{V}$	Right-singular vectors of the SVD
$\boldsymbol{Z}(\omega_f)$	Dynamic stiffness matrix
$\boldsymbol{\Lambda}$	Diagonal matrix with ω^2

Symbol	Description
$\boldsymbol{\Sigma}$	Singular values of a SVD
$\boldsymbol{\Phi}$	Modal matrix $N \times m$ of the full system
$\boldsymbol{\Psi}$	Eigenvectors of FIM
$\boldsymbol{\Psi^{at}}$	Attachment modes for a free-interface CMS
$\boldsymbol{\lambda}$	Eigenvalues of FIM
$\bar{\boldsymbol{\lambda}}$	Non-zero eigenvalues of projected FIM during EfI_3+
$\boldsymbol{\phi_{3i}}$	Partitioned modal matrix corresponding to the i-th node

Subscripts

Symbol	Description
$_{CB}$	Fixed-interface CMS approach
$_{CMS}$	Free-interface CMS approach
$_{\text{EMR}}$	Reduced with EMR
$_{\text{GR}}$	Reduced with GR
$_{\text{IRS}}$	Reduced with IRS
$_{\mathcal{K}}$	Element of the Krylov subspace
$_{\text{KSM}}$	Reduced with the KSM
$_{MR}$	Reduced with MR
$_{\text{SEREP}}$	Reduced with SEREP
$_{\text{SMR}}$	SMR-based selection criteria
$_{a}$	a-set partition of a $N \times 1$ vector or a $N \times m$ matrix
$_{aa}$	a-set partition of a $(N \times N)$ matrix
$_{ao}$	a-set as rows and o-set as column partition of a $(N \times N)$ matrix
$_{\text{cemw}}$	Mass-weighted formulation of the EfI with a Cholesky factorization of the EMR-reduced of the mass matrix $\boldsymbol{M}$
$_{\text{cmw}}$	Mass-weighted formulation of the EfI with a Cholesky decomposition of the mass matrix $\boldsymbol{M}$
$_{\text{exp}}$	Expanded data acquired from a reduced system
$_{\text{full}}$	Value of the full FEM
$_{\text{hyb}}$	Hybrid reduction

Symbol	Description
$_{i+1}$	$(i+1)$-th step of an iteration
$_{ii}$	I-th diagonal term of a matrix
$_{o}$	o-set partition of a $N \times 1$ vector or a $N \times m$ matrix
$_{oa}$	o-set as rows and a-set as column partition of a $(N \times N)$ matrix
$_{\text{obl}}$	Oblique projection
$_{oo}$	o-set partition of a $(N \times N)$ matrix
$_{\text{orth}}$	Orthogonal projection
$_{p}$	Output location of a system
$_{q}$	Input location of a system
$_{\text{red}}$	Value of the reduced representation
$_{\text{rm}}$	Representation of the residual modes
rmw	Mass-weighted formulation of the EfI with a square root decomposition of the mass matrix $\boldsymbol{M}$
$_{s}$	Pre-selected candidate set of DoF for an a-set selection
$_{\text{tm}}$	Representation of the target modes

Superscripts

Symbol	Description
$^{-1}$	Inverse of a matrix
$^{0.5}$	Square root of a matrix
$^{\text{T}}$	Transpose of a matrix
^{at}	Attachment partition during the free-interface CMS reduction
^{c}	Constraint partition during the CMS reduction
$^{\text{g}}$	Generalized inverse of a matrix
$^{\text{ini}}$	Initial values
$^{\rho}$	Residual partition during the free-interface CMS reduction

Acronyms

a-set	Set of active DoF
ADPR	Average Driving Point Residue
AMKE	Average Modal Kinetic Energy
CMS	Component Mode Synthesis
DoF	Degree of Freedom
DPR	Driving Point Residue
ECP	Eigenvector Component Product
EfI	Effective Independence Distribution
EfI+	Effective Independence-Plus Distribution
EfI_3+	Triaxial Effective Independence Expansion
EfI_3	Triaxial Effective Independence-Plus Distribution
EMR	Exact Modal Reduction
FE	Finite Element
FEM	Finite-Element Model
FIM	Fisher Information Matrix
FRF	Frequency Response Function
GR	Guyan/Static Reduction
GUI	Graphical User Interface
ICMS	Iterated Component Mode Synthesis
ID	Intermediate Dimension
IRS	Improved Reduced System
KCMS	Krylov Component Mode Synthesis
KSM	Krylov Subspace Method

MAC	Modal Assurance Criterion
MKE	Modal Kinetic Energy
ModMAC	Modified Modal Assurance Criterion
MoGeSeC	Modal-Geometrical Selection Criterion
MOR	Model Order Reduction
MORPACK	Model Order Reduction Package
MR	Modal Reduction
NRFD	Normalized Relative Frequency Difference
o-set	Set of omitted DoF
POC	Pseudo-Orthogonality Check
RMS	Root Mean Square
RMS_{diag}	Root Mean Square of the principal diagonal of a modal correlation matrix
$RMS_{off\text{-}diag}$	Root Mean Square of the off-diagonal of a modal correlation matrix
SEREP	System Equivalent Reduction Expansion Process
SMR	Stiffness-to-Mass Ratio
SVD	Singular value decomposition
TAM	Test-Analysis-Model
WADPR	Weighted Average Driving Point Residue
WAMKE	Weighted Average Modal Kinetic Energy

Preface

Writing and finishing this thesis was a crazy adventure with many ups and downs. I would like to thank, first of all, my supervisor, Dipl.-Ing. Claudius Lein. It was an honor to work with the most organized person I have ever met and to be guided by his skills and wisdom – always having time for any kind of problems along the way. My next big thanks is directed to my fellow students – David Bernstein and André Müller – for joining this experience with me and being a great source of inspiration. May God bless you!
My next thank you goes to my parents who enabled me to have this experience by leaving their home country and starting a new life in Germany. Thank You!
My final thank you goes to my partner – Sarah Elizabeth Lewis – for looking after my health and keeping my body strong whilst my mind was too busy focusing on other subjects, and also for the constant supply with tea through some of too many longer nights. I love you!

Jan Paulke

1 Introduction

1.1 Motivation

Model Order Reduction (MOR) techniques are employed in various fields of engineering. In order to compare measured data from an experiment with an analytical finite element (FE) model, the measured mode shapes need to be expanded on to the dimension of the analytical information [50]. This expansion process is also able to reduce the set of equations so that the solution to the eigenvalue problem can be computed in a faster manner [16].
Another typical application of the MOR techniques is the on-orbit modal testing [23] which has an additional difficulty regarding the placement of sensors. Because it is not as easy to change the position once the structure is on orbit, an automated selection process is applied to find an optimal set of active positions [23].

However, it can occur that traditional MOR methods cannot produce a satisfactory solution due to the complexity of the analytical model. Accurate methods, on the other hand, are usually also very computationally intensive. This evokes the idea of combining two different MOR in a sequence to achieve the desired outcome [38]. A combination of reduction methods also presents the difficulty of selecting a suitable intermediate dimension (ID). An optimal ID can be obtained using the methods applied to find sets of sensors for an on orbit modal test.

1.2 Objectives

The objectives of this thesis are to find an optimal combination of MOR methods for a two-step approach as well as a selection of a suitable ID. Not only the size of the ID but also the quality of selected DoF are considered.

Through the study of automated selection methods, it has been observed that the selection of a good active set (*a-set*) can strongly influence the result of a MOR. Especially, modal subspace reduction methods benefit from an automated selection algorithm. Hence, one additional

submitted on 01.04.2014; revised edition from 07.07.2014

objective is to investigate the improvement potential of modal subspace reduction methods with the help of automated selection methods.

1.3 Outline of the Thesis

The thesis is structured in six chapters. Whilst the motivation and objectives are mentioned in the first chapter, the theoretical background can be found in the second chapter. There, the emphasis is placed on the individual MOR methods as well as their correlation.

Chapter three introduces several automated selection methods to find an optimal ID, and chapter four presents the requirements as well as recommendations towards its selection. Also, the investigation of possible combinations of MOR methods is considered in this chapter.

The implemented methods are tested on a gear box model in chapter five, and the results are summarized in chapter six.

2 Theoretical Background

This chapter is meant to create a foundation of which a two-step MOR can be developed and an optimal ID selected. Section 2.1 provides a very brief overview how the system matrices and the modal information is acquired because only then can a MOR be performed. The different MOR methods are explained in sections 2.3 to 2.6, and finally, several correlation methods are introduced in section 2.7.

2.1 Finite Element Method

One very popular tool for structural analysis is the FE method [38]. Since the focus of this thesis lies on the MOR, only a brief description is intended. Further details of the FE method can be found in [63] or [33].

The FE method considered in this thesis is based on three assumptions [38]. First, any non-linear elements are not considered for the formulation of the FE model. The second assumption is based on the description of linear material properties, and third, it is supposed to consider only small displacements. In order to develop a discrete formulation of a continuous body, the geometrical body is partitioned into FEs, and the the Ritz method as well as the weak form of the balance law is applied [10].
A system of N second-order differential equations is the result of the discretization process whereas the continuous description is based on partial differential equations [38]. Introducing a displacement vector $\boldsymbol{z}$ of the dimension $N \times 1$ which consists of the node displacements of the FEs, leads to the discrete equation of motion of the full system:

$$\boldsymbol{M}\ddot{\boldsymbol{z}} + \boldsymbol{C}\dot{\boldsymbol{z}} + \boldsymbol{K}\boldsymbol{z} = \boldsymbol{f} \tag{2.1}$$

where the system mass matrix is denoted by $\boldsymbol{M}$, and the damping and stiffness matrices are represent by $\boldsymbol{C}$ and $\boldsymbol{K}$, respectively. The displacement vector in physical space is expressed by $\boldsymbol{z}$. It is important to emphasize the meaning of the term *physical* to avoid any misconceptions [38]. In this thesis, the physical space is referred to as the three dimensional space with an orthonormal base. Although the dimension of the displacement vector $\boldsymbol{z}$ is $N \times 1$, it still

describes information in reference to the 3-D space. The information of other spaces, e.g. the modal space, cannot be interpreted in reference to the basis of the physical space.
The full system's velocity and acceleration vectors are represented by $\dot{\boldsymbol{z}}$ and $\ddot{\boldsymbol{z}}$, respectively, and the vector $\boldsymbol{f}$ describes the applied forces.

2.1.1 Modal Analysis

The modal analysis is applied to determine the characteristic behavior of an undamped system. For this case, the homogeneous equation of motion has to be solved

$$\boldsymbol{M}\ddot{\boldsymbol{z}} + \boldsymbol{K}\boldsymbol{z} = \boldsymbol{0} \tag{2.2}$$

where $\boldsymbol{0}$ represents the $N \times 1$ vector with all elements being equal to zero. The solution of equation (2.2) is a modal matrix $\boldsymbol{\Phi}$ containing the basis of the modal space as column vectors and the diagonal matrix of the eigenvalues $\boldsymbol{\Lambda}$ containing the system's eigenvalues ω^2. The modal matrix and eigenvalues have to solve the following equation

$$(\boldsymbol{K} - \omega_i^2 \boldsymbol{M})\boldsymbol{\Phi}_i = 0, \quad i = 1, 2, ..., N, \tag{2.3}$$

and a more detailed derivation of this equation can be found in ([33],[63]). Because the discrete system of large systems can have thousands of millions of DoF, solving equation (2.3) is not a trivial task. It is very time consuming and sometimes not even possible due to the limited memory.

The difficulty in solving equation (2.2) has caused the development of one of the first MOR methods – the Guyan Reduction (GR) [16]. Before we can move onto MOR methods, another characteristic property requires further explanation.

2.1.2 Frequency Response Function

The frequency response function (FRF) describes the response of system's output p to an excitation with a forcing frequency ω_f onto an input of the system q. For large systems, the FRF is computationally very intensive because it computes an inverse of the dynamic stiffness matrix $\boldsymbol{Z}(\omega_f)$ [45]

$$\boldsymbol{Z}(\omega_f) = (\omega_f^2 \boldsymbol{M} + \mathrm{i}\,\omega_f \boldsymbol{C} + \boldsymbol{K}) \tag{2.4}$$

where i is the imaginary unit. Since the inverse of the dynamical stiffness matrix $\boldsymbol{Z}(\omega_f)$ is not necessarily easy to compute, a different approach is used to calculate the full system's FRF. With the use of the mode shapes, the FRF can be calculated in the following

way

$$h_{pq} = \sum_{\mathrm{i}=1}^{m} \frac{\phi_{ip}\,\phi_{iq}}{-\omega^2 + \omega_f^2 + 2\mathrm{i}\,\zeta_f\,\omega\,\omega_f} \tag{2.5}$$

where ω is the undamped natural frequency of the i-th mode shape, the modal damping coefficient is referred to as ζ_f, the value of the i-th mode at the q-th input is ϕ_{ip}, and ϕ_{iq} expresses the value of the i-th mode shape at the p-th output location [12].
The response matrices can be arranged as elements of the FRF data matrix $\boldsymbol{H}$ which is a function of the dynamic stiffness matrix ($\boldsymbol{H} = \mathrm{f}(\boldsymbol{Z^{-1}})$). One correlation method compares the data matrices of the full system with a reduced representation in order to evaluate the quality of a MOR.

2.2 Model Order Reduction

The objective of a MOR is to be able to solve the equation of motion as presented in equation (2.1) with the help of a reduced representation so that the computation time can be saved. Hence, the full system needs to be partitioned into the active degree of freedom (DoF), which will also be referred to as the a-set, and the omitted DoF, also called the o-set. Equation (2.6) shows the result of such a partitioning

$$\begin{bmatrix} \boldsymbol{M_{aa}} & \boldsymbol{M_{ao}} \\ \boldsymbol{M_{oa}} & \boldsymbol{M_{oo}} \end{bmatrix} \begin{bmatrix} \ddot{\boldsymbol{z}}_{\boldsymbol{a}} \\ \ddot{\boldsymbol{z}}_{\boldsymbol{o}} \end{bmatrix} + \begin{bmatrix} \boldsymbol{K_{aa}} & \boldsymbol{K_{ao}} \\ \boldsymbol{K_{oa}} & \boldsymbol{K_{oo}} \end{bmatrix} \begin{bmatrix} \boldsymbol{z_a} \\ \boldsymbol{z_o} \end{bmatrix} = \begin{bmatrix} \boldsymbol{f_a} \\ \boldsymbol{f_o} \end{bmatrix} \quad . \tag{2.6}$$

In order to be able to map the solution of the reduced representation onto the full system, a linear transformation ([11] [2]) is applied

$$\boldsymbol{z} = \boldsymbol{T}\,\boldsymbol{z_a} \tag{2.7}$$

where $\boldsymbol{z_a}$ is the a-set partition displacement vector, and $\boldsymbol{T}$ is referred to as the transformation matrix. Substituting this relation into the undamped equation of motion results in an overdetermined system of linear equations where the number of unknowns is smaller than the number of equations

$$\boldsymbol{M\,T\,\ddot{z}_a} + \boldsymbol{K\,T\,z_a} = \boldsymbol{f_a} \quad . \tag{2.8}$$

This system of equations does not necessarily have a solution, and finding an approximation is achieved by multiplying equation (2.8) with the transpose of the transformation matrix

$$[\boldsymbol{T}]^{\mathrm{T}}\,\boldsymbol{M\,T\,\ddot{z}_a} + [\boldsymbol{T}]^{\mathrm{T}}\,\boldsymbol{K\,T\,z_a} = [\boldsymbol{T}]^{\mathrm{T}}\,\boldsymbol{f_a} \quad . \tag{2.9}$$

This creates the reduced system of equations where the reduced representations of the mass and stiffness matrices are computed in the following way:

$$\boldsymbol{M}_{\mathbf{red}} = [\boldsymbol{T}]^{\mathrm{T}}\,\boldsymbol{M}\,\boldsymbol{T} \qquad \boldsymbol{K}_{\mathrm{red}} = [\boldsymbol{T}]^{\mathrm{T}}\,\boldsymbol{K}\,\boldsymbol{T} \quad . \tag{2.10}$$

For correlation purposes, the solution of the partitioned homogeneous equation of motion

$$\begin{bmatrix} \boldsymbol{M_{aa}} & \boldsymbol{M_{ao}} \\ \boldsymbol{M_{oa}} & \boldsymbol{M_{oo}} \end{bmatrix} \begin{bmatrix} \ddot{\boldsymbol{z}}_a \\ \ddot{\boldsymbol{z}}_o \end{bmatrix} + \begin{bmatrix} \boldsymbol{K_{aa}} & \boldsymbol{K_{ao}} \\ \boldsymbol{K_{oa}} & \boldsymbol{K_{oo}} \end{bmatrix} \begin{bmatrix} \boldsymbol{z}_a \\ \boldsymbol{z}_o \end{bmatrix} = \begin{bmatrix} \boldsymbol{0} \\ \boldsymbol{0} \end{bmatrix} \tag{2.11}$$

is compared with the expanded results of the reduced eigenanalysis. Figure 2.1 demonstrates the discussed procedure. At first, a transformation matrix is established which in this case,

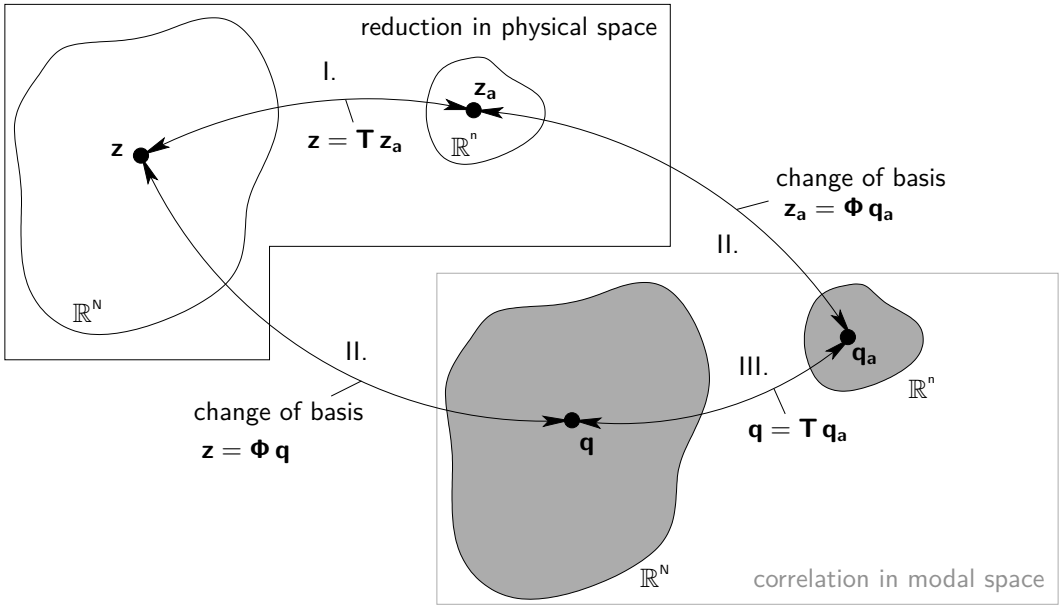

Figure 2.1: Typical Procedure of a Model Order Reduction and Correlation

occurs in the physical space. Then, the eigenanalysis of the reduced representation and the full system is solved. This is indicated by second step – the change of basis – in figure 2.1. During the next step, a comparison of modal information occurs by expanding the reduced modal matrix with the previously determined transformation matrix $\boldsymbol{T}$. If the expanded modal matrix shows a good correlation with the analytical modal matrix of the full system, it is expected that the mapping described by $\boldsymbol{T}$ will also satisfy the equation of motion as described in equation (2.1).

Depending on the subspace which the column vectors of the transformation matrix span, the MOR methods presented in this thesis can be classed into the physical subspace, the modal subspace, the Krylov subspace, and the hybrid subspace reduction methods, respectively. The meaning of a physical subspace is ambiguous, and has been defined in section 2.1 as

a space which information can be referred to the orthonormal basis of a 3-D space. Table 2.1 presents an overview of the MOR methods which are discussed in the following sections.

Table 2.1: Overview of MOR Methods Based on Subspace Spanned by the Transformation Matrix

Physical	Modal	Krylov	Hybrid
GR	MR	KSM	CMS
IRS	EMR		ICMS
	SEREP		Hybrid EMR

2.3 Physical Subspace Reduction Methods

The physical subspace MOR techniques are one of the first developed reduction methods. No modal information is required for the reduction process, however, their approximating nature not always satisfies the desired accuracy. One of the first developed and still commercially used techniques is the GR.

2.3.1 Guyan Reduction

The GR is one of the first model order reduction technique applied to create efficient eigensolutions of a dynamic system ([16], [46]). It is developed from a static analysis where the reduction of the stiffness matrix has been performed [16]. Guyan applied this principal onto the mass matrix to compute the eigenvalues and eigenvectors.
Within the static analysis, it is possible to remove the coordinates of the stiffness matrix where no forces are applied. This leads to the following expression

$$\begin{bmatrix} \boldsymbol{f_a} \\ \boldsymbol{f_o} \end{bmatrix} = \begin{bmatrix} \boldsymbol{K_{aa}} & \boldsymbol{K_{ao}} \\ \boldsymbol{K_{oa}} & \boldsymbol{K_{oo}} \end{bmatrix} \begin{bmatrix} \boldsymbol{z_a} \\ \boldsymbol{z_o} \end{bmatrix} \tag{2.12}$$

where – per definition – the omitted forces are equal to zero $\boldsymbol{f_o} = \boldsymbol{0}$ [16]. The second row of equation (2.12) describes the relationship between the a-set of displacement coordinates $\boldsymbol{z_a}$ and the o-set $\boldsymbol{z_o}$. This relationship allows a displacement mapping from the reduced

representation onto the full system's displacement vector

$$\boldsymbol{z} = \begin{bmatrix} \boldsymbol{I} \\ -\boldsymbol{K}_{oo}^{-1}\,\boldsymbol{K}_{oa} \end{bmatrix} \boldsymbol{z}_a = \begin{bmatrix} \boldsymbol{I} \\ \boldsymbol{D}_{\mathrm{GR}} \end{bmatrix} \boldsymbol{z}_a = \boldsymbol{T}_{\mathrm{GR}}\,\boldsymbol{z}_a \tag{2.13}$$

where $\boldsymbol{I}$ is an appropriately sized $(n \times n)$ unity matrix, and $\boldsymbol{T}_{\mathrm{GR}}$ is the transformation matrix of the GR. The mapping from the active displacement vector to the omitted displacements is performed by $\boldsymbol{D}_{\mathrm{GR}}$, and the reduced mass and stiffness matrices – $\boldsymbol{M}_{\mathrm{GR}}$, $\boldsymbol{K}_{\mathrm{GR}}$ – can now be calculated using equation (2.10). It is demonstrated in equation (2.14) that all elements of the full stiffness matrix contribute to the reduced representation [16]

$$\begin{aligned} \boldsymbol{K}_{\mathrm{GR}} &= \boldsymbol{K}_{aa} - \boldsymbol{K}_{ao}\,\boldsymbol{K}_{oo}^{-1}\,\boldsymbol{K}_{oa} \\ \boldsymbol{M}_{\mathrm{GR}} &= \boldsymbol{M}_{aa} - \boldsymbol{M}_{ao}\,\boldsymbol{K}_{oo}^{-1}\,\boldsymbol{K}_{oa} - (\boldsymbol{K}_{oo}^{-1}\,\boldsymbol{K}_{oa})^{\mathrm{T}}(\boldsymbol{M}_{oa} - \boldsymbol{M}_{oo}\,\boldsymbol{K}_{oo}^{-1}\,\boldsymbol{K}_{oa}) \end{aligned} \tag{2.14}$$

which causes no loss in the structural complexity. Since $\boldsymbol{M}_{\mathrm{GR}}$ consists of mass and stiffness element combinations, the eigensolutions are not exactly preserved [16]. The more influence the inertial forces have on the system's response, the worse the approximation of the GR. Another difficulty occurs in the selection of a good a-set because a poor selection will also create poor results [46]. If experience is not available, an automated selection method would become a very important asset.

To overcome the neglection of the inertial forces during the reduction process, O'Callahan has developed the Improved Reduced System (IRS) [46].

2.3.2 Improved Reduced System Method

The IRS has been developed to overcome the shortcomings of the GR which considers only the static forces in the reduced representation. This creates only a good approximation for a lower frequency range. Another problem is that the quality of the reduction highly depends on the choice of an a-set [46]. Hence, the IRS method includes the inertia forces into the transformation matrix [12], and it is also meant to be relatively insensitive to the choice of an a-set [46].
Just like in the GR, it starts with a static approximation of the omitted displacement vector, as presented in equation (2.12). This time, however, it is not assumed that $\boldsymbol{f}_o = \boldsymbol{0}$, and the formulation of $\boldsymbol{z}_o$ can be expressed as

$$\boldsymbol{z}_o = \boldsymbol{D}_{\mathrm{GR}}\,\boldsymbol{z}_a + \boldsymbol{K}_{oo}^{-1}\,\boldsymbol{f}_o \quad . \tag{2.15}$$

Now, the improved full displacement vector can be calculated using the following equation

$$\boldsymbol{z} = \begin{bmatrix} \boldsymbol{I} \\ \boldsymbol{D}_{\mathrm{GR}} \end{bmatrix} \boldsymbol{z_a} + \begin{bmatrix} \mathbf{0} & \mathbf{0} \\ \mathbf{0} & \boldsymbol{K}_{oo}^{-1} \end{bmatrix} \begin{bmatrix} \boldsymbol{f_a} \\ \boldsymbol{f_o} \end{bmatrix} = \boldsymbol{T}_{\mathrm{GR}}\, \boldsymbol{z_a} + \boldsymbol{S} \cdot \boldsymbol{f} \tag{2.16}$$

where the product $\boldsymbol{S} \cdot \boldsymbol{f}$ is the inertia force adjustment, and $\mathbf{0}$ is an appropriately sized matrix with all elements having the value of zero. O'Callahan proceeds further by explaining the expansion process of the GR-reduced displacement $\boldsymbol{z} = \boldsymbol{T}_{\mathrm{GR}}\, \boldsymbol{z_a}$, and that it can also be applied to the modal vectors of the reduced system

$$\boldsymbol{\Phi}_{\mathrm{exp}} = \boldsymbol{T}_{\mathrm{GR}}\, \boldsymbol{\Phi}_{\mathrm{GR}} \tag{2.17}$$

where $\boldsymbol{\Phi}_{\mathrm{exp}}$ denotes an expanded modal matrix; $\boldsymbol{\Phi}_{\mathrm{GR}}$ is a $(n \times n)$-dimensional matrix acquired using an eigenanalysis of the GR-reduced system. The expanded modal matrix $\boldsymbol{\Phi}_{\mathrm{exp}}$ has the same dimension as the modal matrix of the full system $\boldsymbol{\Phi}$ with the first n mode shapes $(N \times n)$. This expansion of $\boldsymbol{\Phi}_{\mathrm{GR}}$ lacks in the influence of the system's inertia forces because they are not included in the transformation matrix $\boldsymbol{T}_{\mathrm{GR}}$. An improved expansion of $\boldsymbol{\Phi}_{\mathrm{GR}}$ would be

$$\boldsymbol{\Phi}_{\mathrm{exp}} = \boldsymbol{T}_{\mathrm{GR}}\, \boldsymbol{\Phi}_{\mathrm{GR}} + \boldsymbol{S} \cdot \boldsymbol{f} \quad . \tag{2.18}$$

Here, the inertia force adjustment is meant to improve the expansion of the a-set in the modal domain. By finding an expression for $\boldsymbol{f}$ – in the modal domain – the transformation matrix would create an improved reduced system compared to the GR. Equation (2.19) shows the suggested formulation of the inertia force vector [46]

$$\boldsymbol{f} = \boldsymbol{K}\boldsymbol{T}_{\mathrm{GR}}\, \boldsymbol{\Phi}_{\mathrm{GR}} = \boldsymbol{M}\boldsymbol{T}_{\mathrm{GR}}\, \boldsymbol{\Phi}_{\mathrm{GR}}\, \boldsymbol{\Lambda}_{\mathrm{GR}} \tag{2.19}$$

where $\boldsymbol{\Lambda}_{\mathrm{GR}}$ is a diagonal matrix with reduced system's eigenvalues. Now, the improved expanded modal matrix can be computed

$$\boldsymbol{\Phi}_{\mathrm{exp}} = \boldsymbol{T}_{\mathrm{GR}}\, \boldsymbol{\Phi}_{\mathrm{GR}} + \boldsymbol{S} \cdot \boldsymbol{M}\, \boldsymbol{T}_{\mathrm{GR}}\, \boldsymbol{\Phi}_{\mathrm{GR}}\, \boldsymbol{\Lambda}_{\mathrm{GR}} \tag{2.20}$$

which includes an approximation of the inertia forces of the system. Using the information from an eigenanalysis of the reduced system

$$\boldsymbol{K}_{\mathrm{GR}}\, \boldsymbol{\Phi}_{\mathrm{GR}} = \boldsymbol{M}_{\mathrm{GR}}\, \boldsymbol{\Phi}_{\mathrm{GR}}\, \boldsymbol{\Lambda}_{\mathrm{GR}} \quad \Rightarrow \quad \boldsymbol{\Phi}_{\mathrm{GR}}\, \boldsymbol{\Lambda}_{\mathrm{GR}} = \boldsymbol{M}_{\mathrm{GR}}^{-1}\, \boldsymbol{K}_{\mathrm{GR}}\, \boldsymbol{\Phi}_{\mathrm{GR}} \quad , \tag{2.21}$$

leads to a transformation matrix which can create an improved approximation of the modal matrix expansion compared to the standard GR

$$\boldsymbol{\Phi}_{\mathrm{exp}} = \left(\boldsymbol{T}_{\mathrm{GR}} + \boldsymbol{S} \cdot \boldsymbol{M}\, \boldsymbol{T}_{\mathrm{GR}}\, \boldsymbol{M}_{\mathrm{GR}}^{-1}\, \boldsymbol{K}_{\mathrm{GR}} \right) \boldsymbol{\Phi}_{\mathrm{GR}} \quad . \tag{2.22}$$

It can also be applied to expand the active displacement vector $\boldsymbol{z_a}$ [46]. With the IRS transformation

$$\boldsymbol{z} = \begin{bmatrix} \boldsymbol{I} \\ \boldsymbol{D}_{\mathrm{GR}} + \boldsymbol{K}_{oo}^{-1}(\boldsymbol{M}_{oa} + \boldsymbol{M}_{oo}\boldsymbol{D}_{\mathrm{GR}})\boldsymbol{M}_{\mathrm{GR}}^{-1}\boldsymbol{K}_{\mathrm{GR}} \end{bmatrix} \boldsymbol{z_a} = \boldsymbol{T}_{\mathrm{IRS}}\,\boldsymbol{z_a} \quad , \tag{2.23}$$

the reduced mass and stiffness matrices – $\boldsymbol{M}_{\mathrm{IRS}}$ $\boldsymbol{K}_{\mathrm{IRS}}$ – can be calculated using equation (2.10). The IRS method creates the idea of a hybrid MOR because the relationships in the modal domain are being used to find an approximation of the inertia forces of the system. Since the transformation matrix consists only of information from the physical domain, it is classed as a physical subspace reduction.

It is said that not only the reduced stiffness matrix $\boldsymbol{K}_{\mathrm{IRS}}$ is stiffer than $\boldsymbol{K}_{\mathrm{GR}}$ but also the reduced mass matrix $\boldsymbol{M}_{\mathrm{IRS}}$ is less suitable for further orthogonality checks [12]. In order to improve the reduced results, Friswell *et al.* suggest an iterated IRS method ([12], [13]) which converges monotonically to the transformation matrix similar to the SEREP technique. However, the iteratively reduced system would include the rigid mode shapes, and if a certain mode is not observable through the a-set, it is neglected, and a different eigenvalue and mode shape is computed instead [12]. Whereas SEREP has the capability to exclude rigid modes and produces only a result if all mode shapes are observable. For the iterated IRS reduction, however, a poor choice of the a-set does cause a bad convergence rate [12].
Best results are achieved using the following equation

$$[\boldsymbol{T}_{\mathrm{IRS}}]_{i+1} = \boldsymbol{T}_{\mathrm{GR}} + \boldsymbol{S}\cdot\boldsymbol{M}\,\boldsymbol{T}_{\mathrm{GR}}\,[\boldsymbol{M}_{\mathrm{IRS}}^{-1}]_i\,[\boldsymbol{K}_{\mathrm{IRS}}]_i \quad . \tag{2.24}$$

which creates a better approximation than the GR as well as the standard IRS reduction.

2.4 Modal Subspace Reduction Methods

In the modal subspace reduction methods, a relationship between the o-set and the a-set is acquired by using information of the modal subspace. It is a very powerful reduction technique because it is able to precisely map the selected modal information within the frequency range of interest. However, the approximation outside of this range is poor compared to other reduction techniques.

2.4.1 Modal Reduction

The MR is a very easy and straight-forward method which maps the full system onto the modal subspace. Also called the second order modal truncation [35], it uses the full system's eigenvectors $\boldsymbol{\Phi}$ as the transformation matrix

$$\boldsymbol{T_{MR}} = \boldsymbol{\Phi} \quad . \tag{2.25}$$

The reduced representation is obtained by retaining only a certain amount of the mode shapes m, and the reduced mass $\boldsymbol{M_{MR}}$ and stiffness matrices $\boldsymbol{K_{MR}}$ can be calculated using equation (2.10).

Using modal subspace reduction techniques yield two difficulties. First, an eigenanalysis of the full system is required to calculate the eigenvectors within the frequency range of interest, which is very time-intensive for large models.
The second difficulty is the domain of the reduced representation. Because the reduced basis is within a modal subspace, it cannot be used as an ID for a two-step reduction. Also, a transformation onto the physical subspace of the reduced representation is not necessarily trivial. In order to avoid this transformation, Kammer has developed an EMR [21].

2.4.2 Exact Modal Reduction

The EMR is able to create a reduced representation where the dynamic information of the full system in a frequency range of interest is incorporated in the transformation matrix. Like the GR, the EMR is designed to reduce the order of the eigenvalue problem [21] of an undamped system as shown in equation (2.11). In order to find the relationship between the active and the omitted DoF, the modal expansion of the displacement vector is used [21]

$$\boldsymbol{z} = \boldsymbol{\Phi q} \tag{2.26}$$

where $\boldsymbol{q}$ is the $m \times 1$ displacement vector in modal coordinates, which size depends upon the number of retained mode shapes. Partitioning equation (2.26) creates an expression for the modal displacement vector

$$\boldsymbol{z} = \begin{bmatrix} \boldsymbol{z_a} \\ \boldsymbol{z_o} \end{bmatrix} = \begin{bmatrix} \boldsymbol{\Phi_a\, q} \\ \boldsymbol{\Phi_o\, q} \end{bmatrix} \quad \Rightarrow \quad \boldsymbol{q} = \boldsymbol{\Phi_a^g\, z_a} \tag{2.27}$$

where $\boldsymbol{\Phi}_{\boldsymbol{a}}^{\mathbf{g}}$ is the generalized inverse ([4], [56]) of the partition $\boldsymbol{\Phi}_{\boldsymbol{a}}$, which is also referred to as *Moore-Penrose pseudo-inverse* ([15], [32], [61], [42]). The generalized inverse $\boldsymbol{\Phi}_{\boldsymbol{a}}^{\mathbf{g}}$ has to fulfill four *Moore-Penrose conditions* [15]:

$$\begin{array}{llllll} (1) & \boldsymbol{\Phi}_{\boldsymbol{a}}\,\boldsymbol{\Phi}_{\boldsymbol{a}}^{\mathbf{g}}\,\boldsymbol{\Phi}_{\boldsymbol{a}} = \boldsymbol{\Phi}_{\boldsymbol{a}} & (3) & (\boldsymbol{\Phi}_{\boldsymbol{a}}\,\boldsymbol{\Phi}_{\boldsymbol{a}}^{\mathbf{g}})^{\mathrm{T}} = \boldsymbol{\Phi}_{\boldsymbol{a}}\,\boldsymbol{\Phi}_{\boldsymbol{a}}^{\mathbf{g}} \\ (2) & \boldsymbol{\Phi}_{\boldsymbol{a}}^{\mathbf{g}}\,\boldsymbol{\Phi}_{\boldsymbol{a}}\,\boldsymbol{\Phi}_{\boldsymbol{a}}^{\mathbf{g}} = \boldsymbol{\Phi}_{\boldsymbol{a}}^{\mathbf{g}} & (4) & (\boldsymbol{\Phi}_{\boldsymbol{a}}^{\mathbf{g}}\,\boldsymbol{\Phi}_{\boldsymbol{a}})^{\mathrm{T}} = \boldsymbol{\Phi}_{\boldsymbol{a}}^{\mathbf{g}}\,\boldsymbol{\Phi}_{\boldsymbol{a}} \end{array} \quad . \tag{2.28}$$

If the a-set partition $\boldsymbol{\Phi}_{\boldsymbol{a}}$ is of dimension $n \times m$, and the number of rows (n) is larger than the number of columns m, the generalized inverse $\boldsymbol{\Phi}_{\boldsymbol{a}}^{\mathbf{g}}$ can be expressed as [50]

$$\boldsymbol{\Phi}_{\boldsymbol{a}}^{\mathbf{g}} = ([\boldsymbol{\Phi}_{\boldsymbol{a}}]^{\mathrm{T}}\,\boldsymbol{\Phi}_{\boldsymbol{a}})^{-1}[\boldsymbol{\Phi}_{\boldsymbol{a}}]^{\mathrm{T}} \tag{2.29}$$

where the a-set partition $\boldsymbol{\Phi}_{\boldsymbol{a}}$ has to be of full-column rank, which is a minor limitation of this reduction method [21]. In the case of an equal number of rows and columns within the a-set of the modal matrix, the generalized inverse $\boldsymbol{\Phi}_{\boldsymbol{a}}^{\mathbf{g}}$ becomes the inverse of $\boldsymbol{\Phi}_{\boldsymbol{a}}$. The last variant where n is smaller than m is not relevant for reduction purposes because a system can only have as many different mode shapes as its number of DoF.

Having the expression of the modal displacement $\boldsymbol{q}$, a relationship between the a-set and the o-set can be established using equation (2.30)

$$\boldsymbol{z}_{\boldsymbol{o}} = \boldsymbol{\Phi}_{\boldsymbol{o}}\,\boldsymbol{\Phi}_{\boldsymbol{a}}^{\mathbf{g}}\,\boldsymbol{z}_{\boldsymbol{a}} \tag{2.30}$$

and substituting this relationship into equation (2.27) leads to

$$\boldsymbol{z} = \begin{bmatrix} \boldsymbol{z}_{\boldsymbol{a}} \\ \boldsymbol{z}_{\boldsymbol{o}} \end{bmatrix} = \begin{bmatrix} \boldsymbol{I} \\ \boldsymbol{\Phi}_{\boldsymbol{o}}\,\boldsymbol{\Phi}_{\boldsymbol{a}}^{\mathbf{g}} \end{bmatrix} \boldsymbol{z}_{\boldsymbol{a}} \tag{2.31}$$

where $\boldsymbol{I}$ would be the unity matrix of the dimension $n \times n$. This way, the transformation matrix of the EMR is defined as

$$\boldsymbol{T}_{\mathbf{EMR}} = \begin{bmatrix} \boldsymbol{I} \\ \boldsymbol{\Phi}_{\boldsymbol{o}}\,\boldsymbol{\Phi}_{\boldsymbol{a}}^{\mathbf{g}} \end{bmatrix} \quad , \tag{2.32}$$

and the reduced mass end stiffness matrices – $\boldsymbol{M}_{\mathbf{EMR}}$, $\boldsymbol{K}_{\mathbf{EMR}}$ – are being calculated using equation (2.10). Since the dynamic information of the full system is incorporated into the transformation matrix $\boldsymbol{T}_{\mathbf{EMR}}$, KAMMER states that this reduction method is an exact representation of the model's dynamic information over the frequency range spanned by the modal eigenvectors [21]. A minor limitation of the EMR is that the a-set partition of the modal matrix $\boldsymbol{\Phi}_{\boldsymbol{a}}$ has to be of full-column rank [21], which implies a difficulty in selecting active

DoF. If the initial a-set creates a rank deficient modal matrix partition, additional DoF would then have to be selected in order to fulfill the rank criterion.
Another important property of the transformation matrix $\boldsymbol{T}_{\text{EMR}}$ is that its rank will always be the number of the selected active DoF (n) [24]. This will ensure that the reduced mass and stiffness matrices are always positive definite which is not always the case for other reduction methods.

2.4.3 System Equivalent Reduction Expansion Process

The concept of SEREP was developed in 1986 by O'Callahan et al. as an Equivalent Reduction [52]. It was originally used as an efficient method of determining rotational DoF from analytical and experimental data. The reduction process is similar to the EMR in the way that both reduction methods preserve the dynamical information of the system within the selected frequency range of interest. Hence, both methods use the same partitioning as in equation (2.27). Once knowing the expression for the modal displacement vector $\boldsymbol{q}$, O'Callahan replaces it in the following way [50]:

$$\boldsymbol{z} = \begin{bmatrix} \boldsymbol{z_a} \\ \boldsymbol{z_o} \end{bmatrix} = \begin{bmatrix} \boldsymbol{\Phi_a}\, \boldsymbol{\Phi_a^{\mathrm{g}}} \\ \boldsymbol{\Phi_o}\, \boldsymbol{\Phi_a^{\mathrm{g}}} \end{bmatrix} \boldsymbol{z_a} \tag{2.33}$$

where the transformation matrix $\boldsymbol{T}_{\text{SEREP}}$ can also be expressed as

$$\boldsymbol{T}_{\text{SEREP}} = \begin{bmatrix} \boldsymbol{\Phi_a}\, \boldsymbol{\Phi_a^{\mathrm{g}}} \\ \boldsymbol{\Phi_o}\, \boldsymbol{\Phi_a^{\mathrm{g}}} \end{bmatrix} = \boldsymbol{\Phi} \boldsymbol{\Phi_a^{\mathrm{g}}} \quad . \tag{2.34}$$

Using this transformation matrix, creates a different representation of the reduced mass and stiffness matrices ($\boldsymbol{M}_{\text{SEREP}}$, $\boldsymbol{K}_{\text{SEREP}}$) compared to the EMR. If the full system's eigenvalues ω^2 are available, and the eigenvectors $\boldsymbol{\Phi}$ are scaled to unity mass, the reduction can be performed using only the generalized inverse $\boldsymbol{\Phi_a^{\mathrm{g}}}$:

$$\begin{aligned} \boldsymbol{M}_{\text{SEREP}} &= [\boldsymbol{T}_{\text{SEREP}}]^{\mathrm{T}}\, \boldsymbol{M}\, \boldsymbol{T}_{\text{SEREP}} = [\boldsymbol{\Phi_a^{\mathrm{g}}}]^{\mathrm{T}} [\boldsymbol{\Phi}]^{\mathrm{T}}\, \boldsymbol{M}\, \boldsymbol{\Phi} \boldsymbol{\Phi_a^{\mathrm{g}}} = [\boldsymbol{\Phi_a^{\mathrm{g}}}]^{\mathrm{T}} \boldsymbol{\Phi_a^{\mathrm{g}}} \\ \boldsymbol{K}_{\text{SEREP}} &= [\boldsymbol{T}_{\text{SEREP}}]^{\mathrm{T}}\, \boldsymbol{K}\, \boldsymbol{T}_{\text{SEREP}} = [\boldsymbol{\Phi_a^{\mathrm{g}}}]^{\mathrm{T}} [\boldsymbol{\Phi}]^{\mathrm{T}}\, \boldsymbol{K}\, \boldsymbol{\Phi} \boldsymbol{\Phi_a^{\mathrm{g}}} = [\boldsymbol{\Phi_a^{\mathrm{g}}}]^{\mathrm{T}} \boldsymbol{\Lambda}\, \boldsymbol{\Phi_a^{\mathrm{g}}} \end{aligned} \tag{2.35}$$

where $\boldsymbol{\Lambda}$ is a diagonal matrix with the eigenvalues ω^2 of the full model.
Using the transformation matrix $\boldsymbol{T}_{\text{SEREP}}$ to expand experimentally measured data will create a scaling or smoothing within the expanded full space domain [52], which is desirable due to errors in the experimental data or noise measurement [24]. No smoothing effect occurs when the number of targeted mode shapes m is equal to the number of active DoF n. For this case, the generalized inverse would become the inverse $\boldsymbol{\Phi_a}\, \boldsymbol{\Phi_a^{\mathrm{g}}} = \boldsymbol{I}$, and the transformation

matrices of SEREP and EMR would be identical. The selection of active DoF that fulfill this case is, however, not a trivial task, which creates a need for automated a-set selection methods.

Another major difference between both reduction techniques is the rank of the transformation matrix for the cases $n > m$ [24]. Using EMR produces a full-column rank transformation matrix as well as positive definite reduced mass and stiffness matrices. The transformation matrix $\boldsymbol{T}_{\text{SEREP}}$, however, is always only of rank m which causes rank deficient reduced representations. This is not desirable for further simulations. It may still lead to an exact reduction of the full system [46] if n is very close to m, but the exact condition of SEREP is only achieved when $n = m$ [50], which means that this reduction technique must always be used with caution [49].

2.5 Krylov Subspace Reduction Methods

Although the modal subspace reduction methods can preserve the dynamical information of the full model, it can only do so for the targeted mode shapes and frequencies, respectively. Since the response of the full system is characterized by the influence of all mode shapes, the modal subspace reduction methods would never be able to represent the FRF of the full system unless all major mode shapes are included in the transformation matrix. The Krylov-subspace-based method is an alternative technique that is not meant to preserve the mode shapes of the full system. It is designed to approximate the response of the full system which is a combination of all its eigenvectors. This way it implicitly can find and preserve the mode shapes with the largest influence on the FRF within the frequency range of interest.
The notation of the equations will be slightly different to the literature in order to show certain similarities between the MR and the KSM.

Just like the modal domain is spanned by the column vectors of the modal matrix, the Krylov subspace is spanned by column vectors which will be referred to as the *Krylov modes* $\boldsymbol{\Phi}_{\boldsymbol{\mathcal{K}}}$ in this thesis. In order to reduce an undamped equation of motion, the Krylov modes have to be recursively calculated in the following way ([35],[60]):

$$\boldsymbol{\Phi}_{\boldsymbol{\mathcal{K}}} = \left[\boldsymbol{K}^{-1}\boldsymbol{f},\ \left(\boldsymbol{K}^{-1}\boldsymbol{M}\right)\boldsymbol{K}^{-1}\boldsymbol{f},\ \ldots\ ,\ \left(\boldsymbol{K}^{-1}\boldsymbol{M}\right)^{(m_{\mathcal{K}}-1)}\boldsymbol{K}^{-1}\boldsymbol{f}\right] \tag{2.36}$$

where the first vector $\boldsymbol{K}^{-1}\boldsymbol{f}$ is called the starting vector, and the total number of Krylov modes is expressed by $m_{\mathcal{K}}$. The choice of a good starting vector is important for the quality

of the reduced representation. An interesting case occurs during the reduction of the eigenvalue problem as presented in equation (2.11). Because no forces are applied, the starting vector is not fully defined, which means that the KSM computes a different reduced representation for different starting vectors.
The transformation matrix of the KSM is computed similar to the MR in the following way:

$$\boldsymbol{T}_{\text{KSM}} = \boldsymbol{\Phi}_{\mathcal{K}} \quad , \tag{2.37}$$

and the reduced representations of the mass and stiffness matrices in the Krylov subspace are expressed using equation (2.38)

$$\boldsymbol{M}_{\text{KSM}} = [\boldsymbol{T}_{\text{KSM}}]^{\text{T}}\, \boldsymbol{M}\, \boldsymbol{T}_{\text{KSM}} \qquad \boldsymbol{K}_{\text{KSM}} = [\boldsymbol{T}_{\text{KSM}}]^{\text{T}}\, \boldsymbol{M}\, \boldsymbol{T}_{\text{KSM}} \quad . \tag{2.38}$$

In this way, the reduction method is called a one-sided KSM [59]. The two-sided reduction method computes a second Krylov subspace and replaces it with the transposed transformation matrix $[\boldsymbol{T}_{\text{KSM}}]^{\text{T}}$ in equation (2.38).
Computing the Krylov modes according to equation (2.36) tends to create an almost linear dependent transformation matrix [59] which is not recommended for numerical applications. However, there are other methods to compute better Krylov modes, and one of the most popular algorithms is the Arnoldi algorithm.
The Arnoldi algorithm constructs in a simple recursive manner an orthogonal basis of the Krylov subspace ([35], [37]). Because of this, it produces very stable, fast results.
Another major advantage of the KSM is that no selection of an a-set is required because the Krylov subspace is not expressed with physical coordinates. This also means that there is no way to express the reduced representation with physical coordinates, which is sometimes necessary. So the advantage is at the same time a disadvantage depending on the purpose of a model order reduction. An attempt to create a reduced KSM representation in physical coordinates has been made by Koutsovasilis introducing a back-projection approach [34]. This method creates only an approximate of the reduced representation because certain information within the transformation matrix are being neglected during the back-projection.
However, any attempt to create a reduced representation in physical coordinates would require a selection of an a-set which creates the need for an automated DoF selection method.

2.6 Hybrid Subspace Reduction Methods

The hybrid approach is sometimes mistaken with a two-step reduction technique. In order to avoid any misunderstandings, the definition of the hybrid subspace reduction method will be

briefly outlined in this section.
The similarity to a two-step approach is the existence of two transformation matrices – $\boldsymbol{T_1}$ and $\boldsymbol{T_2}$. A hybrid approach, however, uses two different transformation matrices during a one-step reduction, whilst the two-step approach reduces two times, as the name implies. Figure 2.2 illustrates this difference using one possible two-step combination.

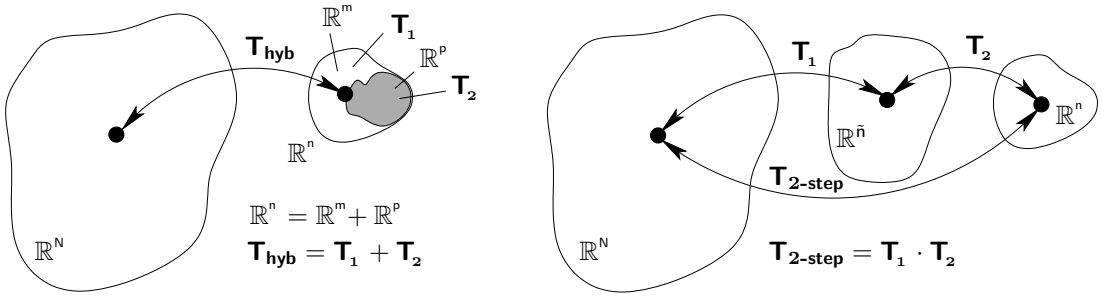

Figure 2.2: Comparison of a Hybrid Reduction (left) and a Two-Step Reduction (right)

The hybrid transformation matrix is computed as a superposition of the two matrices

$$\boldsymbol{T}_{\mathbf{hyb}} = \boldsymbol{T_1} + \boldsymbol{T_2} \tag{2.39}$$

where $\boldsymbol{T}_{\mathbf{hyb}}$ represents the transformation matrix of a hybrid reduction. During a two-step approach, the second transformation matrix $\boldsymbol{T_2}$ depends upon the solution of the first step, and the two-step transformation matrix $\boldsymbol{T}_{\mathbf{2\text{-}step}}$ is computed by a product, as shown in the following equation

$$\boldsymbol{T}_{\mathbf{2\text{-}step}} = \boldsymbol{T_1} \cdot \boldsymbol{T_2} \quad . \tag{2.40}$$

For the hybrid reduction, it is mandatory that the transformation matrices $\boldsymbol{T_1}$ and $\boldsymbol{T_2}$ span two different subspaces, whereas a two-step reduction does not require this restriction. One of the most known hybrid reduction techniques is the CMS.

2.6.1 Component Mode Synthesis

The CMS is a technique mainly designed for substructure coupling purposes [8] which can be a major advantage for large systems. By separating the large model into substructures and creating reduced representations of the substructures, the computation time can drastically be reduced compared to a reduction approach on a full model. After the reduction process, the reduced representations are assembled by synthesizing the modes into a reduced representation of the full model ([19], [26]).
Several different CMS reduction techniques exist ([9], [41], [58]), and they differ mainly by the treatment of the system's normal modes. The normal modes are the eigenvectors of

the substructure. Every substructure usually consists of boundaries (interfaces) to adjacent substructures. One method is to calculate the normal modes for fixed-interfaces [9], which means that the substructure is constraint at its boundaries. The free-interface approach ([41],[58]) uses the mode shapes of an unconstrained substructure.
In order to augment the information of the normal modes, each method uses a different set of modes to account for the static solution. For the fixed-interface approach, constraint modes are being applied, and for the free-interface technique, two different types of modes can be used. Either a set of attachment modes for a constrained model defined by BAMFORD [18] or the inertia relief modes for a free model defined by RUBIN [58] are normally used.
The CMS methods attempt, like the other reduction techniques, to reduce the size of the undamped equation of motion, which is expressed in equation (2.41)

$$\begin{bmatrix} \boldsymbol{M_{aa}} & \boldsymbol{M_{ao}} \\ \boldsymbol{M_{oa}} & \boldsymbol{M_{oo}} \end{bmatrix} \begin{bmatrix} \ddot{\boldsymbol{z}}_{\boldsymbol{a}} \\ \ddot{\boldsymbol{z}}_{\boldsymbol{o}} \end{bmatrix} + \begin{bmatrix} \boldsymbol{K_{aa}} & \boldsymbol{K_{ao}} \\ \boldsymbol{K_{oa}} & \boldsymbol{K_{oo}} \end{bmatrix} \begin{bmatrix} \boldsymbol{z_a} \\ \boldsymbol{z_o} \end{bmatrix} = \begin{bmatrix} \boldsymbol{f_a} \\ \boldsymbol{f_o} \end{bmatrix} \tag{2.41}$$

where the subscript o denotes the omitted set of DoF, which is also referred to as the interior coordinates [9], and the subscript a represents the a-set, also known as the boundary coordinates, which are shared with the adjacent substructures. Hence, the selection of a good a-set does not occur during the CMS reduction. Per definition, the interior DoF are all force free, which means that $\boldsymbol{f_o} = \boldsymbol{0}$. The normal modes are used to approximate the responses of all interior DoF. Therefore, the CMS technique is similar to a modal subspace reduction method because the corresponding part of the transformation matrix spans a modal subspace.
The fixed-interface approach solves the omitted eigenvalue problem

$$(\boldsymbol{K_{oo}} - \omega^2 \boldsymbol{M_{oo}})\boldsymbol{\Phi_o} = \boldsymbol{0} \quad , \tag{2.42}$$

which means that the fixed-interface normal modes, also called the Craig-Bampton modes, have the following expression:

$$\boldsymbol{\Phi_{CB}} = \begin{bmatrix} \boldsymbol{0} \\ \boldsymbol{\Phi_o} \end{bmatrix} \quad . \tag{2.43}$$

The free-interface approach, on the other hand, solves the eigenvalue problem of the full substructure

$$(\boldsymbol{K} - \omega^2 \boldsymbol{M})\boldsymbol{\Phi} = \boldsymbol{0} \quad . \tag{2.44}$$

The effect of the substructure's normal modes is augmented by introducing a second set of modes. For the case of the fixed-interface approach, the constraint modes are used, which are defined as a static response of the substructure due to a unit displacement of one of the active DoF while the rest of the a-set is restrained, and the o-set is force-free [8]. The constraint modes are a static response of the substructure and can be calculated from the

static equation

$$\boldsymbol{K}\boldsymbol{\Psi}^{\boldsymbol{c}} = \boldsymbol{f} \quad \Rightarrow \quad \begin{bmatrix} \boldsymbol{K_{aa}} & \boldsymbol{K_{ao}} \\ \boldsymbol{K_{oa}} & \boldsymbol{K_{oo}} \end{bmatrix} \begin{bmatrix} \boldsymbol{I} \\ \boldsymbol{\Psi_o^c} \end{bmatrix} = \begin{bmatrix} \boldsymbol{f_a} \\ \boldsymbol{0} \end{bmatrix} \quad . \tag{2.45}$$

The second row of equation (2.45) yields the expression of the partition of the fixed-interface constraint modes $\boldsymbol{\Psi_o^c}$, and the following equation shows the definition of the full constraint modes $\boldsymbol{\Psi^c}$:

$$\boldsymbol{\Psi^c} = \begin{bmatrix} \boldsymbol{I} \\ \boldsymbol{\Psi_o^c} \end{bmatrix} = \begin{bmatrix} \boldsymbol{I} \\ -\boldsymbol{K_{oo}^{-1}}\,\boldsymbol{K_{oa}} \end{bmatrix} \quad . \tag{2.46}$$

Since the constraint modes are a static response of the substructure, it is not surprising that it is the same transformation matrix as in the GR. This also means that every other variant of possible constraint modes has to be able to solve the static problem. Introducing the IRS reduction as a replacement of the constraint modes [35] may improve the approximation of higher frequencies of the substructure, however, it will not be able to create a complete solution of the static problem, which the constraint modes should be able to solve.
The transformation matrix of the fixed-interface approach would have the form

$$\boldsymbol{z} = \begin{bmatrix} \boldsymbol{z_a} \\ \boldsymbol{z_o} \end{bmatrix} = \begin{bmatrix} \boldsymbol{I} & \boldsymbol{0} \\ \boldsymbol{\Psi_o^c} & \boldsymbol{\Phi_o} \end{bmatrix} \begin{bmatrix} \boldsymbol{z_a} \\ \boldsymbol{q_o} \end{bmatrix} = \boldsymbol{T_{CB}}\,\boldsymbol{q_{CB}} \quad , \tag{2.47}$$

and the reduced representations of the system matrices are being calculated using equation (2.10). Another alternative for the fixed-interface approach is using block Krylov modes instead of the normal modes [19]. This procedure tends to create very good results and will be referred to as the Krylov Component Mode Synthesis (KCMS) method according to [35].

The free-interface approach is not able to use the constraint modes and relies on the use of the so called attachment modes. The attachment modes are defined as a static response to a unit force applied on one of the active coordinates [8]. However, since the substructure is unrestrained, a rigid body movement would occur. The solution would be either to mathematically exclude the rigid body movement or to calculate the so called inertia relief modes defined by Rubin [58]. Either way, the calculation of the residual flexibility matrix $\boldsymbol{G^\rho}$ is achieved, and the attachment modes can be expressed as columns of the partitioned residual flexibility matrix:

$$\boldsymbol{\Psi^{at}} = \begin{bmatrix} \boldsymbol{G_{aa}^\rho} \\ \boldsymbol{G_{oa}^\rho} \end{bmatrix} \quad . \tag{2.48}$$

Further details on the derivation of the residual flexibility matrix $\boldsymbol{G^\rho}$ are shown in [58], [44]. The transformation matrix for the free-interface method is expressed

as

$$\boldsymbol{z} = \begin{bmatrix} \boldsymbol{z_a} \\ \boldsymbol{z_o} \end{bmatrix} = \begin{bmatrix} \boldsymbol{G^{\rho}_{aa}} & \boldsymbol{\Phi_a} \\ \boldsymbol{G^{\rho}_{oa}} & \boldsymbol{\Phi_o} \end{bmatrix} \begin{bmatrix} \boldsymbol{q_a} \\ \boldsymbol{q_o} \end{bmatrix} \quad . \tag{2.49}$$

However, this transformation would make an assembly of substructures not as convenient compared to the fixed-interface method. Martinez et. al suggest to replace the active modal displacement $\boldsymbol{q_a}$ with the physical active displacement $\boldsymbol{z_a}$ using the first row of equation (2.49) [44]. This would lead to the final expression of the free-interface transformation matrix which is also derived by Rubin:

$$\boldsymbol{z} = \begin{bmatrix} \boldsymbol{z_a} \\ \boldsymbol{z_o} \end{bmatrix} = \begin{bmatrix} \boldsymbol{I} & \boldsymbol{0} \\ \boldsymbol{G^{\rho}_{oa}}\,[\boldsymbol{G^{\rho}_{aa}}]^{-1} & \boldsymbol{\Phi_o} - \boldsymbol{G^{\rho}_{oa}}\,[\boldsymbol{G^{\rho}_{aa}}]^{-1}\,\boldsymbol{\Phi_a} \end{bmatrix} \begin{bmatrix} \boldsymbol{z_a} \\ \boldsymbol{q_o} \end{bmatrix} = \boldsymbol{T_{CMS}}\,\boldsymbol{q_{CMS}} \tag{2.50}$$

The free-interface mass and stiffness matrices can now be formulated using equation (2.10). There are certain advantages of the free-interface CMS reduction over the fixed-interface method [58]. One is that the modal testing could be done on each substructure, and it is easier to create the boundary conditions of the free-interface method during experimental measurements. Another advantages is that the reduction of one component is independent of the adjacent components according to Hintz [18].

2.6.2 Hybrid Exact Modal Reduction

It has been observed that the EMR-reduced mass matrix produces in some cases larger off-diagonal terms in orthogonality checks than the less accurate GR-reduced representation ([22],[24]). Kammer assumes that the reason for this discrepancy is due to a bad representation of the residual modes, where the target modes would be referred to as the mode shapes of interest used in an EMR, and the residual modes would be the eigenvectors excluded from the reduction. Because the GR-reduced mass matrix would in many cases produce a better approximation of the residual modes (although the approximation of the targeted modes would be worse), Kammer developed a hybrid reduction method which combines the preservation of the target modes with the EMR and introduces a better approximation of the residual modes with a GR at the same time. The reduced mass and stiffness matrices will be referred to as matrices of a hybrid EMR.
In order to create the hybrid EMR, a projection method is applied using an oblique projector $\boldsymbol{P}_{\text{obl}}$ [22]. The first step is to introduce an additional partitioning of the full displacement vector $\boldsymbol{z}$ as

$$\boldsymbol{z} = \boldsymbol{z}_{\text{tm}} + \boldsymbol{z}_{\text{rm}} \tag{2.51}$$

where $\boldsymbol{z}_{\mathrm{tm}}$ represents the displacement vector of the target modes, and $\boldsymbol{z}_{\mathrm{rm}}$ is the displacement partition representing the residual modes of the full system. A projector $\boldsymbol{P}$ is used to separate the contribution of the EMR towards the target mode displacement and the GR towards the residual modes.
The idempotency is the requirement for any matrix to be classed as a projector [4] which means that the following expression has to be valid for every projection matrix $\boldsymbol{P^2} = \boldsymbol{P}$. This implies that every projector has to be a square matrix. If a projector is additionally a symmetric matrix ($[\boldsymbol{P}]^{\mathrm{T}} = \boldsymbol{P}$), it is referred to as an orthogonal projector $\boldsymbol{P}_{\mathrm{orth}}$, otherwise it is called an oblique projector $\boldsymbol{P}_{\mathrm{obl}}$ [4].
The oblique projector is used to project the displacement representing the influence of the target modes $\boldsymbol{z}_{\mathrm{tm}}$ onto the subspace spanned by the a-set partitioning of the target mode shapes $\boldsymbol{\Phi_a}$. This way, the displacement would only contribute to the reduced system's dynamics represented by the target modes. On the other hand, the displacement vector $\boldsymbol{z}_{\mathrm{rm}}$ is projected onto the null space of $\boldsymbol{\Phi_a}$ and would only contribute to the dynamics characterized by the residual modes. The transformation matrix of the hybrid EMR is expressed as [22]

$$\boldsymbol{T}_{\mathrm{hyb}} = \boldsymbol{T}_{\mathrm{GR}} + (\boldsymbol{T}_{\mathrm{EMR}} - \boldsymbol{T}_{\mathrm{GR}})\boldsymbol{P}_{\mathrm{obl}} \tag{2.52}$$

where the oblique projector $\boldsymbol{P}_{\mathrm{obl}}$ is defined as

$$\boldsymbol{P}_{\mathrm{obl}} = \boldsymbol{\Phi_a}\,[\boldsymbol{\Phi_a}]^{\mathrm{T}}\,\boldsymbol{M}_{\mathrm{EMR}} \quad . \tag{2.53}$$

Here, $\boldsymbol{\Phi_a}$ is the a-set partitioned with the target mode shapes of interest, and $\boldsymbol{M}_{\mathrm{EMR}}$ is the EMR-reduced mass matrix. The reduced mass and stiffness matrices would be calculated in the usual way as expressed in equation (2.10). A reduced system computed with the hybrid transformation matrix $\boldsymbol{T}_{\mathrm{hyb}}$ will preserve all dynamical information within the frequency range of the target modes, and the residual modes will additionally be approximated using the GR. This leads to a better orthogonality and cross-orthogonality performance compared with the EMR or the GR [22].
Mains suggests that it is also possible to use the SEREP and IRS reduction methods, instead [43]. Another possibility is to exchange the oblique projector with an orthogonal projector

$$\boldsymbol{P}_{\mathrm{orth}} = \boldsymbol{\Phi_a}\,\boldsymbol{\Phi}_{\boldsymbol{a}}^{\mathbf{g}} \tag{2.54}$$

which would create seven additional transformation matrices on top of Kammer's hybrid EMR [43]. In this thesis, however, only the original formulation is considered.

2.7 Model Correlation Methods

The assessment of the reduced representation is a crucial step in MOR. The techniques used in this thesis are developed from a need to correlate experimentally obtained data with an analytical finite element model ([1], [27], [3]). While a comparison of the eigenvectors creates some difficulties, it is very easy and straight forward to compare the eigenvalues of the full an reduced system.

2.7.1 Normalized Relative Frequency Difference

Since the frequencies can be compared directly, one very common way to compare them is to calculate the NRFD vector. In the literature, it is usually calculated in the following way [35]:

$$f_{\mathrm{NRFD}}(i) = \frac{|f_{\mathrm{full}}(i) - f_{\mathrm{red}}(i)|}{f_{\mathrm{full}}(i)}, \quad i = 1, 2, ..., n. \tag{2.55}$$

Figure 2.3 shows an example of a typical NRFD plot. It is important to point out that the

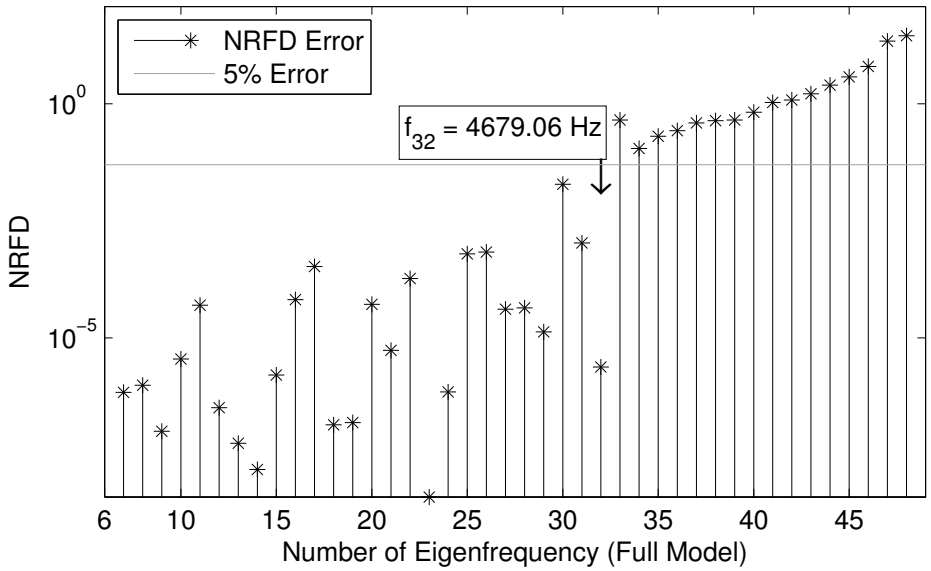

Figure 2.3: Normalized Relative Frequency Difference with Error Limit at 5%

rigid body modes are excluded from all correlations. Hence, the first compared frequency is the 7-th eigenfrequency of the full system. Within Fig. 2.3, the value of the highest frequency below the error limit of 5% can also be observed. This error limit is typically used during model validation and correlation procedures [27]. However, for the purposes of this thesis, the error limit is set to 1% which is valid only for the NRFD.

2.7.2 Modified Modal Assurance Criterion

The Modal Assurance Criterion (MAC) was developed to be able to correlate experimental modal vectors from a measured frequency response function [1]. This was especially needed if a mass matrix, derived from a finite element model, was not available. There are, however, situations in which a MAC may show a correlation between vectors which are actually linear independent [3]. This could be the case when either the modal vectors are incompletely determined or the sensors could not be placed on internal components of the test structure.
In order to gain more insight into the orthogonality of mode shapes, the ModMAC has been developed, also referred to as a weighted modal analysis criterion [1].

The calculation of the ModMAC always occurs at the full model dimension, which means that the reduced modal vectors would have to be expanded using the transformation matrix $\boldsymbol{T}$. Equation (2.56) shows the definition of the ModMAC for real valued modal vectors

$$\mathbf{ModMAC} = \frac{([\boldsymbol{\Phi}]^{\mathrm{T}}\boldsymbol{M}\,\boldsymbol{T}\boldsymbol{\Phi}_{\mathbf{red}})^2}{([\boldsymbol{\Phi}]^{\mathrm{T}}\boldsymbol{M}\,\boldsymbol{\Phi})([\boldsymbol{T}\boldsymbol{\Phi}_{\mathbf{red}}]^{\mathrm{T}}\boldsymbol{M}\,\boldsymbol{T}\boldsymbol{\Phi}_{\mathbf{red}})} \tag{2.56}$$

where $\boldsymbol{\Phi}_{\mathbf{red}}$ is the modal matrix acquired from an eigenanalysis of the reduced system. For complex valued modal vectors, the transpose has to become a conjugate transpose [1]. The values of the principal diagonal of the ModMAC matrix indicate the correlation of the compared mode shapes. A value of 1.0 indicates a perfect correlation, it is usually acceptable to interpret an error of 5% as still accurate. The industry standard uses a value between 0.9 and 1.1 on the principal diagonal and a value less then 0.1 on the off-diagonal terms [43]. Figure 2.4 shows an example of a possible ModMAC plot which will be used throughout this thesis. It can be seen from the figure how many mode shapes correlate within the set error limit of 5%, as well as the Root Mean Square (RMS) values. A low RMS of the off-diagonal terms indicates orthogonality of the modal vectors, and a high value of the diagonal terms indicates a good correlation of the mode shapes.

2.7.3 Pseudo-Orthogonality Check

There are four different possible POC which all can be used either at the full dimension or at the reduced level ([3], [47], [48]). In this thesis, the approach at the reduced model dimension is used. For this case, the POC is calculated as follows:

$$\boldsymbol{POC} = [\boldsymbol{\Phi}_{\mathbf{red}}]^{\mathrm{T}}\boldsymbol{M}_{\mathbf{red}}\,\boldsymbol{\Phi}_{\boldsymbol{a}} \tag{2.57}$$

$$\boldsymbol{M}_{\mathbf{red}} = [\boldsymbol{\Phi}_{\boldsymbol{a}}^{\mathbf{g}}]^{\mathrm{T}}\boldsymbol{\Phi}_{\boldsymbol{a}}^{\mathbf{g}} \quad . \tag{2.58}$$

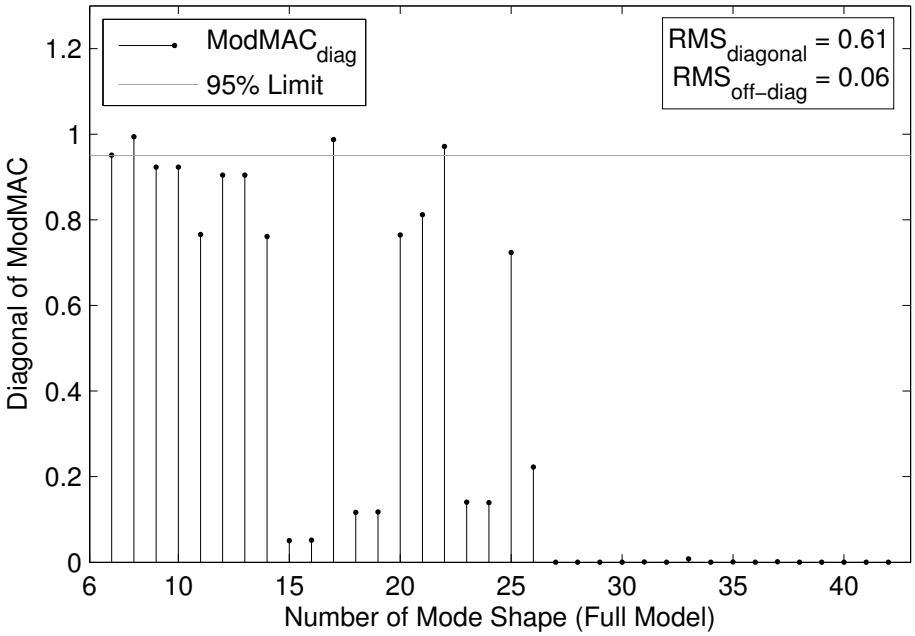

Figure 2.4: ModMAC with RMS values of the diagonal and off-diagonal terms

The a-set partition of the full modal matrix has to be normalized to the reduced mass. It is also important to note that the POC will only compute representative results when the number of active DoF n is equal to the number of retained modes m. For every other case, the POC information is not representative and will not be considered. The plot would be similar to the ModMAC in figure 2.4. For the determination of a good a-set, however, only the RMS values of the principal diagonal and off-diagonal elements are sufficient.

2.7.4 Comparison of Frequency Response Function

The comparison of the FRF occurs by employing a modified $\mathcal{H}_2$-norm which is computed in the following way [10]:

$$\|\boldsymbol{H}\|^2_{\mathcal{H}_2^i} = \frac{1}{2\pi}\int_{f_{\min}}^{f_{\max}} \|\boldsymbol{H}(2\pi f)\|_{\mathrm{F}}\ df \quad . \tag{2.59}$$

The $\mathcal{H}_2$-norm allows the computation of a value which indicates the similarity of the FRF. This value is called the $\mathcal{H}_2$ error and its calculation is expressed in the following equation:

$$\varepsilon^{\mathrm{rel}}_{\mathcal{H}_2}(f) = \frac{\|\boldsymbol{H}(i2\pi f) - \bar{\boldsymbol{H}}(i2\pi f)\|_{\mathcal{H}_2}}{\|\boldsymbol{H}(i2\pi f)\|_{\mathcal{H}_2}}, \quad f \in [f_{\min}, f_{\max}] \quad . \tag{2.60}$$

The $\mathcal{H}_2$ error can be understood as a relative difference by comparing the area between two FRF and relating it to the area under the original system. Simply put, the smaller the $\mathcal{H}_2$

error the better the approximation of the full system's response by the reduced representation.

This concludes the introduction of the MOR methods and some of the possible correlation criteria applied to evaluate the quality of the reduced representation. The next chapter is presenting the automated selection methods for an optimal ID computation which, in turn, is necessary for a successful two-step MOR.

3 Selection of Active Degrees of Freedom

Every outcome of a MOR depends more or less on the selection of the a-set. Good approximations result only if the selected a-set is able to preserve the main information of the full system, and in the case of a two-step MOR, the automated selection methods can be crucial by finding an optimal ID. Due to their importance for a successful MOR, section 3.1 until 3.3 present some of many DoF selection techniques which are investigated in this thesis. The last section (3.4) discusses some methods to evaluate the quality of the selected a-set and their applicability for practical applications.

Several techniques exist to produce an optimal or near optimal a-set, and table 3.1 gives an overview of the methods discussed in this thesis. The selection techniques have been

Table 3.1: Overview of Selection Methods

Non-Iterative	**Iterative Reduction**	**Iterative Expansion**
DPR	EfI	MoGeSeC
ADPR	EfI_3	EfI+
WADPR	mass-weighted EfI	EfI_3+
ECP	mass-weighted EfI_3	mass-weighted EfI+
MKE	SVD-Based	mass-weighted EfI_3+
AMKE	Variance-Based	
WAMKE	SMR-Based	

organized, based on their selection process, into the non-iterative and the iterative selections, respectively. The iterative selection can be achieved in two ways. One is by reducing the size of the candidate set of DoF until the desired a-set is found, which is referred to as the iterative reduction method. The second approach produces a selection in the opposite direction by finding the best candidate and including it into the existing a-set. Because the a-set is expanding with every selected DoF, this type of selection techniques will be referred to as the iterative expansion methods.

3.1 Non-Iterative Methods

The non-iterative selection methods are very appealing due to their fast computation. The procedure of the selection can be seen in figure 3.1. A case of a typical two-step MOR is described,

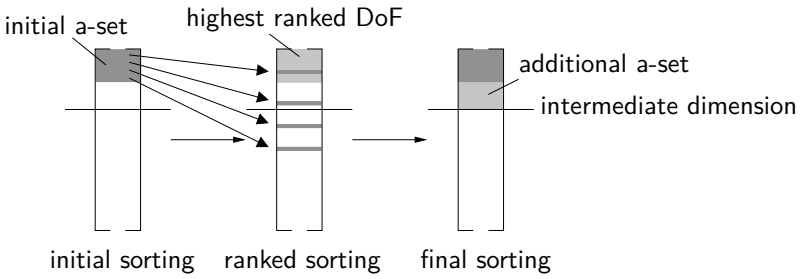

Figure 3.1: Non-Iterative Selection Procedure

where additional DoF are needed for the desired ID. The size of the ID is known, and the aim is to find additional optimal or near optimal active DoF. The selection occurs in two stages. First, all DoF are ranked based on their contribution to a certain criterion. Second, the initial a-set is re-grouped, and additional DoF are selected based on their ranking from step one until the desired size of the ID – or any other criterion – is achieved.

3.1.1 Modal Kinetic Energy and Variants

According to Papadopoulos, Modal Kinetic Energy (MKE) is a visual inspection technique, where a plot for each target mode is used to select the DoF with the largest modal energy over all target modes [53]. This way, the choice of active DoF with the highest kinetic energy is supposed to create the maximum observability of the targeted mode shapes [36]. Kammer uses this approach as a pre-conditioning of the candidate set for his EfI technique, discussed in section 3.2.1 [23].
The following equation presents the calculation of the modal kinetic energy ([53], [6]):

$$\mathbf{MKE} = \mathbf{\Phi}_{\mathbf{tm}} \otimes (\boldsymbol{M}\, \mathbf{\Phi}_{\mathbf{tm}}) \tag{3.1}$$

where $\otimes$ denotes a term-by-term matrix multiplication, and $\mathbf{\Phi}_{\mathbf{tm}}$ describes the target modes in the frequency range of interest. The sum of all elements in one column of the MKE matrix is equal to the value one if the target modes are normalized to unit mass [23].

Average MKE

The Average Modal Kinetic Energy (AMKE) takes the average across the rows of the MKE matrix. Assuming that the number of selected target modes is m, the AMKE can be expressed as

$$\boldsymbol{a}_{\mathbf{MKE}} = \frac{1}{m}\,\mathbf{MKE}\cdot\mathbf{1} \tag{3.2}$$

where $\mathbf{1}$ is a $m \times 1$ vector with each element being equal to one, and $\mathbf{MKE}$ is the result of equation (3.1). Now, the zero motion DoF are being taken into account, which is not the case during the normal MKE procedure [53]. Also, the calculation of the AMKE is meant to be more automatic compared to the standard MKE.

Weighted AMKE

Chung suggests to use the Weighted Average Modal Kinetic Energy (WAMKE) in order to account for the DoF with zero modal kinetic energy [6]. The calculation requires the knowledge of the AMKE vector and the MKE matrix of the system. Equation (3.3) describes the calculation of the WAMKE

$$\boldsymbol{w}_{\mathbf{AMKE}} = \boldsymbol{m}_{\mathbf{min}} \otimes \boldsymbol{a}_{\mathbf{MKE}} \tag{3.3}$$

where $\boldsymbol{m}_{\mathbf{min}}$ is the minimum absolute value across the rows of the MKE matrix [53].

3.1.2 Driving Point Residue and Variants

In a very similar fashion, the Driving Point Residue (DPR) is calculated using equation (3.4)

$$\mathbf{DPR} = \boldsymbol{\Phi}_{\mathbf{tm}} \otimes (\boldsymbol{\Phi}_{\mathbf{tm}}\,\boldsymbol{\Lambda}_{\mathbf{tm}}) \tag{3.4}$$

where $\boldsymbol{\Lambda}_{\mathbf{tm}}$ is the diagonal matrix containing the system eigenvalues associated with the target modes. The selection of the a-set follows the same procedure as the MKE technique. Although Papadopoulos uses the target frequencies, the calculations have been performed using the eigenvalues as mentioned in [36]. There is a limiting factor to both methods since they preclude the placement of sensors at zero motion nodal points ([36], [53]). In order to overcome this problem, the Average Driving Point Residue (ADPR) can be used.

Average DPR

The ADPR is calculated in the same way as the AMKE by computing an average value across the rows of the DPR matrix:

$$\boldsymbol{a}_{\mathbf{DPR}} = \frac{1}{m}\,\mathbf{DPR}\cdot\mathbf{1} \quad . \tag{3.5}$$

Weighted DPR

Consequently, it is possible to calculate the Weighted Average Driving Point Residue (WADPR)

$$\boldsymbol{w}_{\mathbf{ADPR}} = \boldsymbol{d}_{\mathbf{min}} \otimes \boldsymbol{a}_{\mathbf{DPR}} \tag{3.6}$$

where $\boldsymbol{d}_{\mathbf{min}}$ is the minimum in absolute values across the rows of the DPR matrix.

3.1.3 Eigenvector Component Product

The final non-iterative approach presented in this thesis is the Eigenvector Component Product (ECP) which is using only the modal matrix to determine the best location for an active DoF [36]. First, a frequency range of interest is selected with the corresponding target modes $\boldsymbol{\Phi}_{\mathbf{tm}}$. Then, a term-by-term product over all columns of the modal matrix containing only the target modes is calculated [20]. Equation (3.7) demonstrates the computation

$$\boldsymbol{\phi}_{\mathbf{ECP}} = \boldsymbol{\phi}_{\mathbf{1}} \otimes \boldsymbol{\phi}_{\mathbf{2}} \otimes ... \otimes \boldsymbol{\phi}_{\boldsymbol{m}} \tag{3.7}$$

where $\boldsymbol{\phi}_{\boldsymbol{m}}$ denotes the m-th target mode shape, and $\otimes$ is the element-by-element product of the eigenvectors. Just like the MKE and DPR approach, the ECP does not take the zero motion nodes into account [36]. Should this be a problem in any case, Larson et al. suggest to use an absolute value eigenvector sum over the target mode shapes. In both cases, the highest value of the component product – or the sum – would indicate a good sensor location.

The non-iterative approaches are less time consuming compared to the iterative methods, however, it is said that they only produce good results for the GR [29]. Better a-sets for a modal subspace reduction are achieved using the iterative reduction methods.

3.2 Iterative Reduction Methods

The major advantage of iterative reduction methods is their precision. However, it comes with a computational effort. Figure 3.2 demonstrates the selection procedure for a typical two-step MOR application. In order to find additional DoF for an optimal ID, the iterative

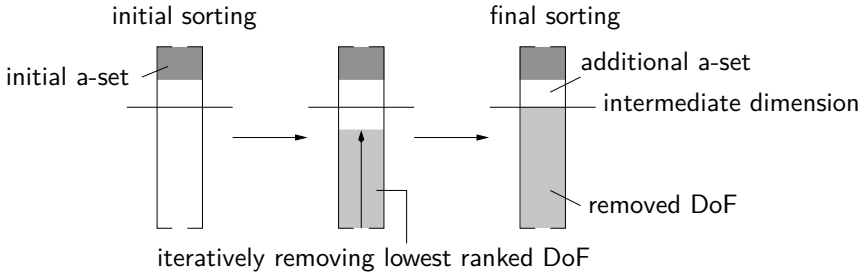

Figure 3.2: Iterative Reduction Methods Procedure

reduction methods rank the candidate set based on a certain criterion. The lowest ranked DoF is removed from the candidate set which is re-ranked after the update. In order to achieve the desired precision, it is mandatory to remove only one DoF per iteration [23] which makes this type of a selection very slow – especially for larger models.

3.2.1 Effective Independence Distribution

One of the most promising iterative reduction methods for selecting the appropriate a-set is Kammer's EfI [23]. In his formulation, he adopts the viewpoint of a structural dynamicist who uses experimental data to validate a finite element model. This means that his main priority is on finding an optimal set of sensors (a-set) on the structure to be able to measure the desired mode shapes. It implies that the information obtained by each sensor has to be as linear independent as possible where every sensor location is represented by the DoF of the model. Because it is an iterative selection of the a-set, Kammer views the selected locations as a sub-optimal selection since it highly depends on the number of deleted DoF during every iterated step.

Due to the computational effort of this method, the first step is a pre-selection of a smaller candidate set. For this step, the MKE method is used. There is no statement as to how big the initial set can be. Smaller models should produce no difficulties in using all DoF for the iteration. However, computing an a-set for bigger models is very time intensive which makes a pre-selection necessary.
After selecting a candidate set, the Fisher information matrix (FIM) $\boldsymbol{A}_{\mathbf{FIM}}$ is formulated as

$$\boldsymbol{A}_{\mathbf{FIM}} = [\boldsymbol{\Phi}_s]^{\mathrm{T}} \boldsymbol{\Phi}_s \tag{3.8}$$

where the pre-conditioned, smaller candidate set of the target mode shapes is described by $\boldsymbol{\Phi_s}$. Maximizing the norm of the FIM will minimize the covariance matrix of the estimate errors [23] as well as maximizing the retained independent information.
In order to obtain the contribution of each DoF to the linear independence of the candidate set $\boldsymbol{\Phi_s}$, the eigenvalues and eigenvectors of the FIM have to be computed. With the results of the eigenanalysis, the following relationship is valid

$$[\boldsymbol{\Psi}]^{\mathrm{T}} \boldsymbol{A_{\mathrm{FIM}}} \boldsymbol{\Psi} = \boldsymbol{\lambda} \quad \Rightarrow \quad \boldsymbol{A_{\mathrm{FIM}}^{-1}} = \boldsymbol{\Psi} \boldsymbol{\lambda}^{-1} [\boldsymbol{\Psi}]^{\mathrm{T}} \tag{3.9}$$

where $\boldsymbol{\Psi}$ represents the eigenvectors and $\boldsymbol{\lambda}$ the corresponding eigenvalues of the FIM, respectively. Now, the EfI can be calculated with the following expression ([30],[40])

$$\boldsymbol{e_D} = (\boldsymbol{\Phi_s} \boldsymbol{\Psi}) \otimes (\boldsymbol{\Phi_s} \boldsymbol{\Psi}) \boldsymbol{\lambda}^{-1} \cdot \mathbf{1} \tag{3.10}$$

where $\otimes$ denotes a term-by-term product, and $\mathbf{1}$ is an appropriately sized column vector with all entries being equal to one. The resulting vector $\boldsymbol{e_D}$ shows the contribution of each DoF to the eigenvalues of FIM and consequently, to the linear independence of the mode shapes $\boldsymbol{\Phi_s}$.
Kammer also suggests an alternative formulation of the EfI. The same vector $\boldsymbol{e_D}$ can be obtained by taking the diagonal entries of

$$\boldsymbol{e} = \boldsymbol{\Phi_s} \boldsymbol{\Psi} \boldsymbol{\lambda}^{-1} [\boldsymbol{\Psi}]^{\mathrm{T}} [\boldsymbol{\Phi_s}]^{\mathrm{T}} \quad , \tag{3.11}$$

and according to equation (3.9), it can be written as

$$\boldsymbol{e} = \boldsymbol{\Phi_s} \boldsymbol{A_{\mathrm{FIM}}^{-1}} [\boldsymbol{\Phi_s}]^{\mathrm{T}} \quad . \tag{3.12}$$

This means that the EfI distribution can be calculated without using the eigenvectors and eigenvalues as expressed in the following equation:

$$\boldsymbol{e} = diag \left(\boldsymbol{\Phi_s} \left([\boldsymbol{\Phi_s}]^{\mathrm{T}} \boldsymbol{\Phi_s} \right)^{-1} [\boldsymbol{\Phi_s}]^{\mathrm{T}} \right) \quad . \tag{3.13}$$

For systems with a very large number of DoF, the alternative calculation becomes much slower compared to the expression in equation (3.10). Since only a small amount of target modes is selected, the FIM is always of a relatively small dimension, and the computation of the eigenvalues and eigenvectors occurs much faster than the multiplication of very large matrices as expressed in equation (3.13). Hence, the former expression with the effective independence distribution vector $\boldsymbol{e_D}$ is used throughout this thesis.

Best results would be achieved by deleting only one DoF per iteration. However, it is also possible to delete up to 10% with no loss of accuracy according to Poston [57].
A second question appears considering different purposes of EfI's applications. Kammer was

interested to find an optimal set of sensor locations to validate an analytical model with experimental data. Which means that there were almost no restrictions towards the sensor locations other than the reachability of each position.
In this thesis, however, it is also possible to have an initial a-set which has to be retained for further simulations. Hence, the deletion of the lowest ranked DoF from the candidate set always affects DoF not belonging to an initial a-set. It is, therefore, important to include a sufficient amount of DoF into the final a-set so that all important locations can be preserved. This would have to be the case for an optimal ID for a two-step MOR.

Triaxial Effective Independence

One limitation of the EfI algorithm is that it only considers every DoF individually. A problem could occur if the use of triaxial sensors for modal vibration tests is required [29]. The same issue happens when further structural analyses of the reduced representation are considered. In both cases, the engineer has to select nodes rather than DoF, which means that a ranking based on nodes is necessary. Since the EfI distribution produces a ranking based on individual DoF, it can create results that are not required. Although an optimum selection occurs for the suggested DoF, it cannot be guaranteed that it would still be an optimal selection in regards to the corresponding nodes. Hence, Kammer and Tinker have improved the standard EfI approach to select an optimal set of nodes instead of DoF. The ranking is applied only for translational DoF, but this method can be adapted to use the rotational DoF as well [29].
The triaxial effective independence distribution vector $\boldsymbol{e_{D_3}}$ can be calculated with the following expression:

$$[\boldsymbol{e_{D_3}}]_i = 1 - det(\boldsymbol{I} - [\boldsymbol{\Phi_3}]_i \boldsymbol{A_{\mathrm{FIM}}} [\boldsymbol{\Phi_3}]_i^{\mathrm{T}}) \tag{3.14}$$

where $\boldsymbol{\Phi_3}$ is the partition of the modal matrix corresponding to one node with three DoF. The 3×3 unity matrix $\boldsymbol{I}$ is in this selection technique always of this size, and the FIM $\boldsymbol{A_{\mathrm{FIM}}}$ is calculated using equation (3.15)

$$\boldsymbol{A_{\mathrm{FIM}}} = \sum_{i=1}^{N_n} [\boldsymbol{\Phi_3}]_i^{\mathrm{T}} [\boldsymbol{\Phi_3}]_i \quad . \tag{3.15}$$

where the total number of nodes is represented by N_n.
Further details on the derivation of the triaxial effective independence (EfI_3) distribution can be found in ([29],[25]). The calculated distribution vector $\boldsymbol{e_{D_3}}$ contains values between zero and one [29]. In a similar way as the original EfI approach, this vector can be sorted and the lowest value deleted from further calculation. Through this iterative procedure where one node is meant to be deleted per iteration, a near optimum set of nodes with translational DoF can be obtained which maximize the determinant of the FIM [25].

3.2.2 Mass-Weighted Effective Independence

There are other variants of the EfI method in the literature considering a mass weighting of the EfI distribution. They usually differ in the way the mass matrix is decomposed, but there are also different ways to reduce the mass matrix during the selection of an optimal a-set.

Square Root GR-Reduced Mass-Weighted EfI

Garvey et al. [14] suggest a mass weighting method where the mass matrix $\boldsymbol{M}$ is expressed as a product of its square root:

$$\boldsymbol{M} = [\boldsymbol{M}]^{0.5}\,[\boldsymbol{M}]^{0.5} \quad . \tag{3.16}$$

Substituting equation (3.16) into the alternative formulation of EfI in equation (3.13) leads to the mass-weighted formulation of the EfI distribution

$$\boldsymbol{e}_{\mathbf{rmw}} = diag\left([\boldsymbol{M}]^{0.5}\,\boldsymbol{\Phi}\,\left([\boldsymbol{\Phi}]^{\mathrm{T}}\,\boldsymbol{M}\,\boldsymbol{\Phi}\right)^{-1}[\boldsymbol{\Phi}]^{\mathrm{T}}\,[\boldsymbol{M}]^{0.5}\right) \quad . \tag{3.17}$$

This can also be achieved using the other formulation of EfI as presented in equation (3.10). It is further suggested [14] that the system mass and stiffness matrices are being reduced using the GR. This approach is very computationally intensive, especially the calculation of the square root of the mass matrix. It is supposed, however, to produce a better a-set than the original EfI method for the GR [28].

Cholesky-Decomposed GR-Reduced Mass-Weighted EfI

Using a similar idea, Coote presents in [7] a mass-weighted formulation of the EfI method without using the square root of the mass matrix. Instead, a Cholesky decomposition

$$\boldsymbol{M} = \boldsymbol{L}[\boldsymbol{L}]^{\mathrm{T}} \quad , \tag{3.18}$$

with $\boldsymbol{L}$ being the lower triangular matrix, is used. In order to make the selection process faster, the rows and columns of the mass and stiffness matrices are deleted. This, however, does not account for a changing mass distribution for every deleted DoF. Hence, it should naturally produce worse results compared to the GR-reduced approach.
The Cholesky-decomposed mass-weighted EfI distribution is expressed in equation (3.19)

$$\boldsymbol{e}_{\mathbf{cmw}} = diag\left([\boldsymbol{L}]^{\mathrm{T}}\,\boldsymbol{\Phi}\,\left([\boldsymbol{\Phi}]^{\mathrm{T}}\,\boldsymbol{M}\,\boldsymbol{\Phi}\right)^{-1}[\boldsymbol{\Phi}]^{\mathrm{T}}\,\boldsymbol{L}\right) \quad . \tag{3.19}$$

Especially for lager models, the Cholesky decomposition as well as the simple deletion of rows and columns within the system matrices create a reasonably fast selection method. However, the speed could not match the original EfI approach.

Cholesky-Decomposed EMR-Reduced Mass-Weighted EfI

A faster and better approach for selecting an optimal a-set could also be achieved by using not only the Cholesky decomposition but also the EMR instead of the slower GR. This idea is also presented in combination with the iterative expansion methods in section 3.3.
Instead of reducing both the stiffness and mass matrices, it is now necessary to only reduce the mass matrix.

$$\boldsymbol{e}_{\mathbf{cemw}} = diag\left([\boldsymbol{L}_{\mathbf{EMR}}]^{\mathrm{T}}\boldsymbol{\Phi}\ ([\boldsymbol{\Phi}]^{\mathrm{T}}\boldsymbol{M}_{\mathbf{EMR}}\ \boldsymbol{\Phi})^{-1}[\boldsymbol{\Phi}]^{\mathrm{T}}\boldsymbol{L}_{\mathbf{EMR}}\right) \tag{3.20}$$

where $\boldsymbol{L}_{\mathbf{EMR}}$ denotes the lower triangular matrix of the EMR-reduced mass matrix $\boldsymbol{M}_{\mathbf{EMR}}$ after a Cholesky decomposition.

3.2.3 Variance Based Selection Method

Another method similar to Kammer's EfI is presented in [62]. Tasker and Liu use not the determinant of the FIM but its trace. Hence, the variance-based selection method focuses on maximizing the trace of the FIM which is also closely related to the linear independence of the column vectors of the modal matrix $\boldsymbol{\Phi}$ [62].
The FIM is being calculated in a similar fashion as in the EfI distribution

$$\boldsymbol{A}_{\mathbf{FIM}} = [\boldsymbol{\Phi}]^{\mathrm{T}}\boldsymbol{\Phi} \tag{3.21}$$

where $\boldsymbol{\Phi}$ is not a pre-conditioned smaller candidate set but the full modal matrix with N DoF and m mode shapes. According to Tasker, a deletion of the i-th sensor causes an increase of the new trace of the covariance matrix $\boldsymbol{A}_{\mathbf{FIM}}^{-\mathbf{1}}$. The increase of the variance $\Delta_i\sigma^2$ can be expressed as [62]

$$\Delta_i\sigma^2 = \frac{[\boldsymbol{\Phi}\boldsymbol{\Phi}^{\mathrm{T}}]^{\mathrm{g}}_{ii}}{[\boldsymbol{I} - \boldsymbol{\Phi}\boldsymbol{\Phi}^{\mathbf{g}}]_{ii}} \tag{3.22}$$

where $\boldsymbol{I}$ is an appropriately sized identity matrix, and the superscript g denotes the generalized inverse of the matrix.
The sorting procedure is similar to the EfI method. For every iteration step, the DoF with the smallest increase in variance $\Delta_i\sigma^2$ are deleted. Hence, the best results appear by deleting only one DoF per iteration.
It is stated [62] that the variance-based selection method performs a better selection than EfI if the minimization of the increase in variance is the main criterion. For the purpose of this

thesis, however, this may not necessarily be the case. According to Tasker and Liu, it is important to retain the DoF with a value of $\Delta_i\sigma^2 = 1$ which might cause problems if the initial a-set has a small $\Delta_i\sigma^2$ value. In this case, a DoF could be deleted which normally would have been retained. This should, however, not cause any difficulties in finding an optimal ID for a two-step MOR due to the larger size of the ID.

3.2.4 Singular Value Decomposition Based Selection Method

The SVD-based approach, introduced by Park [54], is a very similar method to the EfI distribution [53]. Instead of using the modal matrix itself, a SVD decomposition is applied in the following way:

$$\boldsymbol{\Phi} = \boldsymbol{U}\boldsymbol{\Sigma}[\boldsymbol{V}]^{\mathrm{T}} \tag{3.23}$$

where $\boldsymbol{U}$ is the matrix containing the left-singular vectors, and $\boldsymbol{V}$ denotes the right-singular vectors of the modal matrix $\boldsymbol{\Phi}$. The diagonal matrix $\boldsymbol{\Sigma}$ is representing the singular values of the system. Using only the left-singular vectors $\boldsymbol{U}$, a contribution of every DoF to the determinant of the FIM is evaluated using equation (3.24)

$$\boldsymbol{r}_{\mathbf{SVD}} = diag(\boldsymbol{U}[\boldsymbol{U}]^{\mathrm{T}}) \quad . \tag{3.24}$$

Within the vector $\boldsymbol{r}_{\mathbf{SVD}}$ is the contribution of each DoF to the determinant of the FIM. Hence, a high value within $\boldsymbol{r}_{\mathbf{SVD}}$ is retained whilst the DoF with a low value can be deleted [53]. In a similar fashion as the EfI method, the final a-set is selected in an iterative manner.

For all of the so far mentioned iterative methods, modal information is required in order to automatically choose the best DoF. This usually creates a bias selection towards modal reduction methods as the spatial independence of mode shapes is emphasized during the selection procedure. The following iterative selection method is using the system matrices by evaluating the SMR to select the best possible active DoF.

3.2.5 Stiffness-to-Mass Ratio Selection Method

Another approach for an automated selection of active DoF is to use the reduction techniques themselves in order to create the final a-set. Penny et al. show the effects of using the GR as a selection method ([55], [53]). Instead of using modal information, as it is the case for all of the previously introduced selection techniques, the criterion proposed by Henshell is being

evaluated to select the next omitted DoF [17]. For every iteration step, the stiffness-to-mass ratio of the diagonal entries is calculated

$$\boldsymbol{r}_{\mathrm{SMR}} = \frac{[\boldsymbol{K}]_{ii}}{[\boldsymbol{M}]_{ii}} \quad , \tag{3.25}$$

and the DoF with the highest value in $\boldsymbol{r}_{\mathrm{SMR}}$ is reduced out of the mass and stiffness matrices using the GR. This implies that a good selected a-set has to include every DoF with a high inertia so that most of the systems mass is preserved in the reduced model [55].
Rather than calculating the ratio once, the aim is to compute a SMR at each iteration step to take the changes of the deletion of a DoF into account. Although it is suggested to delete only one DoF at a time, the algorithm also includes the possibility to remove more than one DoF per iteration step. This might, however, lead to a removal of an active DoF that would otherwise be retained.

The reduction of the omitted DoF during every iteration step is very time intensive. This is especially the case for larger models. Another difficulty is the structure of the reduced representation matrices since they are fully populated. In order to achieve a faster selection, a simple deletion of rows and columns of the system matrices is applied.

3.3 Iterative Expansion Methods

The iterative expansion methods are a compromise between the fast computation of the non-iterative selection techniques and the precision of the iterative reduction methods. Figure 3.3 demonstrates a selection procedure for an optimal ID. Instead of removing DoF due to little

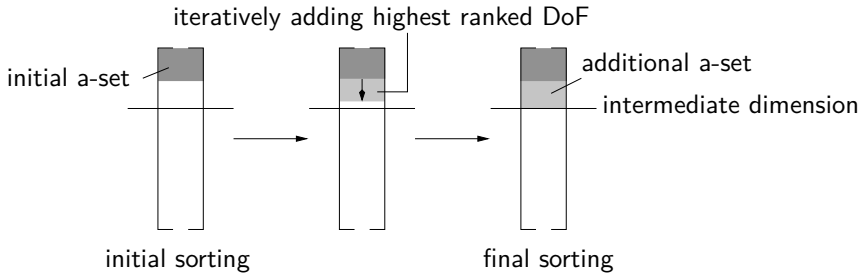

Figure 3.3: Iterative Expansion Methods Procedure

contribution, the iterative expansion methods select the best candidate from the candidate set that has the highest ranking towards a certain criterion. Because the selection occurs in the opposite direction, the computation time is much lower compared to the other iterative

approach. The faster computation comes with a lower precision which might not be acceptable in some cases.

3.3.1 Modal-Geometrical Selection Criterion

The modal-geometrical selection criterion (MoGeSeC) is based on evaluating a weight function vector $\boldsymbol{w}$ [5]. The calculation of the weight function vector contains not only a modal weighting but also a spatial weighting as is demonstrated in the following equation

$$\boldsymbol{w} = diag(\boldsymbol{w_g}[\boldsymbol{w_m}]^{\mathrm{T}}) \tag{3.26}$$

where the geometrical vector $\boldsymbol{w_g}$ and the modal vector $\boldsymbol{w_m}$ have to be calculated for each individual node. The calculation can also be found in [5], and assuming that the weighting vector is computed for a node p and evaluated with previously selected r nodes leads to the following expressions of the geometrical and modal vectors

$$\begin{aligned} w_{g,p} &= \frac{1}{max(\boldsymbol{w_g})} \cdot 1 \Big/ \sum_{i=1}^{r} \left[\frac{1}{(x_p - x_i)^2 + (y_p - y_i)^2 + (z_p - z_i)^2} \right]^{k_1} \\ w_{m,p} &= \frac{1}{max(\boldsymbol{w_m})} \sum_{j=1}^{m} \left[\left(\phi_{p,x}^{(j)}\right)^2 + \left(\phi_{p,y}^{(j)}\right)^2 + \left(\phi_{p,z}^{(j)}\right)^2 \right]^{k_2} \end{aligned} \tag{3.27}$$

where (x, y, z) are the grid coordinates of the nodes, and the normalized mode shapes are represented by $(\phi_{p,x}^{(j)}, \phi_{p,y}^{(j)}, \phi_{p,z}^{(j)})$. The weighting parameters k_1, k_2 are set according to the recommendation to the value of two and one, respectively [5]. The sum of the modal weighting vector uses all target modes m within the frequency range of interest.

The advantage of MoGeSeC is the consideration of nodes rather than individual DoF. By including a physical weighting vector, it also considers spacial independence of the selected a-set. The evaluation of two separate criteria is, on the other hand, very time intensive for larger models.

3.3.2 Triaxial Effective Independence Expansion

The triaxial effective independence expansion ($\mathrm{EfI_3}^+$) is introduced by Kammer in [25]. The purpose is also to find an optimal set of sensor locations for a modal vibration test bast on a ranking of nodes and not individual DoF. The drawback of the precise $\mathrm{EfI_3}$ reduction method is its computationally intensive selection because only one node has to be deleted per iteration [25].

The EfI_3+ algorithm computes in a faster manner the desired a-set because instead of removing nodes with a bad contribution to the observability of the target modes, it selects the best candidate and expands the initial a-set. Since many less nodes have to be added compared to the removal of all other nodes within the candidate set, the EfI_3+ still can produce a solution which maximizes the determinant of the FIM in a much faster computation time compared to the iterative reduction method EfI_3.

By maximizing the determinant of the FIM, it also renders the a-set partition of the modal matrix linearly independent which is a requirement for a successful modal subspace reduction. The FIM is computed as presented in equation (3.8), and depending on the rank of the FIM, two different cases have to be considered.

Case I – Regular Fisher Information Matrix

The simplest case occurs when the FIM is of full rank, which is the case when the initial a-set renders the target modes linearly independent [25]. The first step is the computation of the initial FIM

$$\boldsymbol{A}_{\mathbf{FIM}}^{\mathbf{ini}} = [\boldsymbol{\phi}_{\boldsymbol{a}}^{\mathbf{ini}}]^{\mathrm{T}}\, \boldsymbol{\phi}_{\boldsymbol{a}}^{\mathbf{ini}} \tag{3.28}$$

where the superscript *ini* denotes the initial a-set partition of the modal matrix which creates the initial FIM, as well. The contribution of every node towards maximizing the determinant of the FIM can be evaluated using the following equation

$$[EfI_3+]_i = det(\boldsymbol{I} + \boldsymbol{\phi}_{\mathbf{3i}}[\boldsymbol{A}_{\mathbf{FIM}}^{\mathbf{ini}}]^{-1}\,[\boldsymbol{\phi}_{\mathbf{3i}}]^{\mathrm{T}}) - 1 \tag{3.29}$$

where the (3×3) unity matrix is denoted by $\boldsymbol{I}$, and the partition of the modal matrix of the i-th node is expressed by $\boldsymbol{\phi}_{\mathbf{3i}}$. The EfI_3+ value can be computed for every node of the full system, and the highest ranked node is added to the initial a-set [25]. This procedure is repeated until the desired size of the a-set is achieved.

Case II – Singular Fisher Information Matrix

This is the most common but also most difficult case where the initial a-set does not create a linearly independent partition of the modal matrix. Since the initial Fisher Information Matrix is singular, it contains eigenvalues of zero value, the eigenvectors corresponding to these values are denoted as $\boldsymbol{\psi}_{\mathbf{0}}$. In order to get the best candidate, the FIM of the full candidate set needs to be filtered. This is achieved by generating an orthogonal projector with the initial eigenvectors corresponding to the zero eigenvalues [25]

$$\boldsymbol{P}_{\mathrm{orth}} = \boldsymbol{\psi}_{\mathbf{0}}[\boldsymbol{\psi}_{\mathbf{0}}]^{\mathrm{T}} \quad . \tag{3.30}$$

The orthogonal projection matrix $\boldsymbol{P}_{\text{orth}}$ is used to filter the FIM of the full candidate set $\boldsymbol{A}_{\mathbf{FIM}}$ so that the remaining information is orthogonal to the initial FIM. This means that the best candidate in the projected FIM is most likely to increase the rank of the initial FIM $\boldsymbol{A}_{\mathbf{FIM}}^{\mathbf{ini}}$. The projection is described by

$$\bar{\boldsymbol{A}}_{\mathbf{FIM}}^{\mathbf{ini}} = \boldsymbol{P}_{\text{orth}}\, \boldsymbol{A}_{\mathbf{FIM}}\, [\boldsymbol{P}_{\text{orth}}]^{\mathrm{T}} \tag{3.31}$$

where the projected FIM is expressed by $\bar{\boldsymbol{A}}_{\mathbf{FIM}}^{\mathbf{ini}}$ which is now also a singular matrix. The eigenvectors corresponding to the non-zero eigenvalues of the projected matrix $\bar{\boldsymbol{A}}_{\mathbf{FIM}}^{\mathbf{ini}}$ are used to determine the contribution of every node to the increase of the rank of the initial FIM

$$[Ef{I_3}^{+}]_i = 1 - det(\boldsymbol{I} - \boldsymbol{\phi}_{\mathbf{3i}}(\bar{\boldsymbol{\psi}}\, \bar{\boldsymbol{\lambda}}\, [\bar{\boldsymbol{\psi}}]^{\mathrm{T}})^{\mathrm{g}}\, [\boldsymbol{\phi}_{\mathbf{3i}}]^{\mathrm{T}}) \tag{3.32}$$

where the non-zero eigenvalues of the projected FIM are denoted as $\bar{\boldsymbol{\lambda}}$, and the corresponding eigenvectors are expressed as $\bar{\boldsymbol{\psi}}$. The superscript g refers to the generalized inverse, also called the pseudo-inverse. The node with the highest ranking is included in the initial a-set and this process is repeated until the FIM is of full rank [25]. From this point, the Case-I-procedure can be applied if a further increase of the a-set is necessary.

Mass-Weighted Triaxial Effective Independence Expansion

The mass-weighted variant of $\text{EfI}_3{}^+$ is only briefly explained in this section. The main difference to the previously discussed technique is the mass-weighted modal matrix . If this is acquired, the exact same process follows as presented above. Hence, only the computation of the mass-weighted modal matrix is discussed in this section.
Kammer and Peck suggest to compute the mass-weighted modal matrix in the following way [28]

$$\boldsymbol{\Phi}_{\mathbf{mw}} = \boldsymbol{M}\boldsymbol{T}_{\text{EMR}}\, \boldsymbol{\Phi}_{\boldsymbol{a}} \tag{3.33}$$

where $\boldsymbol{\Phi}_{\mathbf{mw}}$ denotes the mass weighted modal matrix; the mass of the full system is referred to as $\boldsymbol{M}$, and $\boldsymbol{T}_{\text{EMR}}$ and $\boldsymbol{\Phi}_{\boldsymbol{a}}$ are the transformation matrix of EMR and the a-set partition of the not mass-weighted modal matrix, respectively. It is also possible to use different transformation matrices, but Kammer and Peck recommend the EMR [28]. Since the a-set is increasing for every iteration, equation (3.33) has to be evaluated in this form. Compared to the iterative reduction approach, the mass matrix is not fully reduced, but rather a new distribution has to be evaluated with an increasing a-set.

This concludes the presentation of the various selection methods. It is now important to select a measure of goodness to asses the quality of the a-sets produced with different selection approaches.

3.4 Measure of Goodness for Selected Active Set

All of the introduced selection methods produce a sub-optimally selected active partition, and finding a measure of goodness for all the techniques is difficult. Since all selection methods try to optimize a different criterion, it is difficult to compare them without being bias towards one specific method. Penny et. al. [55] suggest several assessment criteria which involve the evaluation of

1. the determinant of the FIM
2. the condition number of the a-set partition of the modal matrix
3. measured energy per mode
4. ModMAC rms error

Another measure of goodness is suggested by Kidder which involves a comparison of the eigenvalues of the active and the omitted partition ([51], [31]).

3.4.1 Determinant and Rank of the Fisher Information Matrix

The determinant of the FIM and its maximization is commonly used for optimal parameter estimation, but it is also a good criterion for optimal sensor placement [29]. By maximizing the determinant, the covariance matrix of the estimate errors is being minimized. Hereby, the most independent information is retained [23]. Penny et. al. point out that using the determinant of the FIM as an assessment criterion has a disadvantage because the value does not necessarily lie within a fixed range [55]. Hence, it cannot be used as an absolute measure of goodness of the selected a-set. It is, however, possible to use it as a relative measure to compare configurations with the same number of DoF [25].

Another measure of goodness appears from the minor limitation of the modal subspace reduction methods where the a-set partition of the modal matrix has to be of full-column rank [21]. In this case, the FIM would also be of full rank, which means that as long as the FIM is not singular, the selected a-set would produce at least with the modal subspace reduction methods a good reduced representation.

3.4.2 Condition Number of the Partitioned Modal Matrix

Unlike the determinant of the FIM, the condition number of the modal matrix indicates the spatial independence of the mode shapes ([62], [30]). It is calculated as the ratio between the largest and the smallest singular value of the partitioned modal matrix [55]. The closer the value to 1.0 the more independent are the partitioned eigenvectors, and an exact value of 1.0 indicates orthogonality of the mode shapes [55]. Hence, an a-set that produces a condition number close to unity is meant to be a good choice.

Whilst this can be regarded as correct for the problem of sensor placements, it has been observed that a reduction using the EMR method can produce very good results with a condition number far higher than 1.0. The other problem occurs when the eigenvectors are normalized to unit mass which means that they are not necessary orthogonal if the mass is not evenly distributed throughout the structure. Hence, achieving a condition number close to one might not even be possible with the whole modal matrix.
It is nevertheless a helpful indicator for a good selection of an a-set, but the expectancy of a small value is not necessary.

3.4.3 Measured Energy per Mode

Another method to assess the selected a-set is to compute the measured energy per mode [55]. The kinetic energy of the first mode would then be calculated using equation (3.34)

$$T_{KE_1} = [\boldsymbol{\phi_1}]^{\mathrm{T}} \boldsymbol{M}\, \boldsymbol{\phi_1} \tag{3.34}$$

where T_{KE_1} denotes the kinetic energy of the first mode, and $\boldsymbol{\phi_1}$ is the first mode shape of the modal matrix. Since the modal matrix is scaled to unit mass, the value of the kinetic energy is equal to one which is also the reference value of the comparison. It is hypothesized that a good a-set will contain within the active partition of the kinetic energy

$$\boldsymbol{T_{KE}} = [\boldsymbol{\Phi_a}]^{\mathrm{T}} \boldsymbol{M_{aa}}\, \boldsymbol{\Phi_a} \tag{3.35}$$

a value close to one since it is desirable to preserve most of the system's energy within the active DoF. It is important to note that the a-set could potentially have a value greater than one [55] which can occur in some circumstances. Another issue is that this criterion is, similar to the determinant of the FIM, a relative measure of goodness which can only be used to compare two a-sets with the same amount of active DoF [55]. Because of this, only one relative measure of goodness is going to be applied. Since the computation of the determinant of the FIM is easier and because of the difficulty in comparing the measured energy per mode directly [55], the determinant of the FIM is used throughout this thesis.

3.4.4 Root Mean Square Error of Pseudo-Orthogonality Check

Although Penny et. al. suggest to use the ModMAC as an assessment criterion [55], in this thesis, a POC is going to be applied since the ModMAC has been defined as a correlation for the full set of DoF. Because a correlation at the reduced set is required, a POC would have to be used, instead. Penny et. al. were using a GR-reduced mass matrix representation for the ModMAC which could have created a bias comparison due to the approximating nature of the GR. Using the SEREP representation of the mass matrix will create better results.
Since the SEREP reduction is applied, the POC can only be evaluated when the a-set partition of the modal matrix is square, which means that the number of active DoF n is equal to the number of target modes m. In every other case, the results of the POC would not be representative and are not evaluated.
After calculating the POC matrix, a RMS value of all off-diagonal terms is being computed. The reference value is the RMS of all off-diagonal terms of the full ModMAC which would be zero because the modal matrix is normalized to unit mass. This implies that the closer to zero the RMS value of the off-diagonal terms is the better the selection of the a-set.
The principal diagonal of the POC is evaluated, as well. It is expected to have a RMS value of one for a good a-set selection.

3.4.5 Eigenvalue Comparison

The eigenvalue comparison was suggested by Kidder [31], and other authors also recommend his criterion ([53], [51]). It is comparing the eigenvalues of the a-set with the results of an eigenanalysis of the o-set. The best selected a-set would have smaller eigenvalues than the smallest eigenvalue of the o-set partition [51]. This is unfortunately not necessarily the case for large models. When only a small number of active DoF is selected, then the smallest eigenvalue of the o-set will also be below the highest eigenvalue of the a-set. This would indicate that more active DoF would have to be included in the final a-set which defeats the objective of creating a reduced representation which is as small as possible. Hence, this criterion is also not going to be applied. Papadopoulos interprets this criterion in such a way, that the best selected a-set would maximize the smallest eigenvalue of the o-set [53]. In this case, a comparison of eigenvalues does also not occur.

4 Two-Step Reduction in MORPACK

This chapter presents the implementation of the two-step MOR within the MORPACK software, as well as the automated selection methods to select an optimal ID. The structure of the software MORPACK is briefly outlined in section 4.1. Implemented selection methods as well as the requirements of an ID with some recommendations are discussed in section 4.2. Finally, section 4.3 presents an overview of possible two-step methods and introduces the proposed pseudo two-step MOR approach.

4.1 Structure of MORPACK

The Matlab-based software MORPACK [35] is developed at the Chair of Dynamics and Mechanism Design at the Technical University of Dresden [39] and has a modular structure to perform various tasks of which one is the reduction of large finite element models. Figure 4.2 demonstrates different modules within MORPACK and highlights the module which was primarily influenced by the work presented in this thesis. The Import module is designed to

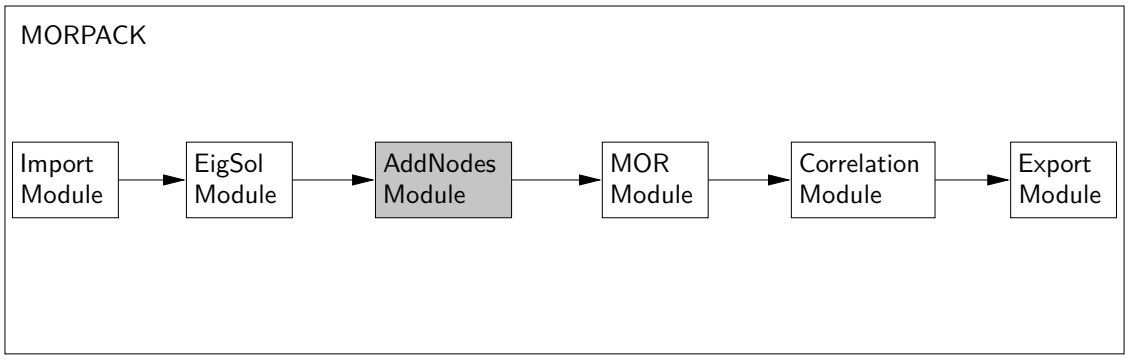

Figure 4.1: Available Modules in MORPACK

import the system matrices and the node list of FE models, and the EigSol module acquires the necessary modal information for correlation and MOR purposes. The discussed selection methods are implemented within the AddNodes module which is designed to enhance the quality of the reduced representation by selecting an optimal a-set. Obviously, the suitable

ID for a two-step MOR is selected within this module, as well. The next module performs the MOR of the FE model, and the results are evaluated using the Correlation module. Should the information be required for further analysis, the Export module is designed to create the desired files for further applications.

The analysis of the AddNodes module is presented in figure 4.2. This is also an example of a typical structure of every module within MORPACK. The options of the various methods,

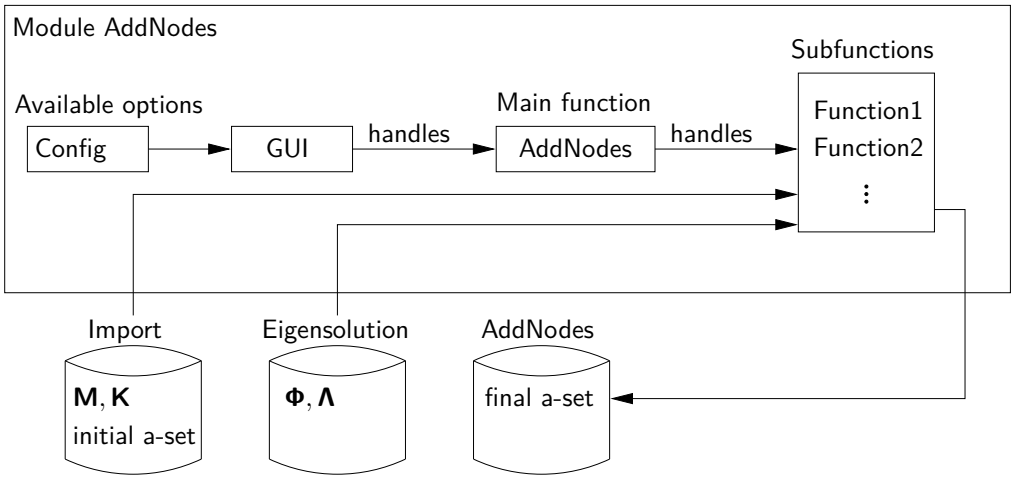

Figure 4.2: Structure of the Module AddNodes in MORPACK

represented by the subfunctions, can be selected through a graphical user interface (GUI), and the selected parameters are exchanged through the handles variable. After the main function of the module is initiated, it has access to all other functions performing each a different selection method. The required information can be found in the Import and Eigensolution folders, respectively. Both are located within the pre-selected working directory. The results are saved into the AddNodes folder, as can be seen in figure 4.2. The main application of the automated selection methods is to find an optimal ID for a two-step MOR.

4.2 Selection of an Intermediate Dimension

The ID has a strong influence on certain aspects of a two-step MOR. Depending upon the size of the ID, it can influence not only the accuracy of the reduction but also the required computational time. It is important to emphasize that not only the size of the ID is a critical factor which has to be considered. Also the location of the selected nodes has a strong influence on the final result. Hence, it is probably more important to decide which nodes to select rather than how many.

4.2.1 Intermediate Dimension Requirements

The requirements of an ID depend upon its application, and a MOR of a large finite element model is only one of possible aspects. In order to classify different IDs, it is necessary to state the attributes of which the goodness is going to be measured against.

Subspace Restriction

The requirement for the ID to be within the physical subspace is a major limitation towards two-step reductions. The reasons for such a constraint are simple because every MOR method maps the reduced information onto a physical space. Hence, the MOR of the second step always maps onto a physical space so that the reduced representation of the first step also has to be within the same space. It is possible, however, to use certain two-step reductions without this restriction which is not considered in this thesis, but could be used for further research. The restriction that the ID has to be within the physical space also excludes some MOR methods from being a possible first step candidate.

Nodes vs. Degrees of Freedom

The other requirement of the ID is the consideration of nodes with their complete set of available DoF. This ensures that the reduced representation also consists of nodes which is necessary for further structural analysis, if intended. However, there are other cases where such an ID is not necessary, e.g. an experimental modal analysis using only uniaxial sensors. Then, it would be required to find an optimal location of DoF instead of nodes. Since this is not of interest for the purposes of this theses, the second requirement of the ID is to contain only nodes with a full set of DoF.

Square Active Partition of the Modal Matrix

The size of the ID depends on the number of active DoF n. For different applications, this number is not necessarily equal to the target mode shapes m within the frequency range of interest. It is very common during a modal test to select many more DoF in order to distinguish the different measured mode shapes. Using an ID where the size of the a-set is larger than the number of target modes will cause a reduced representation which is not preserving the response of the original system. The reason for this lies in the nature of the reduction process using an EMR. When the size of the reduced representation is larger than the number of selected modes, the EMR produces additional, wrong modes of the reduced representation which in turn affects its response to an excitation.
To ensure that the full model's response is preserved within the ID, the a-set partition of the

modal matrix has to be square so that the number of target modes is equal to the number of active DoF.

4.2.2 Implemented Selection Methods

The methods presented in table (3.1) have been implemented, and additional options have been included which are going to be discussed next. For the sake of simplicity, it is easier to differentiate the options for non-iterative, iterative reducing, and iterative expanding methods of which the first options are explained next.

Non-Iterative Options

The implemented options for the non-iterative selection methods are briefly outlined, and an overview is given in table 4.1. Option one is straightforward, but it is very important to

Table 4.1: Available Options for Non-Iterative Selection Methods in MORPACK

No.	Options	DPR	ECP	MKE
1.	Select nodes or DoF	✔	✔	✔
2.	Choose a variant	✔	✘	✔
3.	Exclude rigid modes	✔	✔	✔
4.	Retain initial a-set	✔	✔	✔
5.	Use as a pre-conditioner	✔	✔	✔
6.	Change size of the candidate set	✔	✔	✔
7.	Criterion for ID selection	✔	✔	✔
8.	Mass matrix reduction method	✘	✘	✔

emphasize its function. As opposed to other selection methods, the non-iterative sorting is always ranked by the DoF.
Option one allows the recombination of the translational DoF after the actual ranking process. This means that for one very good DoF usually two badly ranked DoF are included into the a-set, which usually tends to create a larger ID than required.
Option two enables the application of the average and weighted variants of MKE and DPR, respectively, and option three detects the number of rigid modes, if there are any, and excludes them from the calculation.
With option four activated, the initial a-set is recombined after the sorting process. This is also different with other selection methods where an iteration only occurs within the o-set of the system.
The fifth option stems from the idea to use a smaller candidate set for an iterative selection

method. If this option is selected, the non-iterative selection saves the results in the *Temp* directory. From there, the iterative method can access a pre-conditioned, smaller candidate set. This enhances the speed of the iterative reduction methods since only a smaller portion needs to be ranked and sorted.
The gain in computation time is also achieved by using option six and reducing the candidate set beforehand. However, this not a recommended option for a non-iterative selection because it is very likely to cause a loss of important DoF due to the truncation.
There are three different selection criteria implemented in option seven – Rank, Condition Number, and Manual Selection of additional nodes/DoF. While the first two are based upon the FIM or the a-set of the modal matrix, the manual selection neglects any automated selection criteria for an ID. This option should only be used with caution since it is not guaranteed that the proceeding reduction will succeed with a manually selected ID.
The last option is necessary only when a smaller candidate set during the MKE process is selected. In this case, the mass matrix would have to be reduced to the selected size prior to the sorting of the DoF.

Iterative Reduction Options

The various options for the iterative reduction methods are presented in table 4.2. Although some of them are similar to the non-iterative options, they are sill briefly explained, as well. The first option is not available in EfI_3 since it computes a ranking based on nodes. All other

Table 4.2: Available Options for Iterative Reduction Methods in MORPACK

No.	Options	EfI	EfI_3	SMR	SVD	VB
1.	Select nodes or DoF	✔	✘	✔	✔	✔
2.	Select number of target modes	✔	✔	✔	✔	✔
3.	Exclude rigid modes	✔	✔	✔	✔	✔
4.	Retain initial a-set	✔	✔	✔	✔	✔
5.	Criterion for ID selection	✔	✔	✔	✔	✔
6.	Elimination rate selection	✔	✔	✔	✔	✔
7.	Use pre-conditioned candidate set	✔	✔	✔	✔	✔
8.	Change size of the candidate set	✔	✔	✔	✔	✔
9.	Use mass weighting	✔	✔	✘	✔	✔
10.	Diagonalization of mass matrix	✔	✔	✘	✔	✔
11.	Mass matrix decomposition	✔	✔	✘	✔	✔
12.	Mass matrix reduction method	✔	✔	✔	✔	✔

methods compute a ranking based on the DoF, and if option one is selected on nodes, all DoF of the selected node are included in the additional a-set.

Because a selection criterion is implemented based on attributes of the FIM, the number of target modes needs to be specified, which is done with option two.
Option four and five are also available for the non-iterative methods. The criteria of an ID selection are either automated – rank or condition number of the FIM – or manual by selecting the desired number of additional nodes or DoF.
The option six sets the number of deleted DoF during one iteration step based on a selected percentage value.
If option seven is selected, a previously non-iterative selection with its option five activated had to be performed. The solution of the non-iterative sorting is then saved in the *Temp* directory, and the following iterative approach can use a pre-conditioned, smaller sized candidate set to reduce the computation time.
The size of the candidate set would have to be changed with option eight.
Options nine to twelve are related to a mass weighting during the iteration. In order to reduce computation time, the mass matrix can be diagonalized using either only its diagonal or a lumped mass diagonalization procedure. Option eleven activates a decomposition of the mass matrix, and the reduction method is selected with option twelve. It has been observed that for larger models, the mass weighting is too computationally intensive. Hence, the applications are not focused on these last options because it tends to create memory problems due to fully populated reduced mass matrix representations. At the beginning of the iterations, these representations are usually still very large which causes the memory issues.

Iterative Expansion Options

The iterative expansion methods have more or less the same options as the iterative reduction techniques. Hence, the focus will lay only on the additional options which were not mentioned before. A complete overview is presented in table 5.5. The option not used for the iterative expansion methods is the elimination rate for the omitted DoF, because at each iteration only one DoF or node is selected, respectively. Option twelve is MoGeSeC specific and determines the weighting parameters for the modal and spatial weighting vectors.
The last option has been additionally added only for the $\mathrm{EfI}_3{}^+$ algorithm. During the application phase, it has been observed that the computation of a square a-set partition of the modal matrix is made impossible by including rotational DoF into the a-set. Because the rotational DoF do not contribute to the rank of the FIM, it always resulted in an ID which had more DoF n than the selected number of target mode shapes m. Hence, the $\mathrm{EfI}_3{}^+$ algorithm has been modified to exclude nodes with six DoF as an option which could also be expanded for the other selection methods.

Table 4.3: Available Options for Iterative Expansion Methods in MORPACK

No.	Options	EfI+	EfI$_3$+	MoGeSeC
1.	Select nodes or DoF	✔	✘	✘
2.	Select number of target modes	✔	✔	✔
3.	Exclude rigid modes	✔	✔	✔
4.	Retain initial a-set	✔	✔	✔
5.	Criterion for ID selection	✔	✔	✔
6.	Use pre-conditioned candidate set	✔	✔	✔
7.	Change size of the candidate set	✔	✔	✘
8.	Use mass weighting	✔	✔	✘
9.	Diagonalization of mass matrix	✔	✔	✘
10.	Mass matrix decomposition	✔	✔	✘
11.	Mass matrix reduction method	✔	✔	✔
12.	Weighting parameters $k1$, $k2$	✘	✘	✔
13.	Try computing a square a-set partition	✘	✔	✘

4.2.3 Recommended Selection of an Intermediate Dimension

The recommendation towards selecting an optimal ID are regarded not only in the quantitative but also in a qualitative sense. The choice of an ID is always based upon its purpose for the engineer, and in this thesis, the purpose is to create a reduced representation of the full system which can approximate the response to an excitation in the best possible way. This purpose is considered when recommending the criteria for an optimal ID.

Size of the Intermediate Dimension

Computing the response of the full system bears the first difficulty. It is usually handled in such a way that the first m modes are calculated to represent the full system's response. For very large models, it becomes difficult to compute the mode shapes, and usually it is not a very large number. So the size of the ID has to include as many full system modes as possible. It is, however, not a trivial task to select the right a-set which renders the modal matrix partition linearly independent. For this problem, an iterative expansion method seems to suit best. Especially, the results produced by EfI$_3$+ contain the highest potential to fulfill such a criterion.

Consideration of Nodes

All nodes from the initial a-set have to be included to ensure further analysis of the reduced representation. The nodes of the additional a-set, on the other hand, should only have translational DoF. This means that during an additional a-set selection, the nodes with six DoF are not to be included.

This concludes the remarks towards the selection of an optimal ID, and it can be summarized that the size of the ID is based upon the reference of the full system's response. The consideration of any smaller sizes could cause inaccuracies of the reduced representation's FRF.
It is, now, important to establish promising combinations of MOR methods for a successful two-step approach.

4.3 Combination of Reduction Methods

In order to find good combinations for a two-step MOR, it is important to realize the advantages and disadvantages of every individual MOR. The next section attempts to give an overview over the reduction methods implemented within the MORPACK software. Another difficulty arises concerning the availability of modal information of the full system. If a full modal matrix is available, a totally different two-step approach can be applied which would otherwise not even be possible. Finally, a pseudo two-step MOR method is proposed which is meant to reduce in two steps without the knowledge of modal information.
Figure 4.3 presents all possible combinations considered in this thesis.

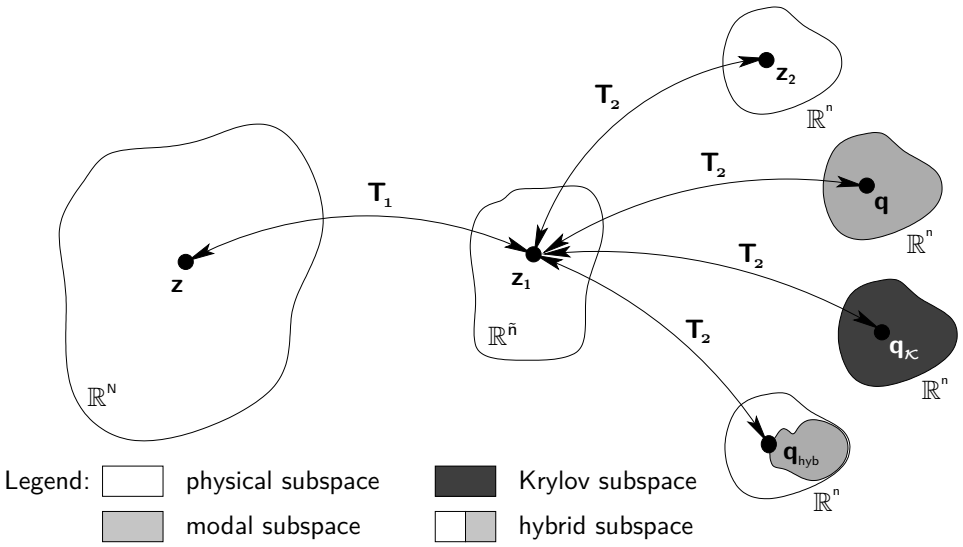

Figure 4.3: Possible Two-Step MOR Combinations

As stated in section 4.2.1, only an ID within the physical space is considered during the first step of the reduction process. However, there are no restrictions towards the second MOR which requires a thorough knowledge of the one-step reductions to choose a good combination.

4.3.1 Overview of All Candidates

This section is meant to give a brief overview over some MOR methods. Hence, the advantages and disadvantages of the individual MORs are simply listed to enhance a better understanding of possible two-step approaches.

Guyan Reduction

Advantages:

- does not require modal information
- simple and straight forward to implement
- meant to be precise in lower frequency ranges (up to 100 Hz)
- reduced representation within physical space

Disadvantages:

- approximating nature due to negligence of inertia forces
- results highly depend on selected a-set
- large a-set for better approximation required
- no criterion available for a final size of the a-set

Improved Reduced System

Advantages:

- initially no modal information required
- iterative nature enhances results
- meant to converge to results of SEREP without using the modal matrix
- reduced representation within physical space

Disadvantages:

- selection of a-set requires modal matrix of full system
- wrong eigenfrequencies too realistic – difficult to distinguish
- iterated procedure is very computationally intensive for large models

Modal Reduction

Advantages:

- preserves the modal information within the reduced representation
- reduction procedure is very fast

Disadvantages:

- reduced representation not within physical space
- computation of full system's target modes required
- does not necessarily preserve full system's response

Exact Modal Reduction

Advantages:

- preserves the modal information within reduced representation if rigid modes are excluded
- reduced representation within physical space
- always produces positive definite mass matrix
- reduction procedure is very fast

Disadvantages:

- computation of full system's target modes required
- selection of optimal a-set is necessary
- unrealistically large additional eigenfrequencies for the case $n > m$ – bad approximation of system's response
- preserves only response of full system when all modes are included

System Equivalent Reduction Expansion Process

Advantages:

- preserves the modal information for the case $n = m$ if rigid modes are excluded
- reduced representation within physical space
- fast reduction procedure

Disadvantages:

- rank deficient reduced mass matrix for the case $n > m$
- computation of full system's target modes is required
- selection of optimal a-set is necessary
- preserves only response of full system when all modes included

Krylov Subspace Method

Advantages:

- approximates directly the response of the full system
- does not require modal information
- easy to distinguish wrong eigenfrequencies

Disadvantages:

- reduced representation not fully within physical space
- more Krylov modes than normal modes required – reduced representation has to be larger than number of target modes m
- no estimator for number of Krylov modes – safest option is to use $2m$

Component Mode Synthesis

Advantages:

- good approximation for a large number of Craig-Bampton-Modes
- easy to distinguish wrong eigenfrequencies

Disadvantages:

- improved approximation only when size of reduced representation increases
- reduced representation not fully within physical space

Improved Component Modes Synthesis

Advantages:

- precise approximation when applied in iterative form
- easy to distinguish wrong eigenfrequencies

Disadvantages:

- reduced representation not fully within physical space
- very time intensive iterated approach
- improved approximation only when size of reduced representation increases

Hybrid Exact Modal Reduction

Advantages:

- same results as SEREP and EMR for the case $n = m$
- better approximation of additional eigenfrequencies for the case $n > m$
- reduced representation within physical space
- always produces positive definite mass matrix

Disadvantages:

- modal information required
- selection of optimal a-set is necessary
- preserves only response of full system when all modes included

4.3.2 Combinations with Modal Information

Since the different advantages and disadvantages of the MOR methods are presented in the previous section, possible combinations for a two-step MOR are, now, considered. It is necessary to differentiate two cases where one case represents the availability of modal information – modal matrix and eigenfrequencies. The other case considers the lack of this information.

The two-step approach is meant to improve the speed of relatively precise MOR that have a large computation time as a drawback. This is definitely the case for the iterative formulations of IRS and ICMS, respectively. Also the KSM reduction is another approach which is not necessarily slow but can produce good approximations.
In order to attempt to improve these three reduction techniques, a first step has to be established that can preserve the response of the full system within the ID. The second requirement is that the ID has to be within the physical space as mentioned in section 4.2.1. Only two of the previously mentioned MOR methods are able to create such an ID – EMR and SEREP. Not only is the computation of the reduced representation relatively fast but also an exact reduced representation can be created due to the fact that the modal information is available. Since the reduced representation is computed by a square a-set partition of the modal matrix, the results of EMR and SEREP are equal. So, it is sufficient to investigate only one approach. For the rest of the thesis, the term SEREP is going to be used to emphasize the fact that the number of selected active DoF n is equal to the number of target mode shapes m. If there is a reason to distinguish both methods, then EMR will be used as well.
Three promising two-step MOR methods have been selected for further investigation in this thesis

1. SEREP-ICMS
2. SEREP-IRS
3. SEREP-KSM

where the iterated approach is going to be applied for both ICMS and IRS, respectively.

4.3.3 Combinations without Modal Information

A totally different situation occurs when no modal information of the full system is available. This could happen if, for some reason, an eigenanalysis is not possible or the results are some-

how not correct. Using a modal subspace reduction in this situation, would cause problems or might not be possible, at all.

The only promising MOR for the first step would be an iterated IRS because it is meant to converge to the SEREP results if the correct nodes are selected. The selection of the a-set, on the other hand, depends on the modal information which makes the computation of an optimal ID difficult. By using the SMR, which does not rely on modal information, it could be possible to find an ID, but it is not likely to be the case.
There is one major problem using the iterated IRS method which makes it impossible to be a first step in a two-step MOR. When IRS is producing an incorrect eigenfrequency, it is not possible to distinguish it without the knowledge of the full systems modal matrix. If SEREP computes wrong eigenfrequencies, they usually have a value of zero or a very high value compared to the rest of the frequencies. This makes them very easy to differentiate from each other which is not the case for the IRS approach.

Hence, a two-step MOR approach without the use of modal information cannot guarantee to be able to successfully create a reduced representation with the desired properties. The newly proposed pseudo two-step, however, attempts to overcome this difficulty by creating a reduced representation which preserves the modal information of the full system without prior knowledge of the its modal matrix.

Pseudo Two-Step

The pseudo two-step combines all previously introduced ideas into one MOR method. The two MOR techniques involved in this process are KSM and SEREP reduction methods. Figure 4.4 demonstrates the procedure. The first step is a KSM reduction to obtain a reduced

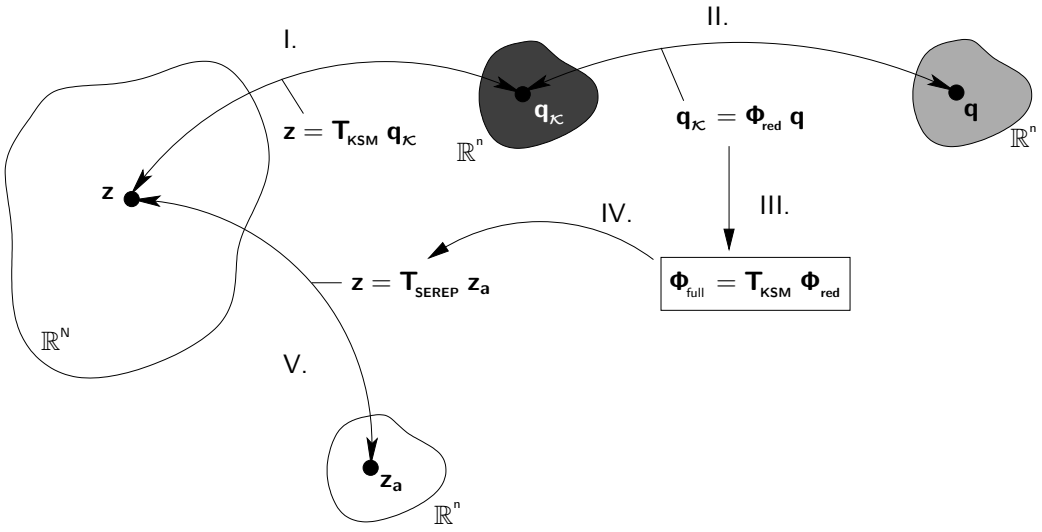

Figure 4.4: Pseudo Two-Step (KSM-SEREP) Procedure

representation. Next, an eigenanalysis is performed to get the reduced modal matrix $\mathbf{\Phi_{red}}$. As a next step, the reduced modal matrix is expanded to the full size of the system using the KSM transformation matrix $\boldsymbol{T}_{\mathbf{KSM}}$. The final step is the reduction of the full system using the modal matrix obtained from the previous step. In order to ensure a correct approximation using the SEREP approach, the $\mathrm{EfI}_3{}^+$ method is applied to select an optimal additional a-set.

Because no ID is necessary, this reduction method is referred to as a pseudo two-step since it uses two consecutive MOR approaches. The results of the pseudo two-step would be the same as the SEREP reduction with available modal information. It is simply a different approach to acquire the modal matrix of the full system. The function *eigs* in Matlab is meant to use a Krylov subspace method, as well.

Since the result depends upon the second step, it still contains the same problems that a modal subspace reduction produces. In order to ensure that the KSM expanded modal matrix contains the correct target modes in the frequency range of interest, it is advisable to use twice as many Krylov modes for the first reduction step.

This concludes the presentation of the two-step MOR in MORPACK, and the introduced methods are tested on a practical application in the next chapter.

5 Applications

The previously presented methods for selecting an optimal ID as well as the two-step MOR variants are tested in this section using an element model of a gear box. In section 5.1, the gear box is briefly described with regards to an optimal ID selection as well as the following MOR procedure. The implemented selection methods are evaluated in section 5.2 where the aim is to find an optimal a-set for the one-step MOR techniques. Two differently sized IDs have been selected for a better comparison, and the selection process is described in section 5.3. The results of the two-step MOR as well as the pseudo two-step are discussed (5.4), the comparison with the one-step approach is performed in section 5.5. Here, a new selection procedure is proposed to improve the FRF approximation of the SEREP reduction for small reduced representations where the idea is presented and the potential discussed. The last section (5.6) compares the hybrid MOR approaches with the two-step results which also concludes the discussion of this chapter. The two-step approaches are compared with the one-step and hybrid MOR techniques, respectively.

5.1 Gear Box Model

The gear box is the same FE model as presented in [39] consisting of a total number of 310335 DoF. It contains 2841 nodes with 6 DoF of which nine are considered as the initial a-set. Another 97761 nodes have no rotational, but all three translational DoF. However, there are also two nodes with incomplete DoF – one node with only 4 and another one with 2 DoF. Both are not included in the ID selection process as well as all rotational DoF that are not part of the initial a-set.
This means that the selection process will have a total amount of 301779 DoF available corresponding to 100593 nodes. Figure 5.1 shows the finite element model of the gear box. The reduced representation is meant to be precise for a frequency range of $2000Hz$. An eigenanalysis has been performed to compute the first 1005 modes of the full system. The first frequency above the desired range is number 68. However, since the reduced representation has to consist of nodes with at least full translational DoF, the number of mode shapes has to be a multiple of three. This means that 69 mode shapes are going to be considered in the reduction process as well as in the correlation of the results. Another important restriction is that the rigid

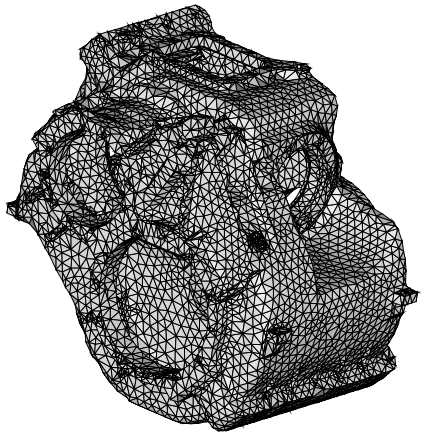

Figure 5.1: Finite Element Model of a Gear Box

modes will be excluded from all calculations. This leads to the final number of mode shapes which are going to be regarded – the first 63 non-rigid modes.

5.2 Selection of Additional Active Nodes

Since the initial a-set consists of nine nodes with a total of 54 DoF, it is now important to find additional active nodes so that the first 63 non-rigid mode shapes can be approximated by the reduced representation. All implemented selection methods have been applied to find, if possible, the additional 3 nodes containing each 3 translational DoF so that an EMR could produce the desired reduced representation.

The selection of additional nodes has been performed for all methods with the rank and the condition number criterion, respectively. The former criterion requires for the FIM to be of full rank, and the latter criterion ensures that the a-set of the modal matrix has a condition number below a certain limit. The choice of the limit highly influences the outcome of the node selection process. For all calculations, the condition number limit was set to 100, which means that the smallest a-set that creates a condition number below this limit is selected.
Table 5.1 presents the results of the non-iterative selection methods without the variants of MKE and DPR, respectively. The second column of table 5.1 shows a reference selection of active nodes. This reference contains the initial a-set and additional nodes to create a square active partition of the modal matrix. For this model, the default sorting already fulfills the rank criterion. It is peculiar that a full rank FIM can have a determinant of a value very close to zero. This seems to happen every time the rank criterion is used and has to be due to numerical issues. However, the reduced representation created with this selection does not show any problems or incompleteness regarding the correlations, which will be discussed at a later stage.

Table 5.1: Results of Non-Iterative Methods using Rank Criterion (white) and Condition Number Criterion (gray)

Measure of Goodness	Ref	DPR	ECP	MKE
1. Recommended quantity of DoF	63	66	63	66
	417	12456	6177	1782
2. Rank of FIM	63	63	63	63
	63	63	63	63
3. Condition number	7.95e6	8.57e5	5.45e6	2.34e6
	90.00	99.84	98.52	97.21
4. Determinant of FIM	0.00	0.00	0.00	0.00
	1e124	9e237	1e218	3e178
5. RMS_{diag} of POC	1.00	-	1.00	-
	-	-	-	-
6. $RMS_{off\text{-}diag}$ of POC	0.00	-	0.00	-
	-	-	-	-
7. Computation time in sec	-	4.4	0.3	6.2
	-	163	112	18.5

A very positive point is that the non-iterative methods are very fast. The sorting of the nodes is finished within seconds as can be observed in table 5.1, where only the ECP method could create a square a-set of the modal matrix. Some of the variants of MKE and DPR are also able to create a square a-set partition which can be observed in table 5.2. Both the ADPR and AMKE are able to create the desired a-set partition. However, the condition number of this partition is higher compared to the reference result in table 5.1. This shows that both methods consider locations only for good observability of the selected mode shapes but neglect the spacial independence of the nodes. Hence, it requires a relatively large amount of additional nodes to achieve an a-set partition below the limit of 100. Although the WAMKE method needs a significantly smaller amount of additional nodes to fulfill the condition number criterion, it is still above the reference example.

The non-iterative selection methods are computationally very fast but only some are able to create the desired results. The main reason is that additional nodes – instead of DoF – are required for an optimal ID. The selection methods, however, rate only the DoF and not the nodes. This results in a biased rating because one selected DoF with a good ranking usually has corresponding DoF with a bad contribution. This distorts the selection process by choosing DoF which would normally not be included.
The non-iterative selection methods could still be used as a pre-conditioner for the iterative

Table 5.2: Results of Variants of MKE and DPR using Rank Criterion (white) and Condition Number Criterion (gray)

Measure of Goodness	ADPR	WADPR	AMKE	WAMKE
1. Recommended quantity of DoF	63	66	66	63
	10545	4068	3570	513
2. Rank of FIM	63	63	63	63
	63	63	63	63
3. Condition number	8.48e6	1.95e6	2.27e6	9.92e6
	99.94	98.41	95.17	95.54
4. Determinant of FIM	0.00	0.00	0.00	0.00
	2e233	5e209	5e199	3e150
5. RMS_{diag} of POC	1.00	-	-	1.00
	-	-	-	-
6. $RMS_{off\text{-}diag}$ of POC	0.00	-	-	0.00
	-	-	-	-
7. Computation time in sec	0.5	0.7	1.6	2.0
	115	35	27	4.8

selection methods. Since the observability of the mode shapes is included in the result, the iterative method could choose from a smaller candidate set, which includes all the important DoF, and increase the linear independence of the final a-set. Because the size of the candidate set is much smaller than the full model, it would reduce the total selection time. A condition number limit of 100 might be too high at this point and would have to be reduced to a value around 30.

Iterative Reduction Methods

The iterative reduction methods reduce, as the name implies, the size of the candidate set by removing the DoF with a low contribution to a selected criterion. The elimination rate for omitted DoF has been set to 1% which is a good compromise between fast computation and exactness of the results. Table 5.3 summarizes the results for both the rank and condition number criterion, respectively. The results of EfI are surprising since it is not able to create a square a-set partition. The problem could be that the selected elimination rate is too high which caused for important DoF to be deleted. The other possibility is the same problem that occurs with the non-iterative selection techniques. A ranking based only on DoF is not good enough for the purposes of selecting an optimal ID. Although the EfI_3 is based on a node ranking, it also does not create a square partition of the modal matrix. Here again, it

Table 5.3: Results of Iterative Reduction Methods using Rank Criterion (white) and Condition Number Criterion (gray)

Measure of Goodness	Ref	EfI	EfI_3	SMR	SVD	VB
1. Recommended quantity of DoF	63	66	66	63	66	66
	417	165	138	597	165	138
2. Rank of FIM	63	63	63	63	63	63
	63	63	63	63	63	63
3. Condition number	7.95e6	1.05e6	8.91e6	6.60e6	1.05e6	2.36e6
	90.00	64.07	98.22	99.73	64.07	82.58
4. Determinant of FIM	0.00	0.00	0.00	0.00	0.00	0.0
	1e124	5e131	4e112	3e132	5e131	5e115
5. RMS_{diag} of POC	1.00	-	-	1.00	-	-
	-	-	-	-	-	-
6. $RMS_{off\text{-}diag}$ of POC	0.00	-	-	0.00	-	-
	-	-	-	-	-	-
7. Computation time in min	-	6	149	10	10	236
	-	7	154	10	13	243

could be the poor choice of an elimination rate of 1% that could have caused this poor result. This is, however, not the case for the EfI_3 result.
In spite of the additional a-set consisting of 12 DoF, the algorithm selected 3 additional nodes of which one had 6 DoF. This shows a general difficulty in selecting optimal node positions. The rotational DoF do not contribute to the linear independence of the a-set modal matrix partition and should be neglected during the selection procedure. This has been implemented with the iterative expansion method EfI_3+, the results shown in table 5.5 have been produced without this setting.

Only SMR is able to achieve the requirements for this example. Regarding the condition number, however, it can be seen that this selection methods does not consider the linear independence similar to the non-iterative examples. The SMR has been performed without reducing the system matrices. It is generally to computationally intensive to reduce the size of the mass and stiffness matrices every iteration even with fast reduction methods like the modal subspace MOR. Because the reduced matrices are fully populated, it creates memory problems. Hence the mass and stiffness reduction has been performed by simply deleting the corresponding rows and columns, which creates only an approximated result.

It already has been observed in [53] that the SVD selection produces the same results as EfI. This is also the case for this example. This implies that within the EfI algorithm occurs a ranking based on a SVD. Since EfI requires less computations time, it is the preferred selection method. The last method presented in table 5.3 bears an interesting result because it seems to compute a better result than EfI. This is more obvious using the condition number criterion. The drawback of the variance-based selection method is its computation time. It is by far the slowest approach of the iterative reduction techniques. Hence, it is not a recommendable to use it for large finite element models.

Change of Elimination Rate for EfI

Since the amount of deleted DoF affects the outcome of the iterative reduction methods, a comparison of the EfI algorithm with different elimination rates has been performed and the results can be seen in table 5.4. The selected nodes have been sorted according to their number and not according to the sorting of the EfI algorithm. Deleting one DoF per iteration,

Table 5.4: Results of the EfI Algorithm with Different Elimination Rates

Measure of Goodness	**1 DoF**	**0.1%**	**1%**	**10%**
1. Recommended quantity of DoF	66	66	66	63
2. Rank of FIM	63	63	63	63
3. Computation time in min	1560	19	6	4
4. Index of selected additional nodes	14641	14641	14641	14047
	67205	67205	52682	38894
	67278	67278	67205	81448
	68181	68181	67278	-

which is meant to be the most precise case, is also not able to create a square a-set partition of the target mode shapes. This indicates that not the elimination rate caused that poor results presented in table 5.3 but the fact that the node of one good ranked DoF has usually two badly ranked corresponding DoF. Hence, a selection method based on node ranking has to be applied in order to achieve an optimal ID.
The same result as the deletion of one DoF at a time is also achieved with an elimination rate of 0.1%, which computes the additional a-set in a fraction of the time. A choice of this selection rate would, nevertheless, not fulfill the set requirements. The surprising result is the 10% elimination rate because it does compute a full ranked FIM within the required dimension. This is, however, only the case for this specific example and should not be generalized. It is obvious that a higher elimination rate leads to a faster computation time which also can be seen in table 5.4.

The main point is that the elimination rate is not the cause for the unsatisfactory results of the EfI algorithm, but the fact that nodes are required for an optimal ID rather than individual DoF. In order to have a fairly precise selection result, an elimination rate of 0.1% is sufficient. So there is no need to delete one DoF per iteration as suggested in literature, at least for this example.

Iterative Expansion Methods

The iterative expansion methods have been using the same settings as the other techniques. Hence, all rotational DoF were considered, but no elimination rate is applied since only one node is added into the additional a-set during every iteration. The results can be observed in table 5.5. All tested methods could achieve the required result for the rank criterion. This

Table 5.5: Results of Iterative Expansion Methods using Rank Criterion (white) and Condition Number Criterion (gray)

Measure of Goodness	Ref	EfI+	EfI_3+	MoGeSeC
1. Recommended quantity of DoF	63	63	63	63
	417	570	105	108
2. Rank of FIM	63	63	63	63
	63	63	63	63
3. Condition number	7.95e6	4.30e6	5.43e6	2.97e6
	90.00	96.88	86.94	90.90
4. Determinant of FIM	0.00	0.00	0.00	0.00
	1e124	3e139	1e105	2e106
5. RMS_{diag} of POC	1.00	1.00	1.00	1.00
	-	-	-	-
6. $RMS_{off\text{-}diag}$ of POC	0.00	0.00	0.00	0.00
	-	-	-	-
7. Computation time in min	-	0.1	4	52
	-	2	23	509

means that the best method to select an optimal ID for a two-step MOR is an iterative expansion approach. It is also very promising how fast EfI+ computes the result for the rank criterion. This matches the speed of the non-iterative methods. Since it only considers individual DoF, the spatial independence cannot be maintained which can be seen in the result of the condition number criterion. Since it selects more DoF than the reference example, it is not recommendable to use this method for an optimal ID selection.
MoGeSeC on the other hand considers not only the modal information but also spatial information to ensure a selection of nodes that can do both – be as spatially apart from each

other as possible and ensure an observability of all mode shapes of interest. Because two criteria have to be evaluated for a relatively large candidate set, this approach is not suited for large systems unless a pre-conditioned smaller candidate set is available.

Best results in table 5.5 are achieved by the EfI_3^+ selection method. It not only is able to fulfill the rank criterion within a reasonable amount of time but also it considers spatial independence by evaluating only modal information and is able to compute the smallest condition number with the least amount of selected additional nodes of all presented selection methods. Hence, this approach is going to be used in order to find an optimal ID for a two-step MOR. During further calculations, it has been observed that the rotational DoF do not contribute to an increase in the rank of the FIM. A modification has been implemented into the EfI_3^+ to optionally neglect such nodes for an ID selection. The results in table 5.5 have been computed without this additional option.

5.3 Optimal Intermediate Dimension

An optimal ID can only be computed for the gear box model because of the possibility to compute a larger amount of modes of the full system. The size of the optimal ID depends on the number of modes that still influence the FRF of the full system within the frequency range of interest. For the gear box model, a frequency range of 2000 Hz is required. A total number of 1005 mode shapes has been computed so that 999 non-rigid modes are available.

It is hypothesized that mode shapes of a higher frequency do not affect the behavior in the lower frequencies. In order to test this assumption, different responses of the full system are compared, and the $\mathcal{H}_2$ up to a maximum frequency of 2000 Hz computed. Table 5.6 presents the results.

Table 5.6: Comparison of $\mathcal{H}_2$ Error Until $f_{\max} = 2033.69$ Hz for Different Intermediate Dimensions

No. of Modes	$\mathcal{H}_2$ error in %
63	89.83
114	8.54
198	6.11
300	**3.11**
399	1.62
498	1.10
600	**0.69**
699	0.49
798	0.26
900	0.12
999	0.00 (Reference)

It can be seen that the $\mathcal{H}_2$ error for the reference number of 999 mode shapes is zero which is also expected. Now, it is assumed that the FRF of the full system is totally described by the influence of these modes. The smaller the number of modes the higher the error compared to the assumed full system's response. This indicates that a larger number of modes is required to describe at least within a certain error bound the FRF.

In order to compare the influence of the ID on the quality of the two-step MOR, two different sizes are selected. The larger size of 600 DoF is below a 1% error limit, and the smaller size of 300 modes produces a $\mathcal{H}_2$ error below 5%. The a-sets for both IDs have been selected using the EfI_3^+ algorithm with option 13 switched on. This means that a square a-set partition of the modal matrix is desired, and a selection of nodes with 6 DoF are neglected due to the little contribution of rotational information towards the rank of the FIM. Table 5.7 lists the required computation times for the a-set selection, but also the computations for the one-step approaches as well as the time needed for an eigenanalysis of the system are presented. This information needs to be considered when comparing the results with other one-step MOR. The two-step approaches can only be an actual alternative when smaller IDs are computed, but this would create only an approximation of the full system's response.

Table 5.7: Computation Time Considerations for the Gear Box Model

Task	No. of Modes	Computation Time in min
Eigenanalysis	100	7
Eigenanalysis	1005	95
EfI_3+	63	5
EfI_3+	114	28
EfI_3+	300	98
EfI_3+	600	309

5.4 Two-Step Model Order Reduction Results

The results of the two-step MOR are discussed in this section for the gear box model presented in section 5.1. Two different sizes of an ID have been selected, but also different sizes of the reduced representation are compared. The choice of the smallest size (63×63) is due to the fact that the first 63 non-rigid modes cover the selected frequency range of interest. The other size (114×114) is the smallest KSM-reduced representation which has and NRFD error of less than 5% for all 63 eigenfrequencies. Hence, not only is the influence of the size of the ID evaluated but also of the final reduced dimension.
Table 5.8 presents the results for the smaller reduced representation using two different IDs. At first, it seems that the size of the ID has completely no influence on the results of the

Table 5.8: Comparison of Reduced Representations ($\mathbf{63 \times 63}$) for Different Sizes of IDs during a Two-Step MOR – 300 DoF (white) and 600 DoF (gray)

Measure of Goodness	SEREP-ICMS	SEREP-IRS	SEREP-KSM
1. No. of matching frequencies	50	57	32
	50	57	32
2. Last matching frequency in Hz	1754.10	1891.81	1341.58
	1754.10	1891.81	1341.58
3. No. of matching modes	47	54	30
	47	55	31
4. $\mathcal{H}_2$ error ($f_{\max} = 2033.69$ Hz) in %	34.38	34.53	31.41
	36.26	39.10	32.88
5. Computation time in min	7	26	7
	20	50	24

two-step MOR. The SEREP-ICMS computes the same number of matching frequencies and modes, respectively. A matching frequency is considered with a maximum NRFD value of 1%,

and a matching mode shape is classified with a maximum difference of 5% on the principal diagonal of the ModMAC matrix.
The matching number of frequencies is not high enough to cover the desired frequency range which indicates that the reduction size cannot be as small as possible and preserve the desired dynamical information of a large model with a complex geometry. Since the frequency range of interest is not fully covered, it is not surprising to find such high error values.
The reason for the difference in the error values is the change of the reference response. It has been stated that the ID is meant to preserve the full system's response, which means that the 300 additional modes of the larger ID still have an influence on the lower frequency response. One reason could be a too low damping value causing this effect. Increasing the damping value, on the other hand, reduced the peaks in the frequency range of interest. Hence, these results can only be compared relatively to each other because a changing reference response seems to have a stronger influence than expected.

A little improvement due to a larger influence can be observed with the other two reduction methods in table 5.8. Each of them are able to match one more mode shape compared to the smaller ID size. This little improvement is, however, very little compared to the extra effort of computing a larger ID.
Although the SEREP-KSM results match the smallest amount of eigenfrequencies, the approximation of the FRF is the best. The increase in the error due to the larger ID is also less compared to the other results. This shows the major advantage of the KSM reduction which approximates the FRF directly instead of trying to match as many mode shapes and frequencies as possible.
This also indicates that the NRFD and ModMAC cannot replace the FRF correlation. On the contrary, a large number of matching modes and frequencies does not guarantee that the response of the full system is correctly approximated. Hence, the MOR methods and correlation techniques have to be carefully selected according to the purpose of the reduction.
The computation time states only the time for each reduction. A consideration of the total time required is considered at a later stage.

Since the influence of the larger ID is very little, table 5.9 presents the results for the second reduction size of 114. A parenthesis around a value represents difficulties during the evaluation process. Especially, the second two reduction methods benefit greatly from the increase of the reduced dimension, whereas SEREP-ICMS improves only slightly. The matching frequency range is just below the required range of interest, and the number of matching mode shapes is smaller compared to the other two reduction techniques. However, the $\mathcal{H}_2$ error decreases when a larger reduction size is chosen. Since this is the case for every two-step approach in table 5.9, it can be said that a good approximation of the full system's FRF requires a larger reduced representation.

Table 5.9: Comparison of Reduced Representations (114×114) for Different Sizes of IDs during a Two-Step MOR – 300 DoF (white) and 600 DoF (gray)

Measure of Goodness	SEREP-ICMS	SEREP-IRS	SEREP-KSM
1. No. of matching frequencies	61	105	65
	60	108	(60)
2. Last matching frequency in Hz	1993.40	2695.66	2055.05
	1973.23	2743.80	1993.40
3. No. of matching modes	56	81	62
	57	87	(60)
4. $\mathcal{H}_2$ error ($f_{\max} = 2033.69$ Hz) in %	12.58	10.07	2.54
	20.38	18.32	4.57
5. Computation time in min	8	24	9
	20	53	95

The large number of matching modes and frequencies for the SEREP-IRS method indicates that the iterated IRS method does converge to the results of a normal SEREP, as stated in [12]. The advantage of the two-step reduction is that the rigid body modes are already excluded by the first step MOR. The number of iterations has been set to 30 since the size of the ID is very small compared to the full system. The FRF response improves much more compared to the SEREP-ICMS reduction.

The greatest improve, however, occurs for the SEREP-KSM MOR. The $\mathcal{H}_2$ errors are the smallest compared to every other reduction method. A surprising effect is that the smaller ID produces better results. It has been observed that the frequency of 1993.40 Hz is missing using the larger ID. The reason of this discrepancy could not be explained, and it is assumed that the cause of this problem are some numerical issues. However, the difference in the $\mathcal{H}_2$ error occurs due to the different reference FRF of the full system when using differently sized ID.
The computation time is slightly out of proportion because at the calculation of the SEREP-KSM results for the larger ID, less computational resources were available, which also is the case for the SEREP-IRS two-step MOR. It is expected that the computation time is very similar to the SEREP-ICMS results.

It can be concluded that the influence of an ID is not as strong as the changing size of the reduced representation. For computational reasons, it is advisable to use the smaller size of 300 DoF. It could also be stated that the a suitable ID should have a $\mathcal{H}_2$ error of less than 5% when compared with the full system's response.

Pseudo Two-Step Model Order Reduction

A slightly different approach has to be taken when using the pseudo two-step MOR. In order to match the first 63 eigenfrequencies of the full system with a KSM reduction, the size of the reduced representation has to be larger than the number of frequencies, as can be observed in table 5.9 and 5.8, respectively. It is the safest approach to use twice as many Krylov modes as the target mode shapes $m_{\mathcal{K}} = 2m$.
An attempt has been made to preserve the 63 target mode shapes of the KSM-expanded modal matrix as well as to preserve all 126 modes computed by the first step. It was not possible to create a square a-set partition of the expanded modal matrix for the second case, and the smallest size to ensure a correct MOR has been found at 147 active DoF. The comparison of both reduced representations can be found in table 5.10 with two different pseudo two-step reductions – KSM-SEREP, KSM-Hybrid EMR. There are no differences

Table 5.10: Comparison of Pseudo Two-Step MOR with 126 Krylov Modes and Different Reduced Dimensions – 63×63 (white) and 147×147 (gray)

Measure of Goodness	KSM-Hybrid EMR	KSM-SEREP
1. No. of matching frequencies	63	63
	(64)	(67)
2. Last matching frequency in Hz	2033.69	2033.69
	2046.70	2083.35
3. No. of matching modes	63	63
	(-)	(63)
4. $\mathcal{H}_2$ error ($f_{\max} = 2033.69$ Hz) in %	22.30	22.30
	-	-
5. Computation time in min	202	174
	269	90

between SEREP and hybrid EMR for the smaller reduction size. This is also expected according to the reduction procedure of both methods. The larger reduction size creates, on the other hand, several difficulties which are indicated by the use of parenthesis.
The hybrid EMR creates a GR approximation of the 84 residual modes. This results in additional eigenfrequencies of the reduced representation which are very similar to the original values. Hence, it is difficult to distinguish the frequencies that have been preserved by the EMR reduction and which ones are the result of the GR approximation. This is also the case for the mode shapes, but it is important to emphasize that the desired mode shapes and frequencies are still produced by the reduced system. The problem is that the response is totally different due to the 84 residual modes.
SEREP produces a different approximation of the 84 residual modes which makes it very

easy to distinguish between residual modes and target modes. The residual frequencies of the reduced representation have either a value of zero or are very large compared to the target frequencies. In this example presented in table 5.10, one residual frequency is equal to zero and the rest is much larger compared to the frequency range of interest. Although the target modes are preserved, the distortion caused by residual modes creates a completely wrong FRF so that it was not even evaluated. The $\mathcal{H}_2$ error would in this cases be far greater than 1.
This implies that the modal subspace reduction methods only produce a good approximation of the response function if all important modes of the system are considered, and when the number of active DoF is equal to the number of target mode shapes. In every other case, the modes and frequencies are still preserved, but the FRF is completely different compared to the full system's response.
The time consideration is also not representative because of the lack of computational resources at the time of the calculations. The most realistic result of the required computation time is the 5376 seconds achieved with a KSM-SEREP reduction. Naturally, the hybrid EMR takes a bit longer due to the additional GR approximation.

Although no prior knowledge of the actual modal information is necessary, the results of the pseudo two-step are still comparable to the one-step SEREP reduction. This is, however, only the case when the a-set partition of the KSM-expanded modal matrix is of full-column rank.

5.5 Comparison to One-Step Model Order Reduction Methods

The computation of the FRF for the one-step MOR is performed by using 600 non-rigid modes of the full system. That means that the comparison of the $\mathcal{H}_2$ error has to include the larger ID results of the two-step MOR. At first, table 5.11 shows the results of the MOR for 2 different sizes of the reduced representation. The values in parenthesis indicate certain difficulties during the evaluation of the results. The GR could not deliver any satisfactory results. Not only creates the existence of rigid modes a difficulty for comparison with other MOR methods which exclude the rigid modes from the reduced representation but also over 50 eigenfrequencies computed by the GR have a value of infinity within the used Matlab software. This means that the results are not good enough for a FRF correlation. The extremeness of such a result is surprising because many commercial FE programs have this reduction method implemented. It is doubtful that a similar result would occur using one of the programs. The important point is that the GR requires, in any case, many more active DoF to create

Table 5.11: Results of One-Step MOR for Different Reduction Sizes – 63 DoF (white) and 114 DoF (gray) – with Results of the Corresponding Two-Step MOR in Square Brackets

Measure of Goodness	GR	Iterated IRS		KSM	
1. No. of matching frequencies	(0)	(53)	[57]	32	[32]
	(0)	(100)	[108]	61	[(60)]
2. Last matching frequency in Hz	-	1799.18	[1891.81]	1341.58	[1341.58]
	-	2607.63	[2743.80]	1993.40	[1993.40]
3. No. of matching modes	-	(49)	[55]	32	[31]
	-	(80)	[87]	60	[(60)]
4. $\mathcal{H}_2$ error ($f_{\max} = 2033.69$ Hz) in %	-	-	[39.10]	54.43	[32.88]
	-	-	[18.32]	5.56	[4.57]
5. Computation time in min	12	163	[24]	67	[9]
	13	200	[53]	103	[95]

a better approximation. For the purposes presented in this thesis, the quality of a GR is not sufficient.

The results of the iterated IRS reduction presented a difficulty as well because of the rigid modes within the reduced representation. This does not occur during the two-step procedure, which is one major advantage of the two-step reduction. By excluding the rigid modes with the first step, the MOR, which usually preserves the rigid mode shapes, can create a representation with only non-rigid modes. For the case of the IRS method, every result is improved using the two-step approach as can be seen in table 5.11. The only drawback is the time required to compute the necessary ID. For a smaller ID, e.g. 300 DoF instead of 600, the computation time for both one-step and two-step reduction would be very similar.

Due to the issues with the SEREP-KSM reduction, the improvements are not very obvious. However, the $\mathcal{H}_2$ error could still be reduced using a two-step procedure. The difference is even stronger when comparing it to the results of the (300×300)-sized ID. The major drawback is the additional time to create the two-step results when considering the time necessary to calculate an optimal ID.

An improvement for the presented one-step MOR can be achieved by using a two-step approach. However, the required additional time does not always justify the improved accuracy.

5.6 Comparison to One-Step Hybrid Model Order Reduction Methods

The hybrid MOR presented in table 5.12 also show similar problems as the previously discussed one-step MOR, and the affected areas are marked with parenthesis. The classic

Table 5.12: Results of Hybrid MOR to Different Reduced Sizes – 63 DoF (white) and 114 DoF (gray) – with Results of the Corresponding Two-Step MOR in Square Brackets

Measure of Goodness	CMS	Iterated ICMS		Hybrid EMR
1. No. of matching frequencies	(3)	(40)	[50]	63
	(54)	(58)	[60]	114
2. Last matching frequency in Hz	660.19	1536.88	[1754.10]	2033.69
	1821.88	1918.70	[1973.23]	2845.22
3. No. of matching modes	-	(39)	[47]	63
	(46)	(56)	[57]	114
4. $\mathcal{H}_2$ error ($f_{\max} = 2033.69$ Hz) in %	-	-	[36.26]	22.30
	-	-	[20.38]	7.74
5. Computation time in min	15	128	[20]	11
	19	137	[20]	13

CMS, which is also implemented in many FE software, shows the same issues as the GR in section 5.5. In both reduced representations, eight eigenfrequencies have the value of zero, and 52 seem to have the value of infinity within Matlab. However, the frequencies, which are not obviously incorrect, perfectly match the full system's eigenfrequencies. It is still surprising how bad both in commercial software implemented MOR perform in this test, which also casts some doubt towards their application and the interpretation of the results.
The same issue is also apparent using the one-step iterated ICMS reduction. Here, the smaller reduced representation produces eight rigid eigenfrequencies and seven of the infinity value. The larger representation computes precisely the six rigid modes with the corresponding frequencies but also 37 infinity, which were all removed for the correlation. It can be seen that the two-step reduction not only prevents such errors but also results in a better approximation of the full system.
There is no difference to the results of the hybrid EMR and the SEREP reduction when the number of active DoF n is equal to the number of target mode shapes m, which can be observed in table 5.12.

5.7 Proposal of a New Approach for Additional Node Selection

The result of the one-step SEREP reduction approach has not been presented, yet. In order to compute the reduced representation, the EfI_3^+ algorithm has been applied to find additional three nodes since the initial a-set consists of 54 DoF, and it is desired to approximate 63 non-rigid modes. The reduced representation is able to represent all target mode shapes and frequencies, however, lacks in a good representation of the FRF. A comparison of the FRF between the KSM is presented in table 5.13 for two different reduction sizes. The subscript *new* indicates the a-set selected with the new approach.

Table 5.13: Comparison of a-sets for SEREP and KSM – Size of Reduction 63 DoF (white) and 114 DoF (gray)

Measure of Goodness	**KSM**	**KSM$_{\text{new}}$**	**SEREP**	**SEREP$_{\text{new}}$**
1. No. of matching frequencies	32	32	63	63
	61	61	114	114
2. Last matching frequency in Hz	1341.58	1341.58	2033.69	2033.69
	1993.40	1993.40	2845.22	2845.22
3. No. of matching modes	32	32	63	63
	60	60	114	114
4. $\mathcal{H}_2$ error ($f_{\max} = 2033.69$ Hz) in %	54.43	48.76	22.30	6.69
	5.56	6.02	7.74	8.67
5. Computation time in min	67	53	1	1
	103	94	2	2

The new node selection method does not change the preservation of the mode shapes and frequencies. However, it strongly affects the FRF as can be observed in figure 5.2. The FRF approximation of the SEREP reduction using the new approach for selecting additional nodes increases compared to the a-set selected with EfI_3^+. In table 5.13, it can be noticed that this improvement only affects the smaller reduced representation because for a smaller number of additional nodes, the impact of selecting a non-optimal node is magnified. It is important to emphasize that both a-sets are completely sufficient to preserve the target mode shapes and eigenfrequencies of the full system.

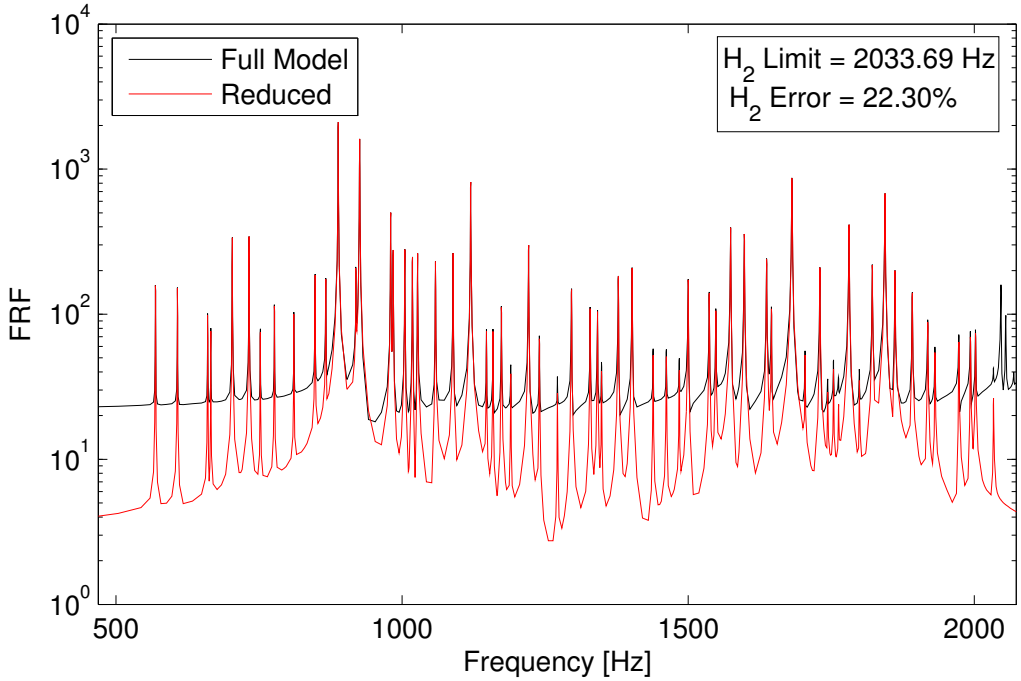

(a) FRF for Additional Nodes Using EfI$_3$$^+$ Algorithm

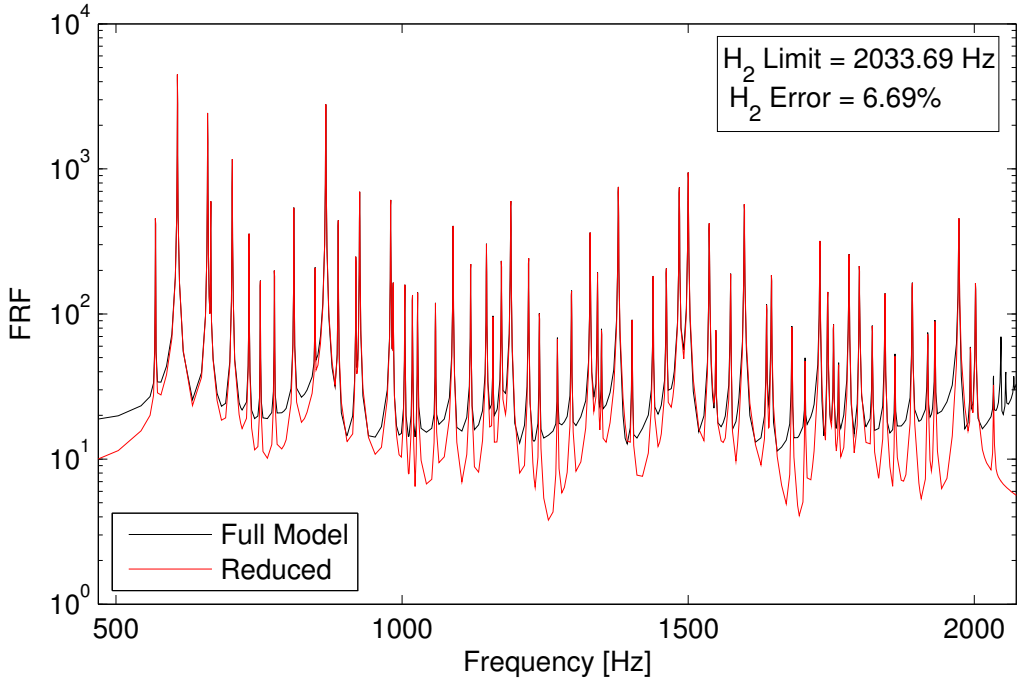

(b) FRF for Additional Nodes New Approach

Figure 5.2: Influence of Node Selection for SEREP reduction on FRF Behaviour

Table 5.14 demonstrates the idea behind the suggested method by presenting the first three additional nodes selected by the EfI_3^+ method with a different number of target modes.

Table 5.14: Results of the EfI_3^+ Algorithm with a Different Number of Target Modes

No. of additional node	63 Modes	114 Modes	300 Modes	600 Modes
1.	54385	14641	14641	14641
2.	62055	24325	4948	24385
3.	25232	62058	5598	5598

Different nodes are selected because the ranking changes with an increasing number of mode shapes. Suddenly, more modal information is within the FIM, and the algorithm chooses the best candidate to preserve as much information as possible. So the selection with 63 target modes will try to preserve totally different modal information as the same method using 600 target mode shapes. The location of the nodes selected by these two examples are presented in table 5.15.

Table 5.15: Location of Additional Nodes Using 63 and 600 Target Modes with EfI_3^+

Node number	X	Y	Z
1. 54385	-439.40	-143.52	-103.89
2. 62055	-337.28	176.92	-428.82
3. 25232	-264.84	-53.119	-587.54
1. 14641	-137.94	-69.41	-180
2. 24385	-138.35	103.18	-142.85
3. 5598	-457.20	191.00	-353.25

Depending on the number of selected target modes, the iterative expansion methods rank the candidate set differently and select a different a-set. The active DoF chosen by the larger number of target modes can preserve the response of the system even for a small reduced representation. The results shown in table 5.13 and figure 5.2 have been achieved by manually selecting the first three additional nodes of the EfI_3^+ result and using this new a-set for a SEREP reduction.

The new approach would have to use a different set of modes which is referred to as the *response modes*. These are the modes which have been pre-defined to be the response of

the full system. It could be as many as 1000 mode shapes or as little as 100. Depending upon the decision of the response mode shape number, an EfI$_3$+ algorithm can be applied to select additional nodes using the response modes instead of the usually suggested target mode shapes. The number of the target modes is defining the size of the reduced representation and is used to exit the iterative selection procedure which occurs once the size of the a-set n is equal to the number of target mode shapes m. This way the reduced representation will preserve the m selected eigenfrequencies and modes, as well as producing a better approximation of the FRF which has been demonstrated in figure 5.2.

The Two-Step MOR methods show interesting capabilities in creating an ID which allows other reduction techniques to safely create a final reduced representation without the typical issues presented during a one-step approach. A proposed pseudo two-step is able to create the accuracy of a modal subspace reduction methods without any modal information available prior to the first reduction step. And finally, the here suggested new selection method for an additional a-set holds the potential to create small reduced representations with an acceptable approximation of the full systems response.

6 Summary and Conclusions

The objectives of this thesis are to find an optimal combination of model order reduction methods for a possible two-step approach. Furthermore, it is necessary to select a suitable ID and to implement the functions into the Matlab-based software MORPACK.
For the selection of an optimal ID, several selection methods are investigated. They can be classified into the non-iterative, iterative reduction, and iterative expansion methods. The suitability of each algorithm is discussed using a FE model of a gear box [39].
For the purpose of the suitable ID selection, the iterative expansion methods produce the best results. The optimal ID is preserving all modal information required to compute the full system's response to an excitation. The modal subspace reduction method SEREP is the best candidate to create such an ID. The partition of the modal matrix has to have an equal number of active DoF and target modes in such a case.
During the iterative expansion method, no rank increase of the FIM occurs when rotational DoF are included. Since they hold redundant information, only translational DoF can be considered to achieve a square a-set partition of the modal matrix. The implemented algorithm EfI_3+ is adapted to exclude nodes with rotational DoF.
Comparison of two IDs show almost no differences in the results of a two-step reduction indicating that a smaller size is sufficient as long as the $\mathcal{H}_2$ error with the full system's response is below 5%. This would have to be validated with more examples which could be part of future research. A stronger influence, on the other hand, is created by the size of the reduced representation.

Three different two-step MOR methods have been compared – SEREP-ICMS, SEREP-IRS, and SEREP-KSM. The latter reduction method produced best results compared also to the one-step KSM technique. The drawback is, however, the requirement of modal information and the additional time for computing an a-set for a suitable ID. A pseudo two-step (KSM-SEREP) is presented to overcome the need for modal information in order to be able to produce results similar to the SEREP one-step approach. The pseudo two-step could also be interpreted as producing the results of the KSM reduction within the physical space.
It has been observed that the KSM produces superior approximation of the system's response compared to the SEREP reduction. This is, however, only the case for a minimal size of the reduced representation. It is often required to have a representation far below this limit, and

the approximation of the SEREP method becomes better compared to KSM.
In order to improve the response for very small reduced representations using the SEREP approach, a new additional node selection method is proposed.

Future research could be concerning the implementation of the new selection approach and to validate the current assumptions. It is also expected that the results of the pseudo two-step would benefit from the new selection method.
Since the problem is the limited size of the reduced representation, another promising reduction approach is suggested by Nimityongskul and Kammer [45]. The suggested reduction method is based on principal component analysis and is meant to be able to preserve more of the FRF of the full system with a smaller reduced representation.
Other variants of the a-set selection like mass-weighting and pre-conditioning with a non-iterative approach have not been pursued. Advantages of the pre-conditioning could be apparent but have not been observed.

7 Zusammenfassung und Ausblick

Das Ziel dieser Arbeit besteht in der Ermittlung einer optimalen Kombination von strukturmechanischen Modellreduktionsverfahren für ein mögliches Zweischritt-Reduktionsverfahren. Dabei soll die Wahl einer geeigneten Zwischendimension getroffen und die Verfahren zur Ermittlung der Zwischendimension in die am Lehrstuhl für Dynamik und Mechanismentechnik entwickelte Software MORPACK implementiert werden.

Für die Ermittlung einer optimalen Zwischendimension werden verschiedene Verfahren untersucht, die in direkte, iterativ reduzierende und iterativ expandierende Verfahren unterteilt werden können. Die Eignung der einzelnen Algorithmen wird an dem Finite-Elemente-Modell eines Getriebegehäuses nach [39] diskutiert, wobei iterativ expandierende Verfahren die besten Resultate liefern. Eine optimale Zwischendimension enthält alle charakteristischen Systemantworten des vollen Systems auf eine Anregung. Die Modalreduktion SEREP erweist sich als bestes Verfahren, um diese zu erzeugen, wobei die Masterpartition der Modalmatrix für diesen Fall quadratisch sein muss.
Beim iterativ expandierenden Verfahren wächst der Rang der Fischer-Informationsmatix nicht an, wenn rotatorische Freiheitsgrade hinzugefügt werden. Daher sind nur Knoten mit ausschließlich Translationsfreiheitsgraden zu wählen. Der implementierte Algorithmus $\mathrm{EfI}_3{}^+$ wird entsprechend angepasst.
Der Vergleich zweier Zwischendimensionen zeigt keinen Unterschied auf das Ergebnis der Zweischritt-Reduktion, wobei die Dimension eine ausreichende Größe hat, wenn der $\mathcal{H}_2$-Fehler im Vergleich zur vollen Systemantwort unterhalb von 5% liegt. Dieses Ergebnis ist jedoch an weiteren Modellen zu validieren und somit Teil zukünftiger Forschung. Einen wesentlich größeren Einfluss auf das Reduktionsergebnis hat die reduzierte Dimensionsgröße.

Es werden drei verschiedene Zweischritt-Reduktionsverfahren verglichen – SEREP-ICMS, SEREP-IRS und SEREP-KSM, wobei letzteres die besten Ergebnisse liefert, was darüber hinaus auch im Vergleich zu einem Einschritt-KSM-Verfahren gilt. Nachteilig wirkt sich die Verwendung und damit Voraussetzung der modalen Größen und die zusätzliche Berechnungszeit für eine geeignete Zwischendimension aus. Ein Pseudo-Zweischritt-Verfahren (KSM-SEREP) wird vorgestellt, welches, ohne modalen Größen zu benötigen, Ergebnisse

ähnlich zum SEREP-Einschritt-Verfahren erzeugt. Das Pseudo-Zweischritt-Verfahren kann auch als KSM-Reduktion in den Anschauungsraum interpretiert werden.
Es wird eine bessere Approximation der Systemantwort durch KSM im Vergleich zu SEREP beobachtet, was jedoch nur bis zu einer minimalen, reduzierte Dimension der Fall ist. Wird, was häufig der Fall ist, eine reduzierte Dimension weit unterhalb dieser Grenze benötigt, liefert SEREP im Vergleich zu KSM bessere Ergebnisse.
Um die Systemantwort für mit reduced with SEREP auf sehr kleine Dimension reduzierte Systeme weiter zu verbessern, wird ein neues Verfahren zur Auswahl zusätzlicher Masterknoten vorgeschlagen.

Weitere Forschungsarbeit ist für die Implementierung der vorgeschlagenen Knotenauswahlmethode und die Validierung der gemachten Annahmen notwendig. Es ist zu erwarten, dass das Pseudo-Zweischritt-Verfahren von dieser Methode profitiert.
Da das Problem der limitierten, reduzierten Dimensionsgröße besteht, wird ein vielversprechendes Reduktionsverfahren nach Nimityongskul und Kammer [45] vorgeschlagen. Das vorgeschlagene Reduktionsverfahren basiert auf einer Hauptwert-Analyse und wird als fähig beschrieben, ein besseres FRF im Vergleich zum vollen System bei kleinerer, reduzierter Dimension zu erzeugen.
Die Untersuchung weiterer Varianten der Masterfreiheitsgradauswahl, wie die Massenwichtung und Vorkonditionierung mit nichtiterativer Näherung wird nicht verfolgt. Vorteile aus der Vorkonditionierung sind vorstellbar, werden jedoch nicht beobachtet.

Bibliography

[1] Allemang, Randall J.: The Modal Assurance Criterion - Twenty Years of Use and Abuse. In: *Journal of Sound and Vibration* (2003)

[2] Anton, Howard; Rorres, Chris: *Elementary Linear Algebra*. John Wiley and Sons, 2005

[3] Avitabile, Peter; O'Callahan, John; Milani, John: Model Correlation and Orthogonality Criteria. In: *Proceedings of the 14th International Modal Analysis Conference* (1988)

[4] Ben-Israel, Adi; Greville, Thomas N.: *Generalized Inverses: Theory and Applications*. Springer-Verlag New York, 2003

[5] Bonisoli, Elvio; Delprete, Cristiana; Rosso, Carlo: Proposal of a Modal-Geometrical-Based Master Nodes Selection Criterion in Modal Analysis. In: *Mechanical Systems and Signal Processing* (2008)

[6] Chung, Y.-T.; Moore, D.: On-Orbit Sensor Placement and System Identification of Space Station with Limited Instrumentations. In: *Proceedings of the 11th International Modal Analysis Conference* (1993)

[7] Coote, J.E; Lieven, N.A.J.; Skingle, G.W.: Sensor Placement Optimisation for Modal Testing of a Helicopter Fuselage. In: *Proceedings of the 24th International Modal Analysis Conference* (2005)

[8] Craig JR., Roy R.: Coupling of Substructures for Dynamic Analysis: An Overview. In: *AIAA Journal* (2000)

[9] Craig JR., Roy R.; Bampton, Mervyn C.: Coupling of Substructures for Dynamic Analysis. In: *AIAA Journal* (1968)

[10] Fehr, J.: *Automated and Error Controlled Model Reduction in Elastic Multibody Systems*, Institut für Technische und Numerische Mechanik, Universität Stuttgart, Dissertation, 2011

[11] Finkbeiner, Daniel T.: *Introduction to Matrices and Linear Transformations.* W. H. Freeman and Company, 1960

[12] Friswell, M.I.; Garvey, S.D.; Penny, J.E.: Model Reduction Using Dynamic and Iterated IRS Techniques. In: *Journal of Sound and Vibration* (1995)

[13] Friswell, M.I.; Garvey, S.D.; Penny, J.E.: The Convergence of the Iterated IRS Method. In: *Journal of Sound and Vibration* (1998)

[14] Garvey, S.D.; Friswell, M.I.; Penny, J.E.: Evaluation of a Method for Automatic Selection of Measurement Locations Based on Subspace-Matching. In: *Proceedings of the 14th International Modal Analysis Conference* (1996)

[15] Golub, Gene H.; Van Loan, Charles F.: *Matrix Computarions.* The Johns Hopkins Universiy Press, 1996

[16] Guyan, Robert J.: Reduction of Stiffness and Mass Matrices. In: *AIAA Journal* (1965)

[17] Henshell, R. D.; Ong, J. H.: Automatic Masters for Eigenvalue Economization. In: *Earthquake Engineering and Structural Dynamics* (1974)

[18] Hintz, Robert M.: Analytical Methods in Modal Component Synthesis. In: *AIAA Journal* (1975)

[19] Häggblad, B.; Eriksson, L.: Model Reduction Methods for Dynamic Analysis of Large Structures. In: *Computers and Structures* (1993)

[20] Jarvis, Brian: Enhancements to Modal Testing Using Finite Elements. In: *Proceedings of the 14th International Modal Analysis Conference* (1991)

[21] Kammer, Daniel C.: Test-Analysis-Model Development using an Exact Modal Reduction. In: *The International Journal of Analytical and Experimental Mechanics* (1987)

[22] Kammer, Daniel C.: A Hybrid Approach to Test-Analysis-Model Development for Large Space Structures. In: *Journal of Vibration and Acoustics* (1991)

[23] Kammer, Daniel C.: Sensor Placement for On-Orbit Modal Identification and Correlation of Large Space Structures. In: *Journal of Guidance, Control, and Dynamics* (1991)

[24] Kammer, Daniel C.: Correlation Considerations - Part 2: Model Reduction Using Modal, SEREP, and Hybrid. In: *Proceedings of the 16th International Modal Analysis Conference* (1998)

[25] Kammer, Daniel C.: Sensor Set Expansion for Modal Vibration Testing. In: *Mechanical Systems and Signal Processing* (2005)

[26] Kammer, Daniel C.; Baker, Mary: A Comparison of the Craig-Bampton and Residual Flexibility Methods for Component Substructure Representation. In: *Structural Dynamics Research Corporation* (1985)

[27] Kammer, Daniel C.; Jensen, Brent M.; Mason, Donald R.: Test-Analysis Correlation of the Space Shuttle Solid Rocket Motor Center Segment. In: *Journal of Spacecraft and Rockets* (1989)

[28] Kammer, Daniel C.; Peck, Jeffrey A.: Mass-Weighting Methods for Sensor Placement Using Sensor Set Expansion Techniques. In: *Mechanical Systems and Signal Processing* (2008)

[29] Kammer, Daniel C.; Tinker, Michael L.: Optimal Placement of Triaxial Accelerometers for Modal Vibration Tests. In: *Mechanical Systems and Signal Processing* (2004)

[30] Kammer, Daniel C.; Triller, M. J.: Efficient Sensor Placement for On-Orbit Modal Identification of Sequentially Assembled Large Space Structures. In: *The International Journal of Analytical and Experimental Modal Analysis* (1992)

[31] Kidder, Robert L.: Reduction of Structural Frequency Equations. In: *AIAA Journal* (1973)

[32] Kielbasiński, A.; Schwetlick, H.: *Numerische lineare Algebra*. VEB Deutscher Verlag der Wissenschaften, 1988

[33] Klein, Bernd: *FEM Grundlagen und Anwendung der Finite-Elemente-Methods im Maschinen- und Fahrzeugbau*. Vieweg und Teubner Verlag, 2010

[34] Koutsovasilis, P.; Quarz, V.; Beitelschmidt, M.: MORPACK interface functionality for importing FE structures into MBS-code via alternative model order reduction methods. (2008)

[35] Koutsovasilis, Panagiotis: *Model Order Reduction in Structural Mechanics: Coupling the Rigid and Elastic Multi Body Dynamics*, TU Dresden, Dissertation, 2009

[36] Larson, C. B.; Zimmermann, D. C.; Marek, E. L.: A Comparison of Modal Test Planning Techniques: Excitation and Sensor Placement Using the NASA 8-Bay Truss. In: *Proceedings of the 12th International Modal Analysis Conference* (1994)

[37] Lehner, Michael; Eberhard, Peter: A Two-Step Approach for Model Reduction in Flexible Multibody Dynamics. In: *Multibody System Dynamics* (2007)

[38] Lein, C.; Beitelschmidt, M.: MORPACK-Schnittstelle zum Import von FE-Strukturen nach SIMPACK. In: *at-Automatisierungstechnik* (2012)

[39] Lein, C.; Beitelschmidt, M.: Impact of Geometry Simplification and Element Size of the FEM-MBS-Coupling-Process. In: *NAFEMS European Conference on Coupled MBS-FE Applications* (2013), November

[40] Li, D.S.; Li, H.N.; Fritzen, C.P.: The Connection Between Effective Independence and Modal Kinetic Energy Methods for Sensor Placement. In: *Journal of Sound and Vibration* (2007)

[41] MacNeal, Richard H.: A Hybrid Method of Component Mode Synthesis. In: *Computers and Structures* (1971)

[42] Maess, Gerhard: *Vorlesungen über numerische Mathematik I.* Akademie-Verlag Berlin, 1984

[43] Mains, Michael L.: Orthogonality for Modal Vector Correlation: The Effects of Removing Degrees-of-Freedom. In: *Proceedings of the Society for Experimental Mechanics Series* (2013)

[44] Martinez, David R.; Carne, Thomas G.; Gregory, Dan L.; Miller, A. K.: Combined Experimental/Analytical Modeling using Component Mode Synthesis. In: *25th Structures, Structural Dynamics and Materials Conference* (1984)

[45] Nimityongskul, Sonny; Kammer, Daniel C.: Frequency domain model reduction based on principal component analysis. In: *Mechanical Systems and Signal Processing* (2010)

[46] O'Callahan, John: A Procedure for an Improved Reduced System (IRS) Model. In: *Proceedings of the 7th International Modal Analysis Conference* (1989)

[47] O'Callahan, John: Development of a General Pseudo Orthogonality Correlation Procedure. In: *Proceedings of International Society for Optical Engineering* (1995)

[48] O'Callahan, John: Correlation Considerations - Part 4: Modal Vector Correlation Techniques. In: *Proceedings of the 16th International Modal Analysis Conference* (1998)

[49] O'Callahan, John: Reduced Model Concepts. In: *Proceedings of the 18th International Modal Analysis Conference* (2000)

[50] O'Callahan, John; Avitabile, Peter; Riemer, Robert: System Equivalent Reduction Expansion Process (SEREP). In: *Proceedings of the 7th International Modal Analysis Conference* (1989)

[51] O'Callahan, John; Li, Ping: A Automatic Selection of Reduced Degrees of Freedom. In: *Proceedings of International Society for Optical Engineering* (1994)

[52] O'Callahan, John; Li, Ping: A Non Smoothing SEREP Process for Modal Expansion. In: *Proceedings of the 12th International Modal Analysis Conference* (1994)

[53] Papadopoulos, Michael; Garcia, Ephrahim: Sensor Placement Methodologies for Dynamic Testing. In: *American Institute of Aeronautics and Astronautics* (1998)

[54] Park, Youn-Sik; Kim, Hong-Bae: Sensor Placement Guide for Model Comparison and Improvement. In: *Proceedings of International Society for Optical Engineering* (1996)

[55] Penny, J. E. T.; Friswell, M. I.; Garvey, S. D.: Automatic Choice of Measurement locations for Dynamic Testing. In: *AIAA Journal* (1994)

[56] Penrose, R.: A Generalized Inverse for Matrices. In: *Mathematical Proceedings of the Cambridge Philosophical Society* (1955)

[57] Poston, Wendy L.: *Optimal Sensor Locations for On-Orbit Modal Identification of Large Space Structures*, The Graduate School of Engineering and Applied Science of The George Washington University, Master's Thesis, 1991

[58] Rubin, S.: Improved Component-Mode Representation for Structural Dynamic Analysis. In: *AIAA Journal* (2075)

[59] Salimbahrami, Behnam; Lohmann, Boris: Krylov Subspace methods in linear model order reduction: Introduction and invariance properties. In: *Sci. Rep.. Inst. of Automation* (2002)

[60] Salimbahrami, Behnam; Lohmann, Boris: Order Reduction of Large Scale Second-Order Systems using Krylov Subspace Methods. In: *Linear Algebra and its Applications* (2006)

[61] Schwetlick, H.: *Numerische Lösung nichtlinearer Gleichungen.* VEB Deutscher Verlag der Wissenschaften, 1979

[62] Tasker, Frederick A.; Liu, Chinchao: Variance-Based Sensor Placement for Modal Identification of Structures. In: *Journal of Guidance, Control, and Dynamics* (1995)

[63] Zienkiewicz, O. C.; Taylor, R. L.: *Finite Element Method: Its Basis and Fundamentals.* Elsevier Butterworth-Heinemann, 2005

List of Tables

2.1 Overview of MOR Methods Based on Subspace Spanned by the Transformation Matrix 7

3.1 Overview of Selection Methods 25

4.1 Available Options for Non-Iterative Selection Methods in MORPACK 45
4.2 Available Options for Iterative Reduction Methods in MORPACK 46
4.3 Available Options for Iterative Expansion Methods in MORPACK 48

5.1 Results of Non-Iterative Methods using Rank Criterion (white) and Condition Number Criterion (gray) 59
5.2 Results of Variants of MKE and DPR using Rank Criterion (white) and Condition Number Criterion (gray) 60
5.3 Results of Iterative Reduction Methods using Rank Criterion (white) and Condition Number Criterion (gray) 61
5.4 Results of the EfI Algorithm with Different Elimination Rates 62
5.5 Results of Iterative Expansion Methods using Rank Criterion (white) and Condition Number Criterion (gray) 63
5.6 Comparison of $\mathcal{H}_2$ Error Until $f_{\max} = 2033.69$ Hz for Different Intermediate Dimensions 65
5.7 Computation Time Considerations for the Gear Box Model 66
5.8 Comparison of Reduced Representations ($\mathbf{63} \times \mathbf{63}$) for Different Sizes of IDs during a Two-Step MOR – 300 DoF (white) and 600 DoF (gray) 66
5.9 Comparison of Reduced Representations ($\mathbf{114} \times \mathbf{114}$) for Different Sizes of IDs during a Two-Step MOR – 300 DoF (white) and 600 DoF (gray) 68
5.10 Comparison of Pseudo Two-Step MOR with 126 Krylov Modes and Different Reduced Dimensions – $\mathbf{63} \times \mathbf{63}$ (white) and $\mathbf{147} \times \mathbf{147}$ (gray) 69
5.11 Results of One-Step MOR for Different Reduction Sizes – 63 DoF (white) and 114 DoF (gray) – with Results of the Corresponding Two-Step MOR in Square Brackets 71

5.12 Results of Hybrid MOR to Different Reduced Sizes – 63 DoF (white) and 114 DoF (gray) – with Results of the Corresponding Two-Step MOR in Square Brackets 72
5.13 Comparison of a-sets for SEREP and KSM – Size of Reduction 63 DoF (white) and 114 DoF (gray) 73
5.14 Results of the EfI_3+ Algorithm with a Different Number of Target Modes . . . 75
5.15 Location of Additional Nodes Using 63 and 600 Target Modes with EfI_3+ . . . 75

List of Figures

2.1 Typical Procedure of a Model Order Reduction and Correlation 6
2.2 Comparison of a Hybrid Reduction (left) and a Two-Step Reduction (right) . . 16
2.3 Normalized Relative Frequency Difference with Error Limit at 5% 21
2.4 ModMAC with RMS values of the diagonal and off-diagonal terms 23

3.1 Non-Iterative Selection Procedure 26
3.2 Iterative Reduction Methods Procedure 29
3.3 Iterative Expansion Methods Procedure 35

4.1 Available Modules in MORPACK 42
4.2 Structure of the Module AddNodes in MORPACK 43
4.3 Possible Two-Step MOR Combinations 49
4.4 Pseudo Two-Step (KSM-SEREP) Procedure 55

5.1 Finite Element Model of a Gear Box 58
5.2 Influence of Node Selection for SEREP reduction on FRF Behaviour 74

A.1 NRFD of SEREP-ICMS with 600 Modes (ID), 54 Active Dof and 9 CB Modes 87
A.2 ModMac of SEREP-ICMS with 600 Modes (ID), 54 Active Dof and 9 CB Modes 88
A.3 FRF of SEREP-ICMS with 600 Modes (ID), 54 Active Dof and 9 CB Modes . 88
A.4 $\boldsymbol{\mathcal{H}_2}$ Error of SEREP-ICMS with 600 Modes (ID), 54 Active Dof and 9 CB Modes 89
A.5 NRFD of SEREP-IRS with 600 Modes (ID) and 63 Active Dof 89
A.6 ModMac of SEREP-IRS 600 Modes (ID) and 63 Active Dof 90
A.7 FRF of SEREP-IRS with 600 Modes (ID) and 63 Active Dof 90
A.8 $\boldsymbol{\mathcal{H}_2}$ Error of SEREP-IRS with 600 Modes (ID) and 63 Active Dof 91
A.9 NRFD of SEREP-KSM with 600 Modes (ID) and 63 Krylov Modes 91
A.10 ModMac of SEREP-KSM with 600 Modes (ID) and 63 Krylov Modes 92
A.11 FRF of SEREP-KSM with 600 Modes (ID) and 63 Krylov Modes 92
A.12 $\boldsymbol{\mathcal{H}_2}$ Error of SEREP-KSM with 600 Modes (ID) and 63 Krylov Modes 93

A Appendix

A.1 Results of Two-Step Model Order Reduction

The results of the two-step MOR for the larger ID size are presented in this section. Please, refer for further figures of the other reduction methods to the enclosed data CD.

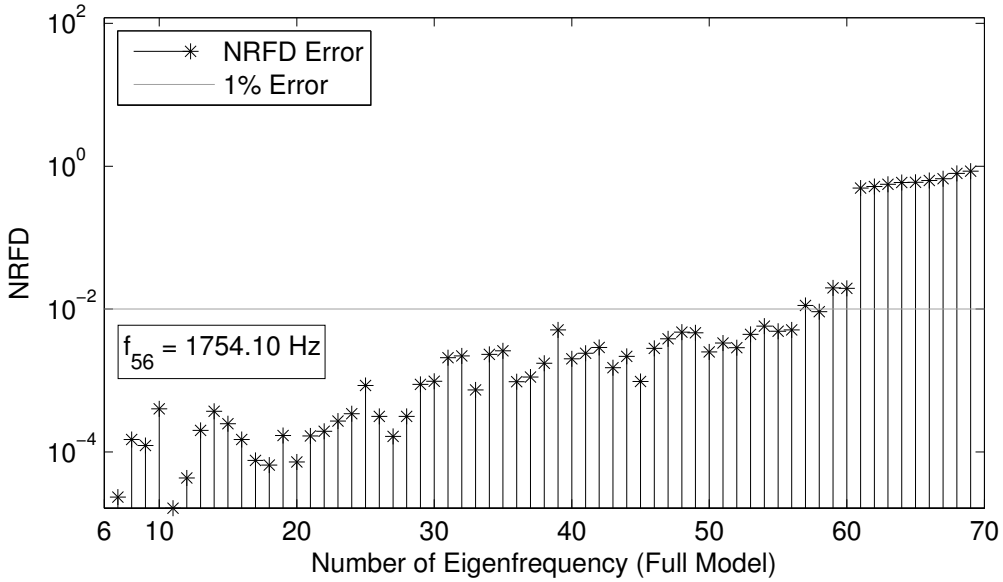

Figure A.1: NRFD of SEREP-ICMS with 600 Modes (ID), 54 Active Dof and 9 CB Modes

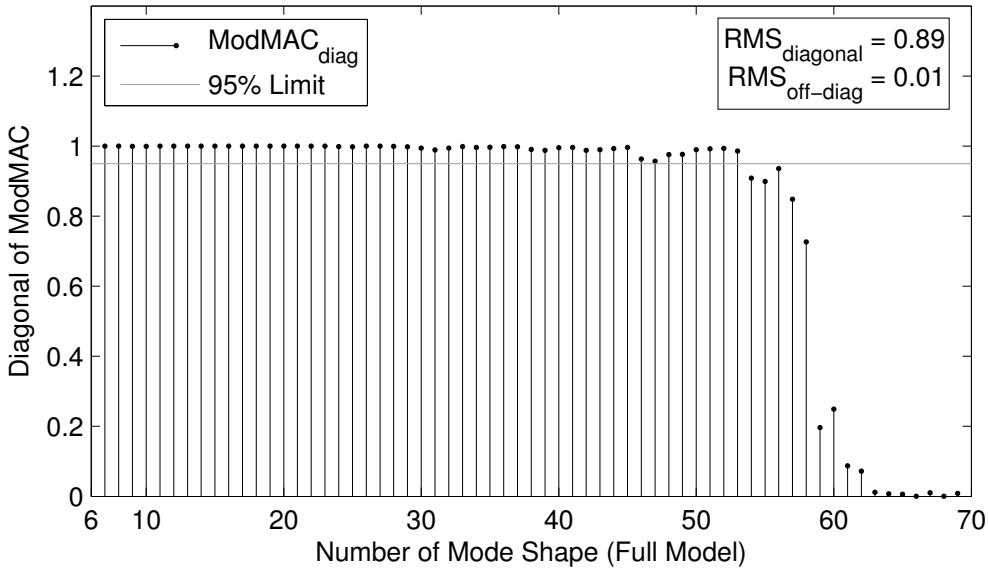

Figure A.2: ModMac of SEREP-ICMS with 600 Modes (ID), 54 Active Dof and 9 CB Modes

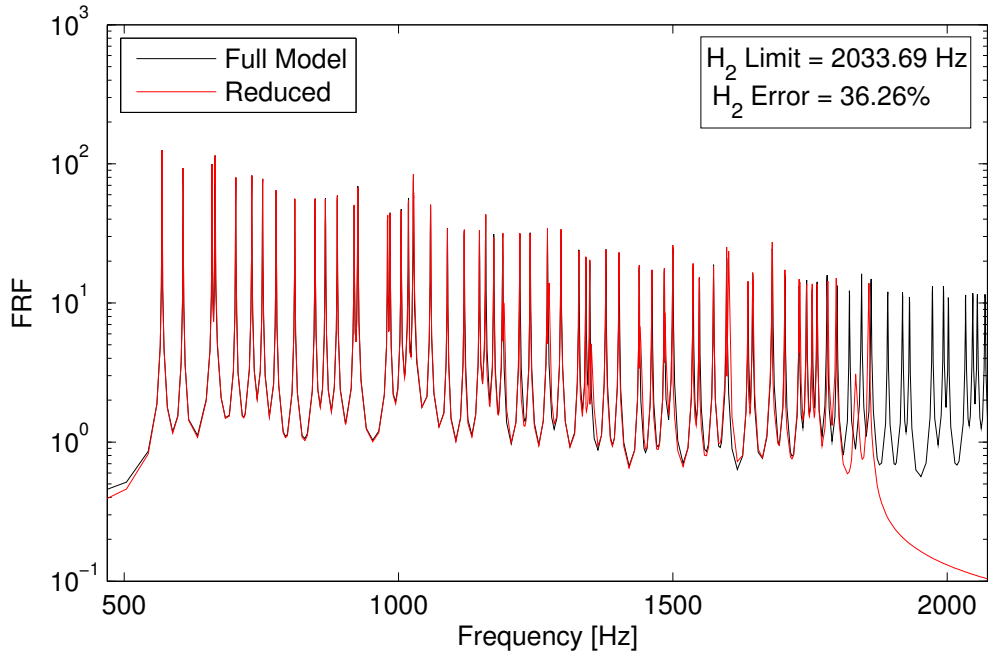

Figure A.3: FRF of SEREP-ICMS with 600 Modes (ID), 54 Active Dof and 9 CB Modes

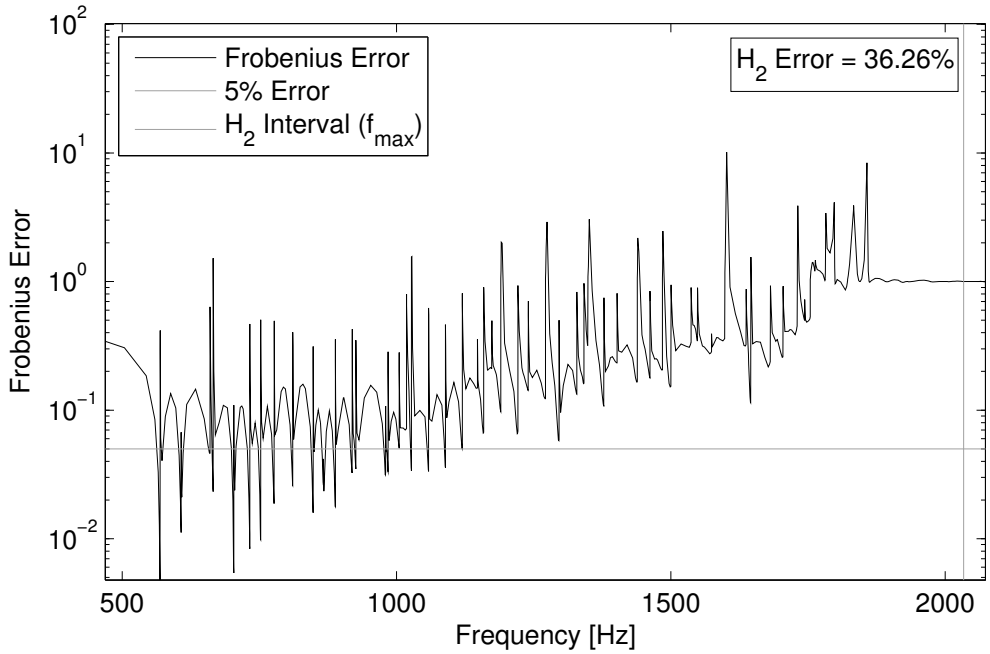

Figure A.4: $\mathcal{H}_2$ Error of SEREP-ICMS with 600 Modes (ID), 54 Active Dof and 9 CB Modes

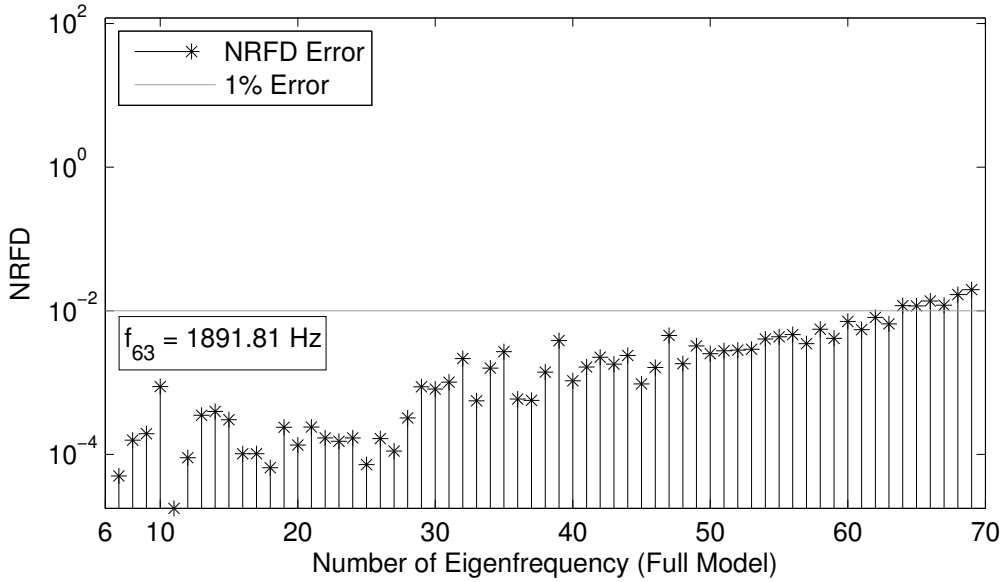

Figure A.5: NRFD of SEREP-IRS with 600 Modes (ID) and 63 Active Dof

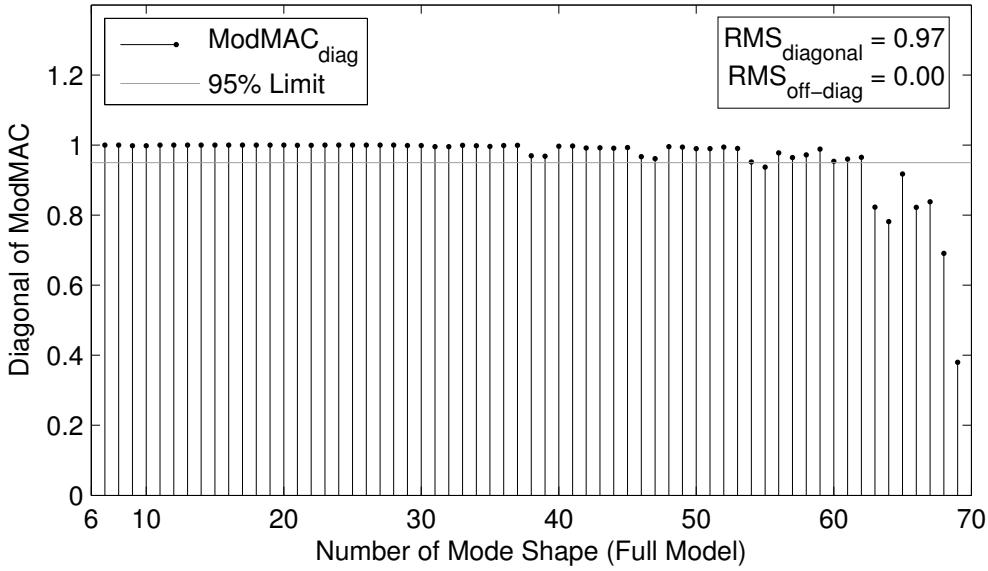

Figure A.6: ModMac of SEREP-IRS 600 Modes (ID) and 63 Active Dof

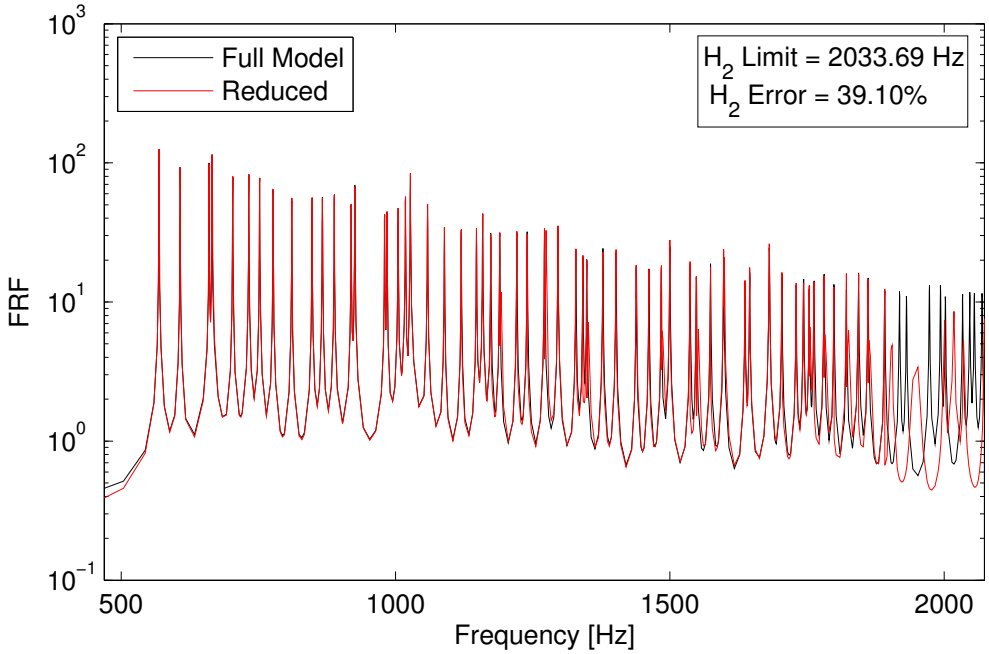

Figure A.7: FRF of SEREP-IRS with 600 Modes (ID) and 63 Active Dof

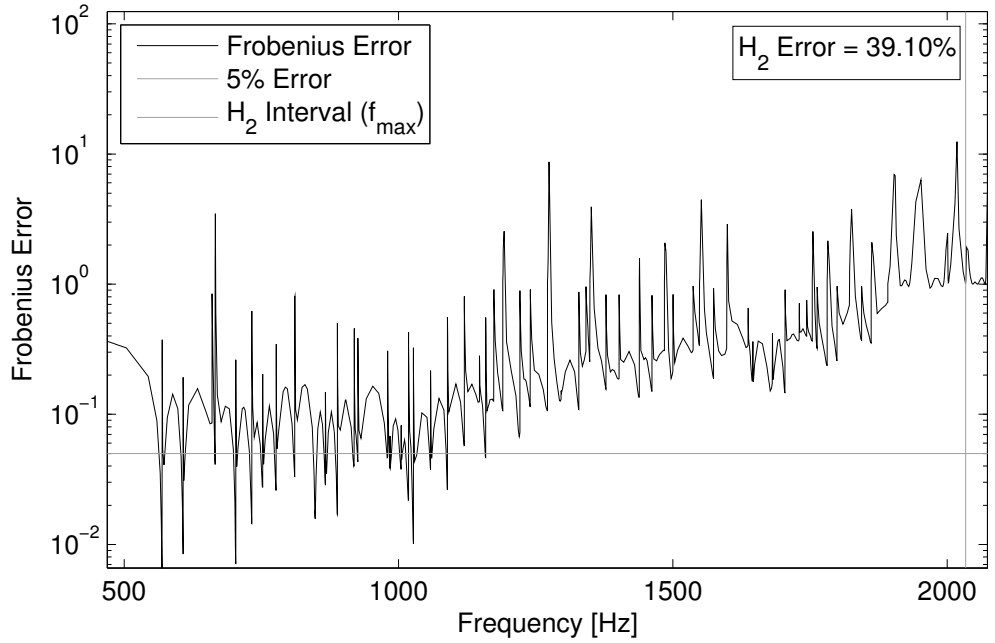

Figure A.8: $\mathcal{H}_2$ Error of SEREP-IRS with 600 Modes (ID) and 63 Active Dof

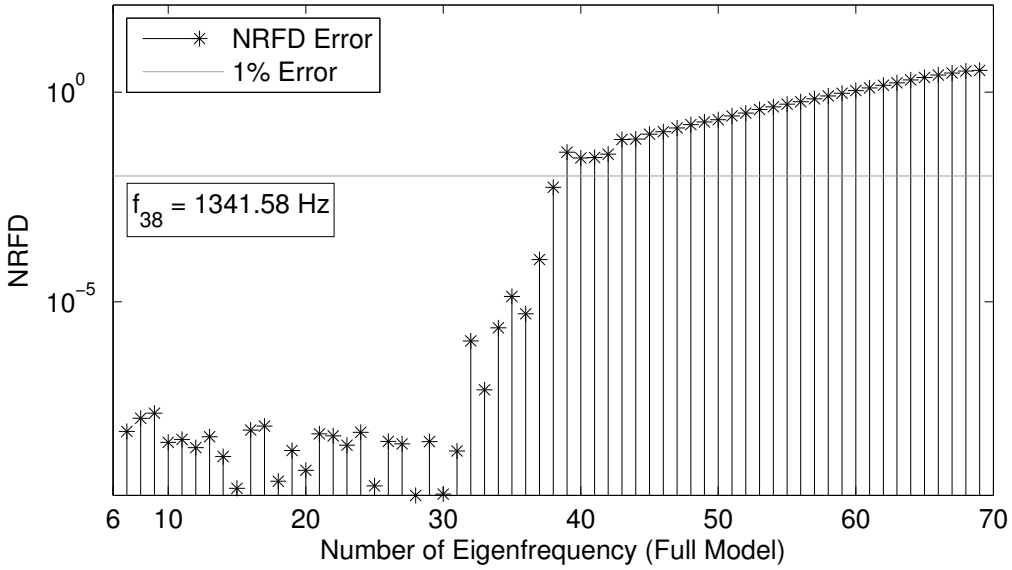

Figure A.9: NRFD of SEREP-KSM with 600 Modes (ID) and 63 Krylov Modes

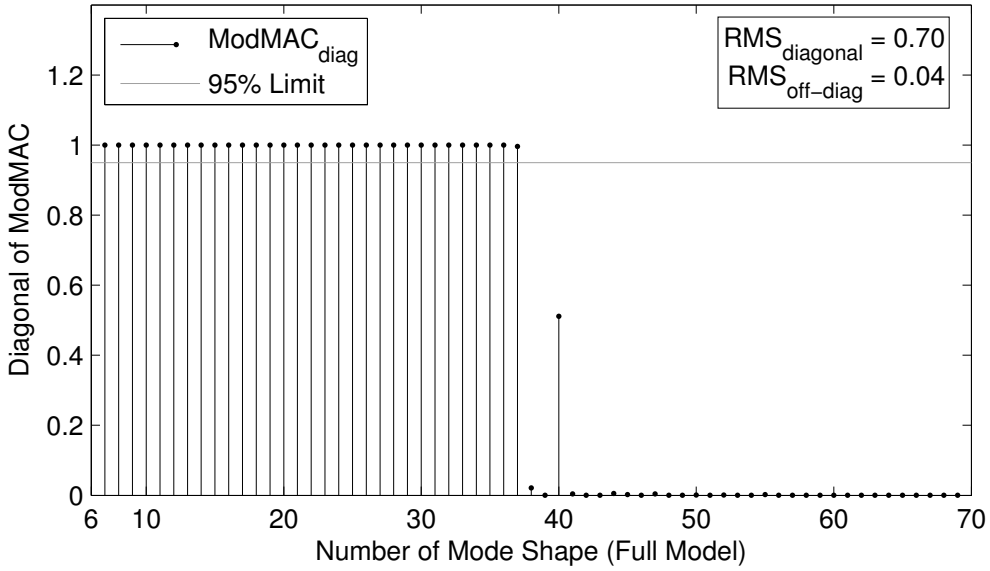

Figure A.10: ModMac of SEREP-KSM with 600 Modes (ID) and 63 Krylov Modes

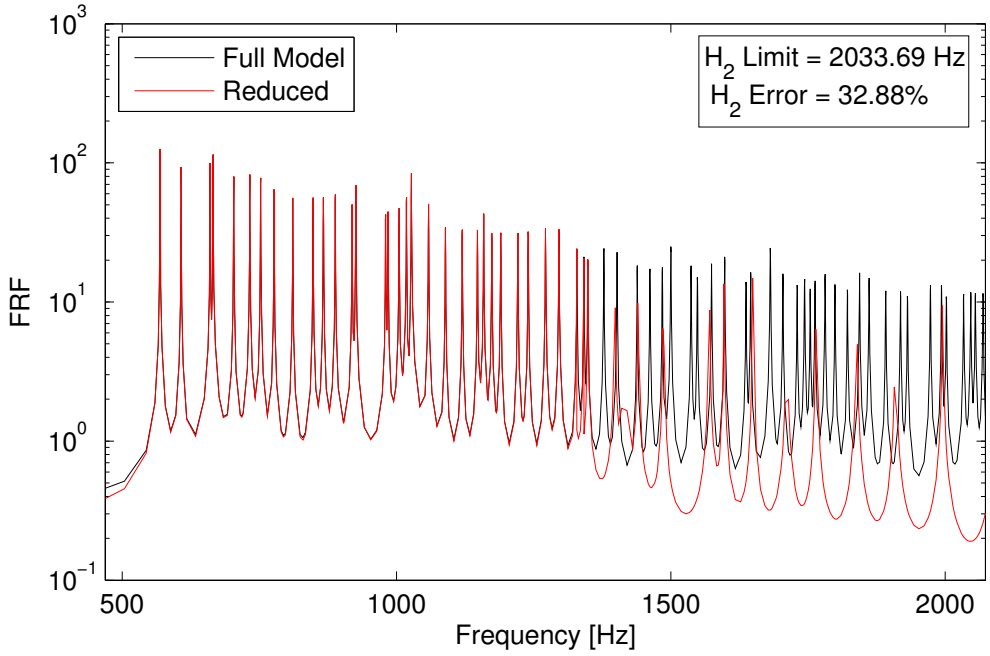

Figure A.11: FRF of SEREP-KSM with 600 Modes (ID) and 63 Krylov Modes

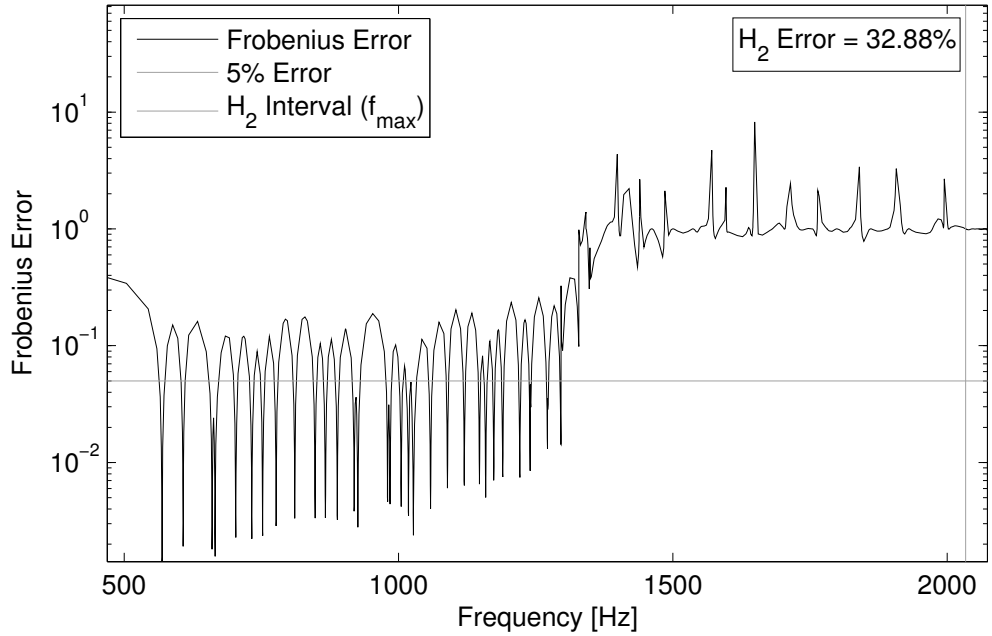

Figure A.12: $\mathcal{H}_2$ Error of SEREP-KSM with 600 Modes (ID) and 63 Krylov Modes

A.2 Data CD